



VALIDATION OF THE AIR FORCE GLOBAL
WEATHER CENTER RELOCATABLE WINDOW
MODEL TOTAL CLOUD FORECAST

THESIS

Edward C. Harris, Second Lieutenant, USAF

AFIT/GM/ENP/97M-07

DISTRIBUTION STATEMENT A

Approved for public release
Distribution Unlimited

DEPARTMENT OF THE AIR FORCE
AIR UNIVERSITY
AIR FORCE INSTITUTE OF TECHNOLOGY

Wright-Patterson Air Force Base, Ohio

DTIC QUALITY INSPECTED 1

AFIT/GM/ENP/97M-07

VALIDATION OF THE AIR FORCE GLOBAL
WEATHER CENTER RELOCATABLE WINDOW
MODEL TOTAL CLOUD FORECAST

THESIS

Edward C. Harris, Second Lieutenant, USAF

AFIT/GM/ENP/97M-07

19970402 073

Approved for public release; distribution unlimited

AFIT/GM/ENP/97M-07

VALIDATION OF THE AIR FORCE GLOBAL WEATHER CENTER
RELOCATABLE WINDOW MODEL TOTAL CLOUD FORECAST

THESIS

Presented to the Faculty of the Graduate School of Engineering
of the Air Force Institute of Technology

Air University

Air Education and Training Command

In Partial Fulfillment of the Requirement for the
Degree of Master of Science in Meteorology

Edward C. Harris, B.S.

Second Lieutenant, USAF

March 1997

Approved for public release; distribution unlimited

VALIDATION OF THE AIR FORCE GLOBAL WEATHER CENTER
RELOCATABLE WINDOW MODEL TOTAL CLOUD FORECAST

Edward C. Harris, B.S.

Second Lieutenant, USAF

Approved:



MICHAEL K. WALTERS, LT COL, USAF
Chairman, Advisory Committee



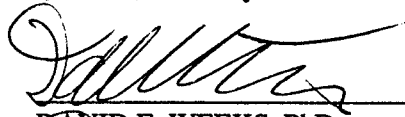
Date



JASON P. TUELL, MAJ, USAF
Member, Advisory Committee



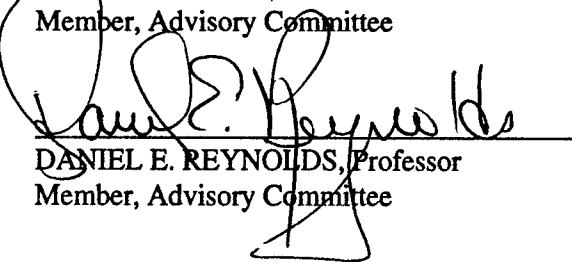
Date



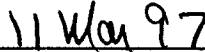
DAVID E. WEEKS, PhD
Member, Advisory Committee



Date



DANIEL E. REYNOLDS, Professor
Member, Advisory Committee



Date

Acknowledgments

This work was supported in part by a grant of HPC time from the DoD HPC Center ASC MSRC Paragon. I would like to thank Mr David Potts of the ASC MSRC for his help and support. His sponsorship into the SCI/VIS lab enabled this study to come to fruition.

I've met some great people at AFIT. Thanks to the faculty, staff, and everyone in the inaugural meteorology class (GM-97M) for all your camaraderie during the last 18 months. I would also like to thank my committee members Major Jason Tuell, Dr David Weeks, and Professor Daniel Reynolds for aiding me in completion of my research. I especially would like to thank my research advisor, Lieutenant Colonel Mike Walters for his knowledge and patience throughout the thesis development. Lt Col Walters is definitely one of the brightest men with whom I've had the pleasure of working.

Finally, I wish to express my heartfelt gratitude to my wife, Tammy, for her love and support throughout our time at AFIT and all the years I've been in school. Without her constant motivation and positive attitude, this would not have been possible. Thanks to my son and daughter, Matthew and Stephanie. The time I've had to spend away from both of them has been challenging, but hopefully they'll see the rewards are greater than the sacrifices. My entire family was always there to cheer me up with their love and support. Most importantly, thanks to God! With Him, all things are possible!

Table of Contents

	Page
Acknowledgments.....	ii
Table of Contents	iii
List of Figures	vi
List of Tables	xiii
I. Introduction.....	1
1.1 Importance of Accurate Cloud Forecasts	1
1.2 AFGWC Cloud Forecasting	1
1.3 Cloud Forecasting Approaches	2
1.3.1 Diagnostic Approach	2
1.3.2 Prognostic Approach	2
1.4 Benchmark.....	3
1.5 Thesis Objective.....	4
1.6 Procedure.....	4
II. Background.....	6
2.1 RWM.....	6
2.1.1 RWM Background.....	6
2.1.2 RWM Limitations.....	9
2.2 Slingo Cloud Forecast Algorithm.....	10
2.2.1 Slingo Background	10
2.2.2 Slingo Limitations	15
2.3 RTNEPH	16

2.3.1	RTNEPH Background	16
2.3.2	RTNEPH Limitations	21
2.3.3	RTNEPH Strengths.....	23
2.4	Previous Studies	24
III.	Methodology	26
3.1	Introduction	26
3.2	Scope	26
3.3	Procedure.....	27
3.3.1	Data.....	27
3.3.2	Slingo Algorithm	27
3.3.3	Grid Transformation and Quality Control	30
3.3.4	Validation Statistics.....	35
IV.	Results.....	40
4.1	RWM Validation for 1 July 1996.....	40
4.1.1	RWM Images	40
4.1.2	RWM Total Cloud Forecast Statistics.....	48
4.2	Persistence Validation for 1 July 1996.	58
4.2.1	Persistence Images.....	58
4.2.2	Persistence Statistics.....	66
4.3	RWM and Persistence Statistics for All Cases	76
4.4	RWM and Persistence Statistics for All Cases and All Times	84
V.	Conclusions and Recommendations	94
5.1	Validation Summary.....	94
5.2	Conclusions	95

5.2.1	Bias	95
5.2.2	Accuracy	96
5.2.3	Correlation	96
5.2.4	Sharpness	97
5.2.5	RWM Overall Total Cloud Forecast Skill.....	98
5.2.6	Summary of Conclusions.....	99
5.3	Recommendations	100
5.3.1	Short-term Recommendations	100
5.3.2	Long-term Recommendations.....	102
Appendices.....		103
Appendix A: GSM Discussion.....		103
Appendix B: High Resolution Analysis System (HIRAS) Description.....		104
Appendix C: Sigma (σ) Coordinate System Description.....		105
Appendix D: The 12 Mandatory Pressure Levels used by RWM.....		106
Appendix E: Slingo FORTRAN Cloud Algorithm.....		107
Appendix F: PV-WAVE Code.....		112
Appendix G: Example of Other Quality Control Data Used.....		139
Appendix H: Chi-Square Test and Results.....		141
Appendix I: Hypothesis Testing.....		143
Bibliography.....		144
Vita.....		146

List of Figures

	Page
Figure 1: The geographical domains of the study. The RWM domain is depicted by the innermost box. The outermost box includes the 9 RTNEPH boxes 35-37, 43-45, 51-53 described and shown in Figures 4 and 5.....	7
Figure 2: Vertical cloud distribution of the Slingo algorithm. (After Slingo, 1987).....	11
Figure 3: Two examples of the maximum overlap method with respect to the ground. Both sketches show low, middle, and high clouds, and have the same total cloud cover using the maximum overlap method. With this in mind, maximum overlap should "overforecast" total clouds.....	15
Figure 4: The Northern Hemisphere domain of the RTNEPH, eighth-mesh grid superimposed on a polar-stereographic projection.....	19
Figure 5: A zoomed view of the 3 x 3 domain of interest used for this study.....	20
Figure 6: An example of one day's coverage by one sunsynchronous satellite. Clear areas represent no coverage, light shading represents 1 satellite pass, and dark shading represents 2 or more satellite passes in a day. (After Kidder and VonderHaar, 1995).	22
Figure 7: Correctly matching up continuous analysis for each RWM forecast required two or three days of data. The top portion of the figure represents the 00 UTC RWM and the bottom portion of the figure represents the 12 UTC RWM.....	27
Figure 8: The untrimmed domain of the 3 x 3 RTNEPH boxes (192 x 192 grid points) of RTNEPH data for 1 July 1996 at 00 UTC, showing total cloud (represented from 0% (black) to 100% (white)).....	30
Figure 9: The trimmed RTNEPH for same date and time as Figure 8. Only the corresponding grid points (129 x 129) within the domain of the RWM are used (refer to Figure 1). Window proportions are different from Figure 8; now it covers the same region as the RWM domain.....	31
Figure 10: The RTNEPH data after interpolation with the same data used in Figure 8 and Figure 9. The data is now displayed in the properly arranged 64 x 64 grid points to match the horizontal resolution of the RWM. RTNEPH data now has the same resolution as the RWM as described in the text.	33

Figure 11: The top-right box represents the RWM forecast with the pixel values converted to bytescales. The magnitude of the individual pixel brightness represents percent of cloud occurrence. A value of zero is represented by a black pixel with brightness of zero, while a value of 100 is represented by a white pixel with brightness of 255. The top-left box represents the RTNEPH analysis for the corresponding time as the RWM forecast. The bottom-left box represents the amount and relative location of RWM total cloud underforecast, and the bottom-right box represents the amount and relative location of RWM total cloud overforecast. For the bottom two boxes, the brighter and more numerous the pixels, the more incorrect the forecast.	40
Figure 12: As Figure 11, for the initial (0) hour RWM forecast. The bottom-right box shows nearly complete absence of overforecast total clouds. Lack of clouds in the upper-right box shows the poor quality of initial RWM moisture data. The initial RWM field lacks convection, which can be seen in the upper-left box of the RTNEPH analysis.....	41
Figure 13: As Figure 11, for the 6-hour RWM forecast. There is a significant increase in total clouds from the initial hour as the RWM moisture begins to increase in the forecast model.....	42
Figure 14: As Figure 11, for the 12-hour RWM forecast.	43
Figure 15: As Figure 11, for the 18-hour RWM forecast. The overforecast areas continue to increase, while the underforecast areas continue to remain relatively high.	44
Figure 16: As Figure 11, for the 24-hour RWM forecast.	45
Figure 17: As Figure 11, for the 30-hour RWM forecast. The same general synoptic structure can be seen in both RWM and RTNEPH. Organized areas of the RWM forecast show clearly defined clear and cloudy areas. Although some areas within the images appear to have no cloud, a closer look at the data showed there are clouds with low coverage (very low brightness). For example, a cloud pixel with a 5% coverage will show up as a faint gray pixel (bytescale of approximately 25), which is barely visible.....	46
Figure 18: As Figure 11, for the 36-hour RWM forecast. Regions of organized underforecast and overforecast total clouds indicate the forecast is too slow or too fast.	47
Figure 19: The RWM 00 UTC mean error scatter plot. Mean error value is steadily decreasing (improving). This indicates a negative bias throughout this forecast with a tendency to improve over time. Removing the initial (0) hour shows the tendency to slightly improve over time. Notice a big improvement between the 0- and 6-hour forecasts, with a slower change afterwards. The negative mean error value indicates the model's tendency to underforecast total clouds through the 36-hour period. For descriptive statistics, refer to Table 4.....	49

Figure 20: RWM total cloud forecast RMSE for 1 July 1996 at 00 UTC. The trend suggests slow improvement of the RWM forecast over time; however, the initial (0) hour of the RWM is so poor the trend of the RMSE values without the initial (0) hour (Figure 21) shows the forecast RMSE increases with time. For descriptive statistics, refer to Table 5 .	50
Figure 21: RWM total cloud forecast RMSE without the initial (0) hour. Without the initial hour, the scatter plot clearly shows a decrease in forecast performance through time. Refer to Table 5 for descriptive statistics.	51
Figure 22: RWM total cloud forecast 0-19 score. Black dots depict RWM 0-19% clear forecast decreasing over time and asterisks depict RTNEPH. The 30-hour RWM forecast appears to be the closest to the true state of the RTNEPH 0-19 score. This plot, along with the values in Table 6 below, clearly shows the RWM overforecasts the clear (0-19) condition through 36 hours. Refer to Table 6 for descriptive statistics.	52
Figure 23: RWM 81-100 score (cloudy). Black dots show RWM 81-100% total cloud forecast, and asterisks show RTNEPH 81-100% total cloud analysis. As with Figure 22, the 30-hour forecast is the closest forecast to the true state. This plot indicates the RWM significantly underforecasts cloudy conditions with respect to the RTNEPH and shows moisture spin-up through 36 hours relatively steady after the 6-hour forecast. The RTNEPH analysis shows relatively little change. Refer to Table 7 for descriptive statistics.	53
Figure 24: RWM PFC with and without point (0,0). Black dots represent the RWM total cloud forecast with point (0,0), while the asterisks represent the RWM total cloud forecast without point (0,0). The percentage forecast correct without the (0,0) point is very poor. For descriptive statistics, refer to Table 8.	54
Figure 25: As Figure 24, except for PFC ± 5 with and without point (0,0). Without the point (0,0), the PFC is still poor, with a mean of less than 10% correct. For descriptive statistics, refer to Table 9.	55
Figure 26: The RWM vs RTNEPH Pearson correlation coefficient for 1 July 1996 at 00 UTC. For descriptive statistics, refer to Table 10. Almost no correlation exists between the RWM and the RTNEPH.	56
Figure 27: Skill scores of the RWM MSE with respect to persistence MSE and the skill score of RWM Brier Score with respect to persistence Brier Score. Black dots show RWM skill compared to persistence. The skill score is mostly negative, with no significant change through time. The asterisks show the RWM skill score with respect to Brier Score. RWM forecast skill is negative, indicating overall poor skill scores but skill improving over time. For descriptive statistics, refer to Table 11.	57
Figure 28: As Figure 11, except top-right box represents the persisted initial (0) hour RTNEPH forecast.	58

Figure 29: As Figure 28, for the initial (0) hour of persistence “forecast.” Underforecast and overforecast, bottom left and bottom right, are empty because the “forecast” is perfect.	59
Figure 30: As Figure 28, this figure represents the 6-hour persistence “forecast.” The qualitative underforecast and overforecast of persistence images. The two bottom images in this figure show nearly equal amount of error with the error fairly evenly distributed. There are no large regions of persisted data in the RTNEPH analysis; if there were, there would be large black areas.	60
Figure 31: As Figure 28. This figure represents the 12-hour persistence “forecast.”	61
Figure 32: As Figure 28, for the 18-hour persistence “forecast.”	62
Figure 33: As Figure 28, for the 24-hour persistence “forecast.”	63
Figure 34: As Figure 28, for the 30-hour persistence “forecast.”	64
Figure 35: As Figure 28, for the 36-hour persistence “forecast.”	65
Figure 36: Persistence mean error is perfect at the initial hour, by definition. With the exception of the 24-hour “forecast,” persistence mean error decreases throughout the forecast period, indicating the “forecast” is becoming poorer. For descriptive statistics, refer to Table 12.	66
Figure 37: The initial (0) hour has a RMSE of zero, by definition. The RMSE increases rapidly over time, then remains relatively steady. Based on these results, persistence accuracy decreases over time. Without the initial (0) hour (Figure 38, next page), persistence forecasts show a gradual decrease in accuracy over time. For descriptive statistics, refer to Table 13.	67
Figure 38: Same as Figure 37, without the initial (0) hour. This scatter plot now clearly shows a decrease in performance through time. For descriptive statistics, refer back to Table 13.	68
Figure 39: Persistence 0-19 score asterisks indicate persistence 0-19% cloud forecast remains the same over time against the RTNEPH (black dots). The best (perfect) score occurs at the initial (0) hour where they are both the same. The near match of the 24-hour forecast is an indication of the diurnal tendency in the persistence forecast. The RTNEPH 0-19 score is not constant, which indicates the lack of persistence in RTNEPH. For descriptive statistics, refer to Table 14.	69
Figure 40: As Figure 39, except this figure shows the 81-100 score for persistence. The persistence 81-100 values, represented by asterisks, remain steady over time against the RTNEPH analysis. As in Figure 39, the 24-hour persistence for the 81-100% occurrence for total cloud is also similar. For descriptive statistics, refer to Table 15.	70

Figure 41: Black dots represent the persistence PFC with point (0,0), and the asterisks represent the persistence PFC without point (0,0). Without the initial (0) hour, the remaining points change little with time. For descriptive statistics, refer to Table 16.	71
Figure 42: As Figure 41, except this figure shows persistence without the initial (0) hour. The persistence accuracy decreases through the forecast period. The persistence "forecast" performs consistently better than the RWM. For descriptive statistics, refer back to Table 16.	72
Figure 43: As Figure 41, except persistence PFC ± 5 with point (0,0) is represented by black dots, the persistence PFC ± 5 without point (0,0) is represented by asterisks. Without the initial (0) hour, the remaining points are similar. For descriptive statistics, refer to Table 17.	73
Figure 44: As Figure 43, except this figure shows persistence PFC ± 5 without the initial (0) hour. Persistence performs much better than the RWM. The performance does decrease through time, as would be expected. For descriptive statistics, refer back to Table 17.	74
Figure 45: The Pearson Correlation Coefficient for persistence against RTNEPH. The mean correlation is just larger than zero except for the initial (0) hour. The persistence forecasts and RTNEPH analyses are poorly correlated. Relatively low correlation at 6 hours suggests many of the RTNEPH grid points are refreshed within 6 hours over the North American Window. For descriptive statistics, refer to Table 18.	75
Figure 46: This plot shows a negative bias (underforecast of total clouds) through the entire forecast period. The RWM does show significant improvement over the first 6 hours with gradual improvement until the 36-hour forecast. A mean error of zero indicates a perfect forecast with respect to the RTNEPH. For descriptive statistics, refer to Table 19, next page.	76
Figure 47: Persistence has a small negative bias tendency through time. However, the 24-hour persisted RTNEPH has a median bias of near zero. This can be expected with diurnal convective cloud changes during the late spring and early summer. For descriptive statistics, refer to Table 19.	77
Figure 48: The RWM RMSE indicates the initial (0) hour is very inaccurate. The RWM total cloud forecast RMSE value decreases (improves) significantly at the 6-hour forecast, and oscillates slightly through the forecast period. An RMSE median value of more than 50 for all periods for the RWM indicates a very inaccurate forecast. For descriptive statistics, refer to Table 20, next page.	78
Figure 49: The persistence initial (0) hour is perfect, by definition. Persistence accuracy then rapidly decreases at the 6-hour forecast, slowly worsens through time, with a slight improvement at 24 hours. For descriptive statistics, refer to Table 20.	79

Figure 50: This figure shows the RWM total cloud forecast and the RTNEPH total cloud analysis is poorly correlated at all forecast times. For descriptive statistics, refer to Table 21, next page.....	80
Figure 51: Persistence against RTNEPH shows perfect correlation at the 0 hour. The correlation then drops to near zero. The remaining persistence hours show a slightly higher correlation than the RWM (Figure 50). The low correlation at 6 hours suggests the RTNEPH is not highly persistent in the North American Window and does not bias the persistence measures of accuracy. For descriptive statistics, refer to Table 21.....	81
Figure 52: RWM Cramer Statistic indicates no linear relation between the RWM and RTNEPH. For descriptive statistics, refer to Table 22.....	82
Figure 53: The Cramer Statistic for persistence begins as nearly perfect, then rapidly drops off at 6 hours. The Cramer Statistic then remains relatively steady through the remainder of the forecast period. For descriptive statistics, refer to Table 22.....	83
Figure 54: RWM and persistence mean error. This plot clearly shows the RWM has a negative bias. Refer to Table 23 for descriptive statistics.....	84
Figure 55: The RWM mean absolute error is greater than that of persistence. Refer to Table 24 for descriptive statistics.....	85
Figure 56: The RWM and persistence RMSE. This is another example of the RWM's total cloud forecast inaccuracy during the late spring and early summer. Refer to Table 25 for descriptive statistics.....	86
Figure 57: The RWM Pearson Correlation Coefficient for all cases and all times is lower than the correlation for persistence. For descriptive statistics, refer to Table 26.	87
Figure 58: RWM and persistence Cramer Statistic for all cases and all times. The RWM shows no linear relation to the RTNEPH, while persistence is slightly higher. For descriptive statistics, refer to Table 27.....	88
Figure 59: RWM PFC without point (0,0) and including the five diagonals either side of the main diagonal. This figure indicates poor performance of the RWM in forecasting total clouds with a heavy reliance on the point (0,0). Only a slight improvement in percentage forecast correct is seen when including the additional 10 diagonals. This figure shows most of the RWM's skill comes from forecasting 0% total cloud. For descriptive statistics, refer to Table 28.	89
Figure 60: As Figure 59, except Figure 60 shows persistence PFC. There is less of a difference from the persisted "forecast" and RTNEPH when including the point (0,0). This figure shows less of the persistence "forecast" skill comes from forecasting 0% total cloud. For descriptive statistics, refer to Table 29.	90

Figure 61: The RWM significantly overforecasts clear conditions (0-19) by approximately 30% and underforecasts the cloudy conditions (81-100) by approximately 17%. For descriptive statistics refer to Table 30.....	91
Figure 62: Cumulative Skill Score of the RWM. For descriptive statistics, refer to Table 31.	92
Figure 63: Persistence closely resembles the RTNEPH total cloud amount. Persistence and RTNEPH scores differ by only 3%. For descriptive statistics, refer to Table 32.....	93
Figure 64: Surface analysis for 1 July 1996 at 00 UTC.....	139
Figure 65: RWM chi-square test of association for all cases through time. Values becoming less positive over time indicates a trend towards dependence of the RWM against the RTNEPH. However, the values all indicate strong independence of the RWM against the RTNEPH. Refer to Table 33 for descriptive statistics.	142

List of Tables

	Page
Table 1: An example of the initial RWM forecast array with the initial RTNEPH analysis, after binning from the original 101 x 101 array, to a 10 x 10 array. The rows are represented by the RWM values and the columns are represented by the RTNEPH values. Each array is binned into a 10 x 10 array with each row and column representing 10 data points except the final row and column which contains eleven values due to the odd size of the original array.....	34
Table 2: An example of the initial Persistence “forecast” (rows) against the initial RTNEPH analysis (columns). A diagonal clearly exist, indicating a perfect correlation between the forecast and analysis data. Table format is the same as Table 1. This is an example of the initial (0) hour persistence forecast.....	35
Table 3: Statistical measures and abbreviations defined for the other tables in this section. Each table is a quantitative summary of its respective figure.....	48
Table 4: Descriptive statistics for Figure 19 for the RWM 00 UTC model forecast for 1 July 1996. The overall mean and median are negative.....	49
Table 5: Descriptive statistics for Figure 20.....	50
Table 6: Descriptive statistics for Figure 22. The statistics show the significant overforecast of clear conditions by the RWM.....	52
Table 7: Descriptive statistics for Figure 23. This table shows the RWM underforecast cloudy conditions with a mean and median less than half of the RTNEPH.....	53
Table 8: Descriptive statistics for Figure 24. Without the (0,0) point, the forecasts are very poor.....	54
Table 9: Descriptive statistics for Figure 25. Without the (0,0) point, the forecast would still have low PFC scores.....	55
Table 10: Descriptive statistics for Figure 26.....	56
Table 11: Descriptive statistics for Figure 27. The initial (0) hour is not shown.....	57
Table 12: Descriptive statistics for Figure 36.....	66
Table 13: Descriptive statistics for Figure 37 and Figure 38.....	67
Table 14: Descriptive statistics for Figure 39.....	69
Table 15: Descriptive statistics for Figure 40.....	70

Table 16: Descriptive statistics for Figure 41 and Figure 42. Even without the (0,0) point, persistence performs relatively well.....	71
Table 17: Descriptive statistics for Figure 43 and Figure 44.....	73
Table 18: Descriptive statistics for Figure 45.....	75
Table 19: Descriptive statistics for Figures 46 and 47.	77
Table 20: Descriptive statistics for Figures 48 and 49.	79
Table 21: Descriptive statistics for Figures 50 and 51. This statistic is the RWM against the RTNEPH and persistence against the RTNEPH.	81
Table 22: Descriptive statistics for Figures 52 and 53.	83
Table 23: Descriptive statistics for Figure 54. The RWM clearly underforecasts total clouds with respect to the RTNEPH analysis data. Persistence has relatively little bias.....	84
Table 24: Descriptive statistics for Figure 55 for all cases and all times.	85
Table 25: Descriptive statistics for Figure 56.....	86
Table 26: Descriptive statistics for Figure 57.....	87
Table 27: Descriptive statistics for Figure 58.....	88
Table 28: Descriptive statistics for Figure 59.....	89
Table 29: Descriptive statistics for Figure 60.....	90
Table 30: Descriptive statistics for Figure 61.....	91
Table 31: Descriptive statistics for Figure 62.....	92
Table 32: Descriptive statistics for Figure 63.....	93
Table 33: Descriptive statistics for Figure 64.....	142

Abstract

Air Force Global Weather Center's (AFGWC) Relocatable Window Model (RWM) total cloud forecasts were validated using data for selected days in May, June, and July, 1996. Forecasts were generated twice daily (00 UTC and 12 UTC) to determine the RWM's ability to accurately forecast total cloud cover during the late spring and early summer. The RWM forecasts were post-processed using the Slingo cloud forecast algorithm and compared against AFGWC's operational real-time nephanalysis (RTNEPH) cloud analysis model. As a minimal-skill baseline comparison to the RWM's total cloud forecast, the RTNEPH initial analysis hour was persisted and evaluated against the same RTNEPH analysis as the RWM forecasts.

The results indicate RWM total cloud forecasts did not show improved skill, sharpness, accuracy or bias when compared against RTNEPH persistence through the 36-hour forecast period. The results also suggest the Slingo algorithm, as tested, is not appropriate for use in the RWM as an accurate total cloud forecast method for the late spring and early summer months. The RWM's total cloud forecast performance during the late spring and early summer over the North American Window should be improved in the short term by incorporating convective parameterization within the Slingo algorithm or replacing the Slingo algorithm with an alternative algorithm designed for more accurate and skillful total cloud forecasts. While the suggested short-term improvements are incorporated into the RWM, the results of this and other related studies must be carefully communicated to the operational users of the RWM products to be useful. In the long term, the RWM should be replaced with a state-of-the-art forecast model capable of forecasting clouds deterministically, rather than diagnostically.

VALIDATION OF THE AIR FORCE GLOBAL WEATHER CENTER RELOCATABLE WINDOW MODEL TOTAL CLOUD FORECAST

I. Introduction

1.1 Importance of Accurate Cloud Forecasts

Weather influences nearly every aspect of military operations. Missions such as air refueling, air-to-air intercept, airlift, airdrop, air-to-ground weapons delivery, and aerial reconnaissance are important Department of Defense (DoD) interests. It is crucial for military forecasters to have correct cloud forecast guidance at their disposal to assist the DoD in the successful completion of those interests. In addition, commanders require timely and accurate weather forecasts to effectively and efficiently exploit aerospace power. The effective integration of accurate cloud forecasts into combat operations can significantly influence decisions regarding weapon selection and targeting options. Accurate total cloud forecast coverage, horizontal resolution, and refresh rate are some of the extremely important characteristics of an accurate cloud forecast model which the Air Force Global Weather Center (AFGWC) uses to support the DoD and other national programs.

1.2 AFGWC Cloud Forecasting

The AFGWC has produced global cloud forecasts using numerical weather models for approximately 30 years. With the escalating performance of computers, AFGWC has been attempting to improve its cloud forecasts on smaller (higher-resolution) scales. The AFGWC produces a cloud forecast visualization using an adapted Relocatable Window Model (RWM) (Mathur, 1983). This study will determine the RWM's performance in forecasting total clouds. The AFGWC is considering implementation of operational cloud forecasts based on the RWM

with Slingo algorithm post-processed clouds. The RWM uses a diagnostic approach to forecast clouds, which is one of two fundamental approaches to cloud forecasting.

1.3 Cloud Forecasting Approaches

This section discusses the two fundamental approaches to cloud forecasting.

1.3.1 Diagnostic Approach

The RWM uses a diagnostic approach to forecast clouds. The diagnostic approach uses governing equations which do not use time derivatives to forecast cloud water deterministically. The forecast will produce, at a moment in time, an estimate of cloud cover based on the distribution of other model variables, such as temperature and relative humidity. This approach is the least computationally demanding of the two approaches, and neglects many of the physical and dynamical effects of the atmosphere. However, with the improved performance of computers, it is becoming feasible to deterministically forecast clouds from first principles. The alternative approach to forecasting clouds is the deterministic (or prognostic) approach.

1.3.2 Prognostic Approach

The prognostic approach solves differential equations for conservation of water substances (i.e., cloud water, rain water, ice, etc.) to deterministically forecast the distribution of clouds. The prognostic approach neglects fewer necessary parameters than the diagnostic approach and includes more realistic physical and dynamical mechanisms to more accurately forecast the true state of the complex atmosphere. In order to realize the full potential of today's computers, and to more accurately model the true state of the atmosphere, the prognostic approach should be used. Other agencies have incorporated this approach into forecasting regional clouds and the results appear encouraging. For example, Hodur (1993)

discusses the potential of the recently developed Coupled Oceanographic and Atmospheric Mesoscale Prediction System (COAMPS) which deterministically forecasts clouds down to a 5 km resolution. The atmospheric prediction component of COAMPS features non-hydrostatic physics, explicit moisture physics and aerosols, and improved data assimilation. The COAMPS has been designed to provide the high-resolution, relocatable prediction capability required for effective and efficient support of military operations.

1.4 Benchmark

The ability to accurately forecast total cloud cover is a critical test of a model's cloud forecast performance. A poor total-cloud forecast indicates individual cloud layers are probably forecast inaccurately as well. This study focuses on the total cloud cover because it is the most basic of cloud forecasts. Correctly forecasting total clouds is a prerequisite for successful cloud forecasts at specific locations and times.

The documentation of the RWM and the adapted Slingo algorithm's performance will serve as a benchmark for one of today's operational military weather forecast models. The accuracy of all numerical weather models and their respective algorithms should be validated to determine their relative operational effectiveness. Once the results are determined, the algorithm or model should be improved or replaced as appropriate. With the answers to questions regarding a model's performance, commanders will be more effectively and efficiently able to make the crucial operational decisions. Communicating the results of a model's performance to the operational forecaster will allow effective implementation of those decisions, which will inevitably lead to improved cloud forecasting support to the customer.

1.5 Thesis Objective

This thesis serves to qualitatively (through subjective analysis) and quantitatively (through objective analysis) validate the performance of the AFGWC RWM with an adapted Slingo algorithm-based (1980, 1987) late spring and early summer total cloud forecast.

1.6 Procedure

The real-time nephanalysis (RTNEPH) is used in this study to validate the RWM total cloud forecast. The RWM is post-processed with the Slingo algorithm, without convective parameterizations, for selected days in May, June, and July, 1996. The days were selected based on the availability of RWM forecasts and the associated RTNEPH validation data for an entire 36-hour period. The RWM cloud forecasts were generated twice daily (00 UTC and 12 UTC) retrospectively for May, June, and July, 1996 to sample the North American late spring and early summer. A side-by-side comparison of the RWM total cloud forecast against a forecast based on persistence of RTNEPH is also performed, to provide a minimal skill baseline. This is accomplished through the RTNEPH initial analysis hour persisted against the entire 36-hour analysis.

The background and specifics of the RWM, Slingo algorithm, RTNEPH, and previous studies are described in the second chapter. Chapter three contains the methodology of the validation and discusses the scope and fundamental processes of the study. Chapter three also describes the grid transformations and the statistics calculated for the RWM forecast validation. Chapter four includes the results of the study, with a discussion of the statistical results for a representative 36-hour forecast example and summary statistics of all cases with all forecast times. The final chapter includes the conclusions and recommendations.

This concludes the introduction necessary for the remainder of the thesis. The next chapter discusses the background of the forecast model, forecast algorithm, and analysis model which were used to perform the validation.

II. Background

2.1 RWM

This chapter begins by discussing the general characteristics of the RWM, the Slingo algorithm, and the RTNEPH analysis model. The chapter concludes with a discussion of related studies.

2.1.1 RWM Background

During the late 1970's, Air Weather Service (AWS) and AFGWC recognized a need for a weather model capable of producing a regional-scale meteorological forecast anywhere in the world (Pace, 1989). During the early 1980's, a committee reviewed the regional-forecast models under development and concluded the best candidate was a Quasi-Lagrangian Model (QLM) developed at the National Meteorological Center (NMC). The QLM was based on an earlier model known as the Quasi-Lagrangian Nested Grid Model (QNGM) (Mathur, 1983). The QLM's main function at NMC was to track hurricanes in a non-operational environment (Neel *et al.*, 1993). Mathur's QLM was imported by AFGWC and adapted to meet military needs (Wonsick, 1996 personal communication). The AFGWC's implementation of the QLM is known now as the RWM.

The RWM receives its source data (00 UTC and 12 UTC) and generates 36-hour forecasts twice per day for three fixed and four contingency windows. The three fixed window grids cover North America, Asia, and Europe, while the four remaining windows can be relocated anywhere around the world. Future references to RWM refer only to the geographical North American fixed window. The North American Window was chosen for validation due to the availability of a higher observation density associated with the RTNEPH. This higher density of observations and availability of data should result in a more accurate analysis for validation.

The specific grid corners for the North American window are: 44.2°N, 144.4°W; 64.7°N, 44.6°W; 13.3°N, 108.8°W; 19.6°N, 69.4°W, as shown in Figure 1. The RWM data is stored on a polar-stereographic grid composed of 61 x 61 (3,721) grid points, with a horizontal resolution of 50 nautical miles (NM), true at 60° N. Each gridpoint represents the centroid of the spatial grid. Therefore, the areal coverage of the RWM-based forecast products is approximately 3000 NM x 3000 NM (Figure 1).

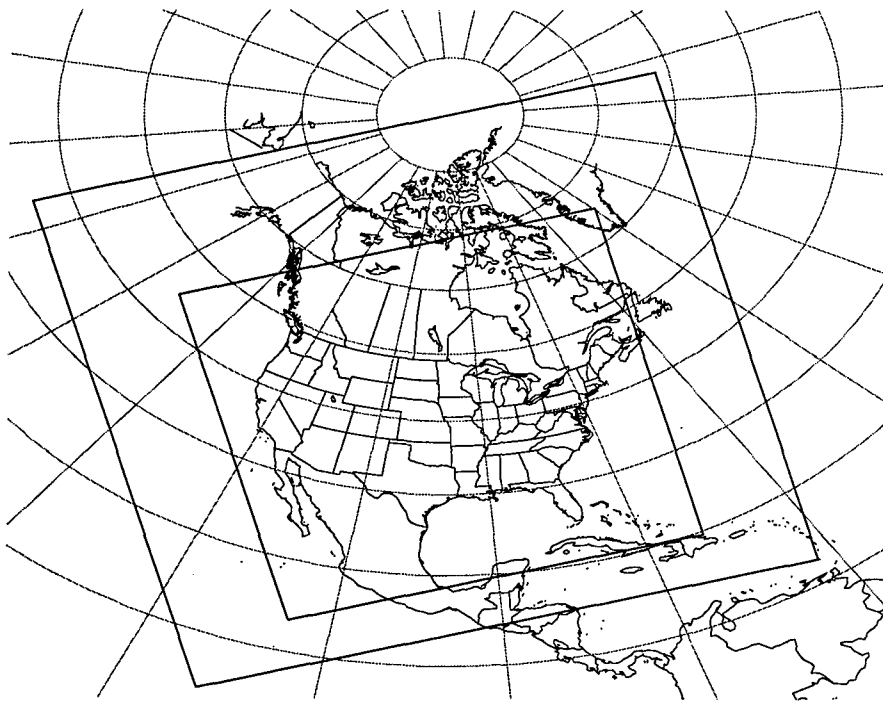


Figure 1: The geographical domains of the study. The RWM domain is depicted by the innermost box. The outermost box includes the 9 RTNEPH boxes 35-37, 43-45, 51-53 described and shown in Figures 4 and 5.

The implementation of the RWM used for this study incorporated 3-hourly lateral boundary conditions from the 2.5° x 2.5° AFGWC Global Spectral Model (GSM), and a rigid top boundary condition with damping. The GSM (Appendix A) specified the large-scale features entering or

leaving the RWM domain. The GSM did not use RTNEPH analysis information to derive its initial moisture analysis. The High Resolution Analysis System (HIRAS), as described in Appendix B, provided the initial conditions for the GSM and the initial boundary conditions for the RWM. For more detailed information, the reader is referred to Stobie, 1986 and Neel *et al.*, 1993. On 8 January 1997, the Navy Operational Global Atmospheric Prediction System (NOGAPS) replaced the GSM as initial fields and boundary conditions for the RWM (Cantrell 1997, personal communication).

For this study, the RWM used HIRAS for its initial conditions and the GSM for its boundary conditions as input into the Relocatable Window Analysis Model (RWAM) for its first-guess analysis fields. The RWM continues to use the RWAM for initialization as of this writing. The RWAM uses an interpolation of the HIRAS global analysis from mandatory pressure levels to the RWM horizontal and vertical grid structure. The RWAM provided temperature, winds, moisture, and pressure as input for the RWM. The GSM forecast database provided boundary layer data, winds, pressure, and temperature (Neel *et al.*, 1993) at a coarse spatial resolution. The RWM also incorporated real-time soil moisture, snow depth, and ground temperature analysis provided by AFGWC's analysis models. The input sea-surface temperatures were provided by the U. S. Navy's sea-surface temperature analysis.

The RWM forecast has two cycles (00 UTC and 12 UTC) and produces forecasts on sigma levels (Appendix C) for horizontal wind components, vertical velocity, potential temperature, specific humidity, and other weather parameters at up to 36 predefined atmospheric levels for forecasts out to 36 hours. The sigma-level forecast variables are then post-processed to generate forecasts on mandatory pressure levels (Appendix D) of vertical velocity, cloud amounts at low, middle, and high levels, total cloud amounts, wind speed and direction, temperature, moisture, and pressure.

The RWM uses a basic boundary-layer physics package which transfers sensible and latent heat over the ocean when the sea surface temperature is greater than the air temperature.

Terrain-dependent drag coefficients model the surface friction (Neel *et al.*, 1993).

Forecast products from the RWM are available to world-wide DoD installations via the Air Force Weather Information Network (AFWIN), the Air Force Dial-In Subsystem (AFDIS), and the Automated Weather Distribution System (AWDS). For a more detailed discussion of the RWM, the reader is referred to Mathur (1983).

2.1.2 RWM Limitations

It is well known that the moisture fields of forecast models, without the true initial moisture conditions, undergo an adjustment during the forecast from the initial state. The RWM moisture problem was complicated by the fact that the RWM did not use its own forecasts as first-guess fields in the analysis. Instead, the RWM relied on an interpolated analysis, or zero-hour forecast, from the GSM. As will be shown later, the RWM tried to develop a three-dimensional moisture field during the forecast period which is consistent with its own physical parameterization of moisture. Since the RWM used the HIRAS as its initial conditions, its starting moisture will be that of the HIRAS and not of the RTNEPH. The RWM does not account for the land surface processes and solar or terrestrial radiative processes (Neel *et al.*, 1993). Without radiation, no diurnal cycle is forecasted. The RWM also is limited in its physics. The RWM parameterizes only basic physical processes such as air-sea exchange of sensible and latent heat.

Documentation of the RWM has been very limited. In addition, previous studies validating the RWM's performance are not well documented. This study will validate the RWM total cloud forecast performance, using the Slingo cloud algorithm (Appendix E), against the RTNEPH, and

will serve as a benchmark for the performance of the RWM cloud forecast scheme as implemented by AFGWC.

2.2 *Slingo Cloud Forecast Algorithm*

This section discusses the Slingo algorithm's background and limitations.

2.2.1 *Slingo Background*

The Slingo (1980) algorithm was implemented in May 1985, within the European Centre for Medium-Range Weather Forecasts (ECMWF) medium range forecast model. The algorithm uses a diagnostic approach to reproduce the main features of a cloud field by relating the large-scale meteorological features associated with a cloud distribution to model variables (Slingo, 1980). The RWM cloud forecast model validated in this study is an AFGWC implementation of the Slingo (1980, 1987) algorithm. The Slingo algorithm produces a diagnosis of cloud cover and liquid water content from the Slingo's large-scale parameters for low-, middle-, high-, and total-cloud cover, at each RWM grid point. The total cloud cover is empirically derived by summing the individual cloud layers without exceeding 100%.

The Slingo algorithm is based on a diagnostic approach in which the forecast cloudiness is empirically related to the large-scale model variables. Empirical functions were developed to represent the probability of clouds occurring under specific atmospheric conditions (i.e., static stability (S), relative humidity (RH), and vertical velocity (ω)). The respective equations (Equations 1-8) are described on the following pages. The Slingo output includes percent cloud occurrence, from clear (0%) to cloudy (100%) in 1% increments. The Slingo algorithm allows four different cloud types (Figure 2). The clouds represented in Figure 2 are convective (cumulus (Cu), cumulonimbus (Cb)), high (cirrus (Ci)), middle (altostratus (As), altocumulus (Ac)), and low (stratus (St), stratocumulus (Sc)). This study only validates the total cloud forecasts. The Slingo algorithm breaks the forecasted clouds up into four levels (including

convection) of clouds. The low-level clouds range from 8 mb above the surface to 800 mb. The restriction of 8 mb above the surface is designed to eliminate the formation and dissipation of fog. The middle cloud ranges from 800 mb to 450 mb, and the high cloud from 450 mb to 250 mb.

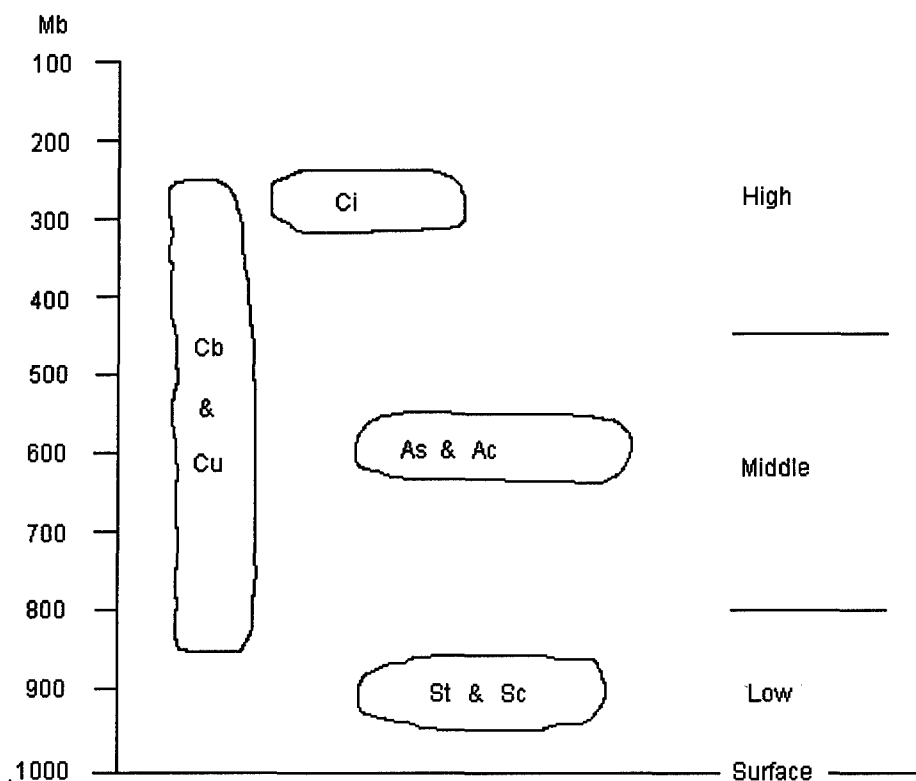


Figure 2: Vertical cloud distribution of the Slingo algorithm. (After Slingo, 1987)

The AFGWC restricts the Slingo cloud forecasts to between 980 mb and 215 mb. From this point on, total cloud cover forecasts for a gridpoint will be assumed to represent the fractional cloud cover within the grid volume represented by the grid point as viewed from above.

The Slingo algorithm uses a quadratic cloud-relative humidity (RH) relationship (Equations 1, 2, and 5) for stratiform clouds in the free atmosphere (above the boundary layer). For a more detailed explanation of the Slingo algorithm, the reader is referred to Slingo (1980, 1987), and Appendix E, which describes the Slingo algorithm as implemented by AFGWC in the RWM.

Fractional coverage of frontal and extratropical cirrus (high-level clouds) is determined from a function of RH and given by the equation:

$$C_H = [Max\{0.0, \frac{(RH - 0.8)}{0.2}\}]^2, \quad (1)$$

where C_H represents the fractional coverage of high-level clouds.

Fractional coverage of middle-level clouds, which are assumed to be formed primarily from extratropical systems and tropical disturbances, are parameterized by:

$$C_M = [Max\{0.0, \frac{(RH_C - 0.8)}{0.2}\}]^2, \quad (2)$$

where

$$RH_C = RH(1.0 - C_C), \quad (3)$$

and C_M represents the fractional coverage of middle-level clouds.

The term C_C , in Equation 3, refers to the convective cloud cover. The AFGWC has set the value of C_C to zero, thus, the RWM implementation of Slingo does not include convective clouds.

With this simplification, Equation 3 becomes:

$$RH_C = RH \quad (4)$$

Low-level clouds are often the most difficult to predict due to the many physical and dynamical effects which influence them. Some of the physical effects include the complexity and dependency on the thermal and moisture structure of the boundary layer, cloud-top entrainment, turbulent fluxes of heat, moisture and momentum, radiative cooling, and diabatic

heating. Slingo (1987) categorizes low clouds into two classes: those associated with extratropical fronts and tropical disturbances, and those that occur in relatively quiescent conditions related directly to the boundary layer. The low-level clouds associated with extratropical fronts and tropical disturbances are parameterized by:

$$C'_L = \left[\text{Max}\left\{0.0, \frac{(RH_c - 0.8)}{0.2}\right\} \right]^2, \quad (5)$$

where C'_L represents the fractional coverage of low-level clouds associated with extratropical fronts and tropical disturbances.

However, if there is subsidence, i.e. vertical velocity (ω) > 0 :

$$C_L = C'_L(-10.0\omega) \quad \text{if } \omega \geq -0.1 \text{ Pa s}^{-1}, \quad (6a)$$

$$C_L = C'_L \quad \text{otherwise} \quad (6b)$$

In Equation 6b, C_L represents the fractional coverage of low-level clouds. The quadratic function (Equation 5) of RH is modified for low-level clouds in the case of weak upward or downward vertical motion (allowing no low-level clouds in areas of subsidence).

The ω in Equation (6a) is intended to delineate frontal clouds in the extratropics, and suppress the excessive cloudiness which otherwise would occur in the subtropics (Slingo, 1987).

The fractional coverage of the low-level clouds which occur in relatively quiescent conditions related directly to the boundary layer, and low-level inversions in temperature and humidity, is given by:

$$C'_L = -6.67 \frac{\Delta\theta}{\Delta p} - 0.667 \frac{\Delta\theta}{\Delta p}, \quad (7)$$

where $\frac{\Delta\theta}{\Delta p}$ is the lapse rate (K mb^{-1}) below 750 mb.

Where low-level inversions exist, boundary layer clouds are modeled as a function of the strength of the low-level inversion. An additional dependence on relative humidity at the base of the inversion (RH_{BASE}) is used to prevent clouds from forming under dry inversions:

$$\begin{aligned} C_L &= 0 && \text{if } RH_{BASE} < 0.6 \\ C_L &= C'_L \left\{ 1.0 - \frac{(0.8 - RH_{BASE})}{0.2} \right\} && \text{for } 0.6 \leq RH_{BASE} \leq 0.8 \\ C_L &= C'_L && \text{otherwise.} \end{aligned} \quad (8)$$

The Slingo algorithm forecasts layers of clouds which have bases and tops constrained to sigma-layers (Appendix C) for the four cloud types shown in Figure 2. The convective cloud may fill any number of layers from 850 mb to 250 mb. The cumulus convection is parameterized by the Kuo-scheme; however, for re-emphasis, the parameterization of cumulus convection is omitted by AFGWC in the current implementation of the Slingo algorithm.

Accurately inferring cloud layers from a three-dimensional moisture field is critically important to the operational forecaster and the individual levels at which clouds are forecasted are important to Air Force operations. The Slingo cloud geometry used for calculating total cloudiness is a maximum overlap method with cloudiness between 0 (for clear) and 1 (for overcast) shown in Figure 3. For example, for fractional cloud coverage for low, middle, and high clouds of 10, 20 and 30% respectively, the maximum overlap would yield a total overlap of 60% total cloud coverage. For a detailed discussion of the Slingo algorithm, refer to Appendix E.

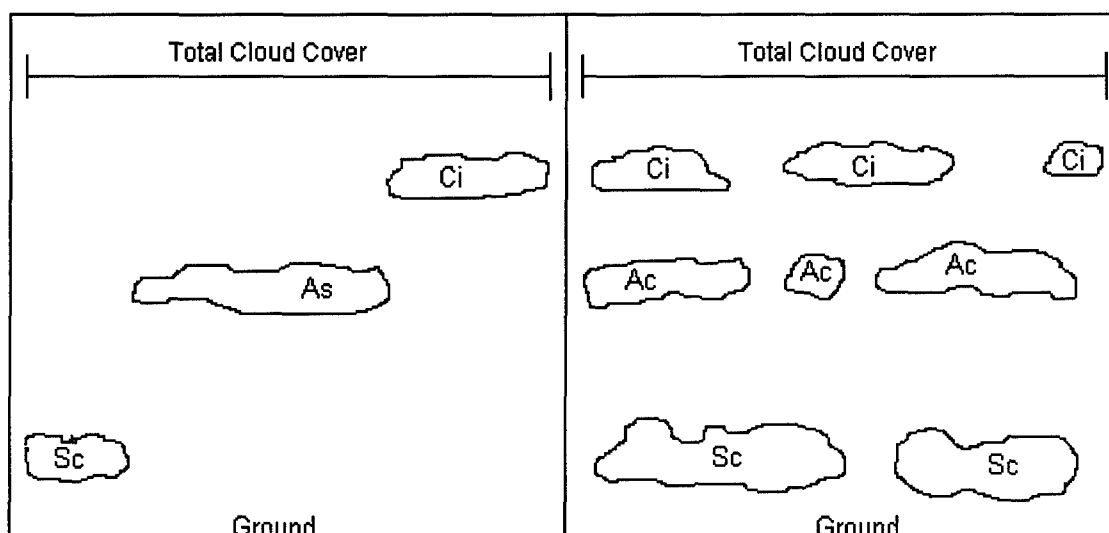


Figure 3: Two examples of the maximum overlap method with respect to the ground. Both sketches show low, middle, and high clouds, and have the same total cloud cover using the maximum overlap method. With this in mind, maximum overlap should “overforecast” total clouds.

Due to data availability and limited computational resources, this study’s scope has been restricted to late spring and early summer. Since the convective parameterization is set to zero, condensational heating will now only occur in saturated flow with a scale resolvable by the model, which has a relatively coarse horizontal resolution of 50 NM for the RWM. Diagnostic cloud schemes are attractive for forecasting large scale cloudiness features due to their simplicity. However, they lack a sound physical basis for forecasting and, thus, have several limitations.

2.2.2 *Slingo Limitations*

In addition to the discussion in Section 1.3.1, Tiedtke (1995) discusses several limitations of diagnostic cloud schemes such as the Slingo algorithm. First, diagnostic cloud schemes contain no realistic representation of cloud formation due to cumulus convection. This representation is especially true in this study since the convective parameterization is set to zero.

In addition, the model does not incorporate realistic treatment of cloud related processes. When treating clouds diagnostically, the subgrid cloud processes, cloud microphysics, and optical cloud properties are not taken into account (Tiedtke, 1995). Second, by manually or automatically retuning the model variables (i.e., critical RH, ω , and S), diagnostic relationships can significantly affect the output parameter (cloud vs no-cloud decision) for the cloud forecast. For example, if the critical-RH value for cloud forecasts is set to 80%, a diurnal tendency may indicate that the critical-RH value should be linearly adjusted up to 90% throughout the day. Finally, incomplete hydrological cycles, such as storage and reevaporation of liquid cloud water, are not considered. The reader is referred to Tiedtke (1995) for a more in-depth discussion of diagnostic cloud schemes.

2.3 RTNEPH

This section describes the background, limitations, and strengths of the RTNEPH, which is used as ground truth in this study.

2.3.1 RTNEPH Background

The RTNEPH replaced the 3-Dimensional Nephanalysis (3DNEPH) at AFGWC on 1 August 1983. The RTNEPH was developed for the initialization of trajectory based cloud forecast models run at AFGWC (Crum, 1987) and was designed to maximize the probability of cloud detection (Hamill *et al.*, 1992). In this study, the RTNEPH is assumed to most closely resemble the true state of the total cloud cover. A Phillips Laboratory (PL) 30-month study also used RTNEPH total cloud output as validation against a modified Slingo algorithm (Nehrkorn *et al.*, 1994).

Most of the data analyzed by the RTNEPH comes from the Defense Meteorological Satellite Program (DMSP), conventional cloud observations, National Oceanic and Atmospheric

Administration (NOAA) polar-orbiting satellites, surface analyses, radiosondes, and aircraft. Surface observations are updated hourly with each observation encompassing a radius of 20 NM to 50 NM (Neel *et al.*, 1993). A manual quality control (referred to as a bogus) is also employed during each analysis cycle.

To perform the bogus, an analyst looks for problem areas in the analysis. Once a problem is identified, the problem is corrected, discarded, or additional meteorological information is added to the analysis data and the corrected product is returned to the system for further analysis (Stobie, 1986). The bogus process uses all available satellite imagery (DMSP, NOAA, and Geostationary Operational Environmental Satellite (GOES)), conventional data, and the analyst's own experience.

Input of the available satellite data is essential to producing an RTNEPH analysis for a given grid point. The AFGWC also collects all available conventional data from the Automated Weather Network (AWN) and incorporates the data into the RTNEPH. The next step of the RTNEPH is the merging of the satellite and conventional analysis. If recent satellite data or conventional data are not available, the RTNEPH will persist the cloud analysis data from the previous RTNEPH analysis.

The RTNEPH dataset consists of total cloud amount and up to 4 distinct layers of clouds, where each grid point contains cloud coverage, geopotential height of the layered cloud bases and tops, time of observation, and diagnostic information (Campana, 1995). The RTNEPH data is then archived in a 1 to 30 million polar-stereographic projection database storing total and layered cloud amounts, cloud bases and tops, and cloud types with a horizontal resolution of approximately 48 km (47.625 km resolution true at 60°N). The RTNEPH is broken up into 64 (eighth-mesh) nephanalysis boxes per hemisphere (Figure 4). Each RTNEPH box has 4,096 grid

points with a 25.715 NM¹ resolution, true at 60°N, and 36,864 total grid points, all vertically located on up to 4 floating levels. The distance between RTNEPH gridpoints is defined relative to the AFGWC whole-mesh grid, where the whole-mesh gridpoints are 381 km apart at 60°N (Zamiska and Giese, 1995). Thus, an eighth-mesh grid has resolution of 1/8th of 381 km, or 47.625 km between gridpoints at 60°N. The polar-stereographic projection is centered at the poles relative to the Earth's surface. Because of the Earth's curvature, resolution increases toward the poles and decreases toward the equator. The four corner RTNEPH boxes of each hemisphere are not used, thus, each hemisphere contains 60 boxes of data. With 4,096 grid points in each box, there are 245,760 grid points per hemisphere. Each of the 64 boxes contains an array of 64 x 64 analysis points. The particular region which will be used in this study consists of a 3 x 3 array of 9 boxes, specifically, boxes 35-37, 43-45, and 51-53. These nine boxes (Figure 5) constitute the 36,864 total grid points in a region larger than that of the RWM (refer back to Figure 1).

The RTNEPH domain is an eighth-mesh grid, projected onto a polar-stereographic projection, regularly spaced in longitude, but irregularly spaced in latitude. The RTNEPH has a horizontal resolution between grid points of 25 NM (roughly 48 km), true at 60°N latitude. For the area of interest (Figure 5), RTNEPH's (0,0) coordinate was located at the top left of each RTNEPH box, with index values increasing to the east and south. The RWM, on the other hand, consisted of a nominal 50 NM horizontal resolution between grid points, with the (0,0) coordinate located at the bottom left of the grid, increasing to the east and north. Using PV-WAVE[®], a product of Visual Numerics, Inc.[®], the RWM arrays were inverted to match the array layout of the RTNEPH.

¹ Where 25.715 NM = 47.625 km, based on the international nautical mile (1 nautical mile = 1852 meters)

The RTNEPH's performance was designed to maximize the probability of detecting clouds, with less emphasis on cloud height, thickness, and determination of cloud type. If multiple sources of data are available to the RTNEPH, the RTNEPH will use the cloudiest one, provided other timeliness and proximity criteria are met. Clouds are identified as high clouds when their tops are greater than 6,500 m, middle clouds when their tops are greater than 3,000 m but less than or equal to 6,500 m, and low clouds when their tops are less than or equal to 3,000 m.

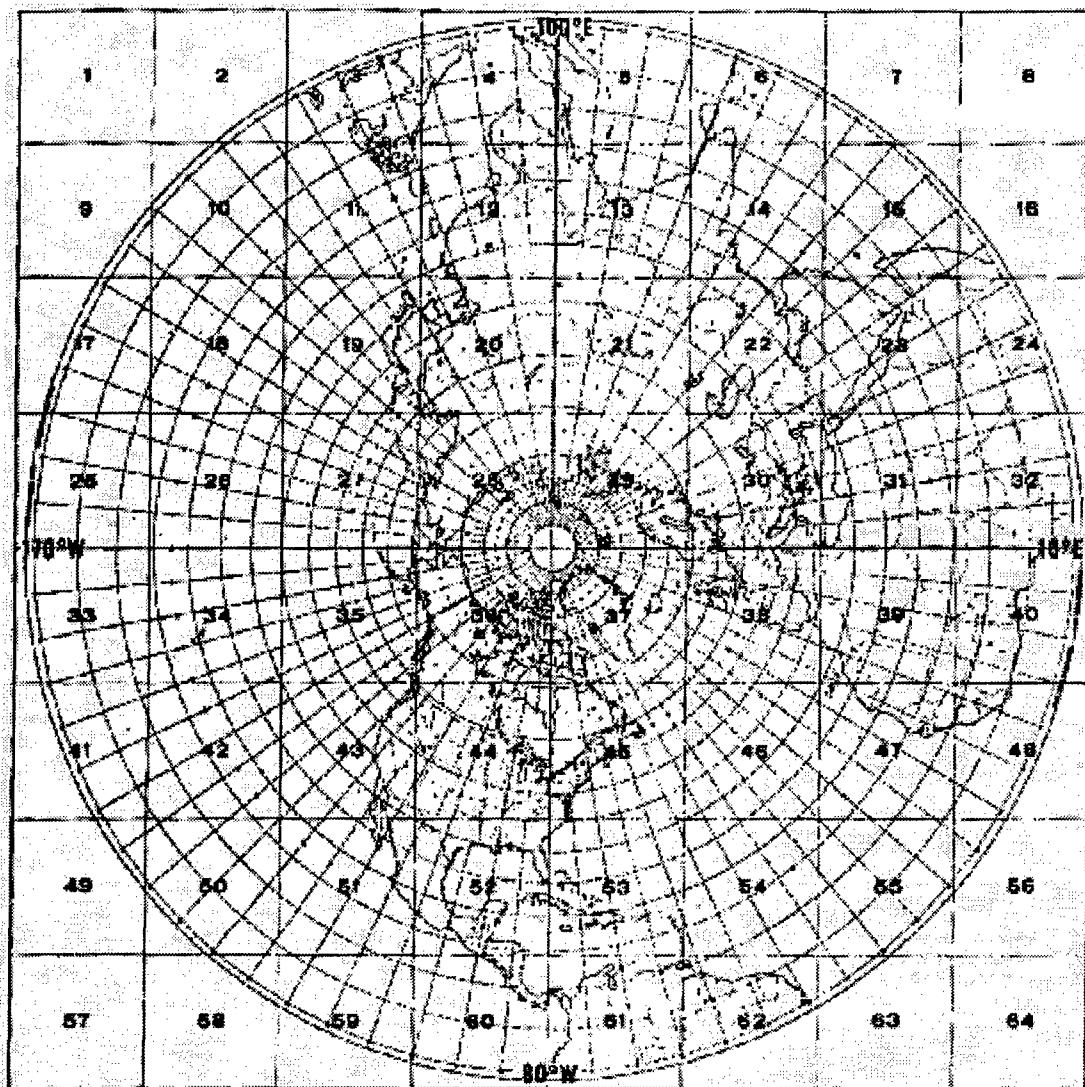


Figure 4: The Northern Hemisphere domain of the RTNEPH, eighth-mesh grid superimposed on a polar-stereographic projection.

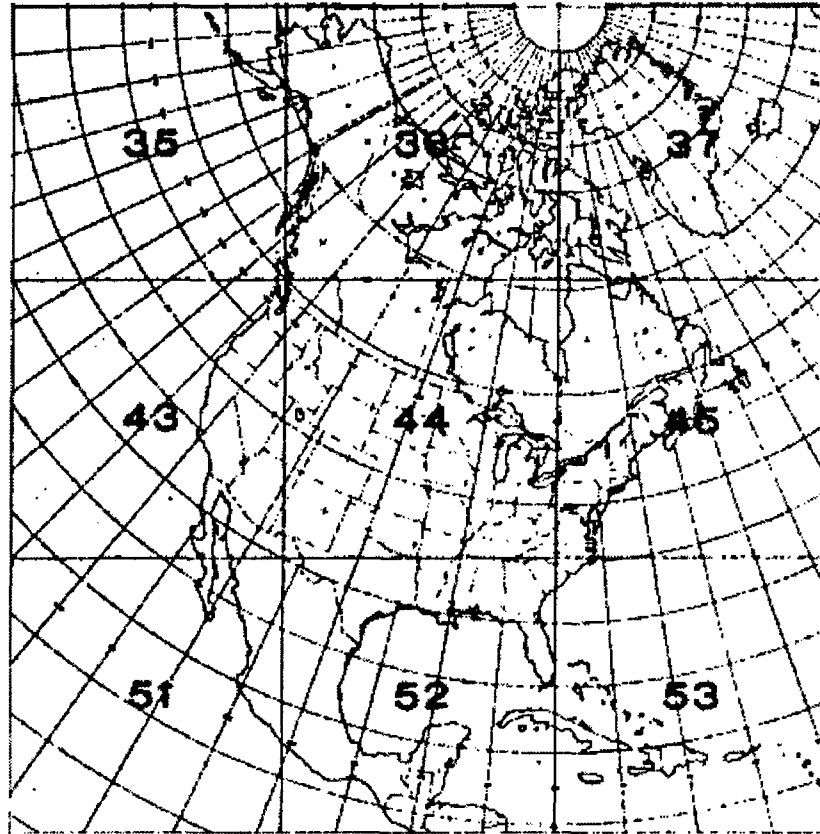


Figure 5: A zoomed view of the 3 x 3 domain of interest used for this study.

The three vertical levels range from the surface to nearly 22,000 m above mean sea level, with a vertical resolution of 30 m between levels below 6,000 m, and 300 m between each level at or above 6,000 m. Once the levels are determined, the cloud-typing processor attempts to distinguish between cumuliform and stratiform clouds. The processor accomplishes this by examining the infrared (IR)-grayshade and visible (VIS) variance. The greater the variance, the more cumuliform the cloud. For example, a cloud type of cumulonimbus is determined when the cloud-top height is greater than 5,486 m (18,000 ft) with a mean IR brightness temperature less than 228 K (Hamill *et al.*, 1992).

The RTNEPH is a global cloud analysis model (Hamill *et al.*, 1992) and has several distinct advantages and improvements over its predecessor (3DNEPH). With the RTNEPH's four

floating cloud layers, each RTNEPH grid point containing cloud cover, geopotential height of the layered cloud bases and tops, diagnostic information, and time of observation, can give greater vertical resolution than the 3DNEPH which provided only 15 fixed layers. If there are more than four cloud layers in the RTNEPH, extra layers will be merged with the closest cloud base. A maximum of eight layers may be merged to fit into the four floating layers. More than eight layers will result in the lowest layer not being counted.

2.3.2 RTNEPH Limitations

The RTNEPH analyses have known problems in data sparse regions where the RTNEPH analysis contains a large percentage of interpolated, or spread data. Spread data is used in areas with few reporting stations which yields large blocks of identical data. These blocks have sharp boundaries that often contrast sharply with adjacent RTNEPH points, based on satellite data or surface observations (USAFETAC/UH-86/001 Rev). Even in North America where the observation network is relatively dense, many RTNEPH reports may include spread data. However, in data sparse regions of the earth, spread data may be used almost exclusively. The use of spread data leads to a more inaccurate and unrepresentative analysis, especially in data sparse regions. The RTNEPH grid points which surround an isolated regularly reporting station contain spread data (Hamill *et al.*, 1992).

Another RTNEPH limitation is its lack of frequent updates of satellite data, especially in tropical regions not revisited as often by the current DMSP or NOAA polar-orbiting satellite (Figure 6).

Another limitation of the RTNEPH is its vulnerability to misidentify clouds and cloud amount. When there is no VIS data available, the RTNEPH has a tendency to miss warm, low stratus clouds as well as to underestimate high, thin cirrus clouds, or falsely place cirrus at lower-than-appropriate elevations. Also, the RTNEPH has problems with the satellite's over- or under-

interpretation of clouds along coastlines due to problems in choosing a representative background temperature to represent the gridpoint during the satellite analysis (Campana, 1995).

The RTNEPH requires a high-quality, VIS-derived and IR-derived surface temperature analysis to determine the background temperature needed for cloud identification. The IR-derived analysis is only from a single channel, and the RTNEPH has been known to mislocate fields through geolocation errors (Neel *et al.*, 1993). The RTNEPH decision algorithm is such that the colder IR data or brighter VIS data, the more likely it is to be cloudy. This is another limitation of the RTNEPH's performance and is especially true since the RTNEPH relies mostly on its IR-derived nephanalysis. An example of this occurs when low stratus clouds develop at night, associated with low-level inversions, or develop over snow and ice or other very cold background scenes. Another limitation of the RTNEPH is small-scale clouds are under-interpreted due to the satellite resolution and the RTNEPH's inability to model cloud thicknesses for latitude or seasonal variation.

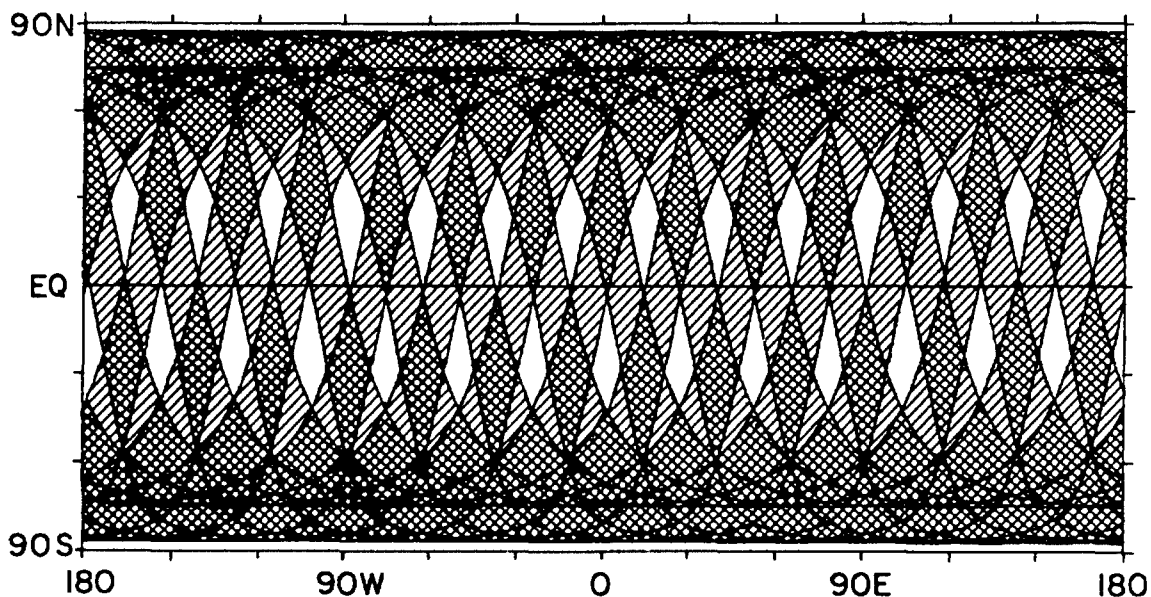


Figure 6: An example of one day's coverage by one sunsynchronous satellite. Clear areas represent no coverage, light shading represents 1 satellite pass, and dark shading represents 2 or more satellite passes in a day. (After Kidder and VonderHaar, 1995).

The RTNEPH also has limitations discriminating cloud vs no cloud. The RTNEPH uses an AFGWC's surface temperature model and water vapor attenuation scheme which also has limitations. This algorithm has a root-mean-square error (RMSE) of approximately 3-4 K in estimating the true IR clear-column temperature (Hamill *et al.*, 1992). The accuracy of RTNEPH's layered cloud amounts is even more suspect, another strong reason for only using RTNEPH's total cloud cover as verification in this study. Unless a point is supplemented with a conventional observation, the RTNEPH has no way of detecting low- and middle-level clouds when there is an obscuring high-level cloud deck, or of assigning an accurate cloud thickness (Hamill *et al.*, 1992). Despite this critical description of the RTNEPH's limitations, it does have many strong characteristics.

2.3.3 RTNEPH Strengths

The RTNEPH has many strengths which make it a very good ground truth measure of the total cloud amount of the atmosphere. The RTNEPH can process a quarter-orbit of satellite data in approximately five minutes, making the RTNEPH processing fast (Neel *et al.*, 1993). Besides the advantages of the manual bogus, other strengths are inherent within the RTNEPH, as discussed in a recent study by Campana (1995). Campana (1995) determined over 80% of the RTNEPH analysis data points were valid within three hours of the synoptic observation time. Also, there were rarely more than two distinct cloud layers (6% of the data had three cloud layers, while 1% of the data had four cloud layers). Incorporating VIS satellite data enhances the quality of the RTNEPH's total cloud cover output (Neel *et al.*, 1993), and thus would make the daytime VIS total cloud analysis even more accurate. Hamill *et al.*, (1992) noted the initial intent of the RTNEPH was to maximize the probability of cloud detection. Hamill did, however, identify a tendency for the RTNEPH to over-estimate clear and overcast (cloudy) situations, while under-estimating partly cloudy situations.

The RTNEPH's performance was studied by Lowther *et al.*, (1991) and the results indicated that seasonal variation plays a significant role in the accuracy of the RTNEPH total cloud-cover analysis. The most accurate analysis was for the summer months. Also, more problems occurred in the polar latitudes due to the RTNEPH's analysis difficulty in separating ice and snow from low-level clouds. The overall results concluded the RTNEPH and surface total cloud-cover reports were in good agreement.

The RTNEPH's relatively high horizontal resolution, bogus, and its inclusion of conventional as well as satellite-derived observations, make it an invaluable analysis tool, especially in data-rich areas. The RTNEPH even updates the background brightness field to ensure no contamination by cloud, snow, or sunglint. For a more detailed discussion of the RTNEPH, the reader is referred to AFGWC/TN-88/001, AFGWC/TN-79/003, and USAFETAC/UH-86/01 (Rev).

2.4 Previous Studies

Phillips Laboratory (PL), accomplished a 30-month study (Nehrkorn *et al.*, 1994) evaluating numerical weather prediction models and cloud forecasts from the Advanced Physics Global Spectral Model. Four separate months of 1989 forecasts were evaluated out to four days (96 hours). Root-mean-square errors (RMSE), mean forecast error, correlation, sharpness, and skill scores of total cloud cover forecasts were evaluated against RTNEPH data. As in the current study, RTNEPH data was used as the true state of the atmosphere in the PL study. A PL modification of the Slingo algorithm was also validated, with results indicating Slingo-derived total cloud forecasts had the largest RMSE of the schemes considered. Persistence forecasts were also used in the PL study for comparison and proved superior to the Slingo forecasts, even out to 36 hours. The reader is referred to the PL study (Nehrkorn *et al.*, 1994) for further discussion of the Slingo algorithm's performance as implemented at PL and the use of

persistence for validation. The only other study which closely resembles the validation performed in this paper is the ongoing study of the RWM by AFGWC.

The AFGWC is documenting the strengths and weaknesses of the RWM for the North American and Asian Windows as of this writing. However, AFGWC has completed preliminary validation for the RWM windows over Europe, Central Africa, and Southeast Europe and the Middle East. Only the RWM European Window will be discussed here. The RWM European Window is similar to the North American Window because of its location in the Northern Hemisphere, its relatively high density of observation data, and its midlatitudes location. The results of the RWM European Window study suggest the RWM forecasts compare favorably with other military models. In addition, the RWM has a positive moisture bias at 700 mb and above. The RWM forecasts retained moisture and did not "rain out" the moisture. This retention of moisture would cause the RWM to underforecast rainfall areas and rainfall accumulation, and overforecast mid- and high-level cloud amount. Relative humidities of more than 75% are usually common throughout the forecast cycle, especially near deep troughs and lows. In summary, the AFGWC study indicates the RWM overforecasts mid- and high-level cloud amounts. One could also infer the model would overforecast low-level clouds based on the RWM European Window study. More detailed information may be found at the Universal Resource Locator (URL) for the AFGWC Home Page at <http://afwin.offutt.af.mil:443/news.html>, as of 27 February 1997, study dated 5 December 1996.

This concludes the background of the models and algorithms used in this study. The next chapter discusses the methodology used to perform the validation.

III. Methodology

3.1 Introduction

This section discusses the steps taken to perform the subjective and objective analysis in this study.

3.2 Scope

This study validates the RWM 00 UTC and 12 UTC total cloud forecasts (expressed in whole percentages of total cloud cover between 0% and 100%, in 1% increments) from selected days in May, June, and July, 1996. The validation days were selected based on the availability of both the RWM forecasts for the 00 UTC and 12 UTC model forecast runs in 6-hour increments and the corresponding RTNEPH analyses.

Matching the corresponding forecast and analysis days and hours required careful planning and programming to ensure the correct days and hours properly matched. For example, the 00 UTC model output of the RWM from any given day had to be matched up to two consecutive RTNEPH days; however, the corresponding 12 UTC RWM output required three days of RTNEPH data (Figure 7). If either the RWM or RTNEPH data were not present, or proved through examination to be corrupt, the data were not used. The RWM 00 UTC forecast required the 0-, 6-, 12-, and 18-hour analyses of the first day of the RTNEPH (refer to Figure 7). Day two of the RTNEPH data consisted of the 0-, 6-, and 12-hour analyses, which corresponded to the 24-, 30- and 36-hour forecasts of the RWM. However, the RWM 12 UTC forecast model run required day one of the RTNEPH's 12- and 18-hour analysis (corresponding to RWM's 0- and 6-hour forecast), day two of the RTNEPH's 0-, 6-, 12-, 18-hour analysis (corresponding to the 12-, 18-, 24-, and 30-hour RWM forecast), and, day three of the RTNEPH's initial (0) hour (corresponding to the RWM's 36-hour forecast).

Forecast Hour:	00	06	12	18	24	30	36
RWM 00Z Forecast:							
Day:	1	1	1	1	2	2	2
RTNEPH Analysis:							
Analysis Hour:	00	06	12	18	00	06	12

Forecast Hour:	00	06	12	18	24	30	36
RWM 12Z Forecast:							
Day:	1	1	2	2	2	2	3
RTNEPH Analysis:							
Analysis Hour:	12	18	00	06	12	18	00

Figure 7: Correctly matching up continuous analysis for each RWM forecast required two or three days of data. The top portion of the figure represents the 00 UTC RWM and the bottom portion of the figure represents the 12 UTC RWM.

3.3 Procedure

This section describes the forecast and analysis products, software, resources, and the fundamental methods used to validate the RWM total cloud forecasts.

3.3.1 Data

The RWM forecast fields and RTNEPH analysis data were compressed and saved by AFGWC on 8 mm tapes. If a day, or a series of days, was not properly copied, or had corrupt data, those days were not used.

3.3.2 Slingo Algorithm

The AFGWC provided the FORTRAN code for their implementation of the Slingo algorithm (Appendix E). The Slingo algorithm was adapted to the specific configuration of the

Air Force Institute of Technology's computing environment and FORTRAN compiler. The algorithm includes the main driver (to forecast clouds from the three-dimensional moisture field within the RWM) for the Slingo cloud diagnosis method. The main driver includes several subroutines which are described below.

The first subroutine initializes block data used by the main driver, while the second subroutine prompts the user for the month, day, and hour of the RWM database. The second subroutine also allows the user to input critical-RH values to be used for the cloud or no-cloud decisions for the low, middle, high, and convective cloud types. In the Slingo implementation of this study, fixed values of the critical parameters were used at AFGWC's request. The next subroutine opens the database pointer file and reads the pointer file information into an array. The fourth and fifth subroutines initialize cloud amounts, bases and tops, and retrieve parameters from the RWM database, respectively. The sixth subroutine extracts a parameter for a given sigma level and forecast hour from the RWM database. The lapse rate in the lowest five sigma layers is determined in the next subroutine. If the lapse rate exceeds a specified threshold, a maximum lapse rate is set and the subroutine returns the maximum lapse rate, its level, and the RH at the specific level. The eighth subroutine takes the RWM parameters on a regular vertical (sigma grid) spacing and interpolates to create an expanded sigma data array. The Slingo subroutine then diagnoses clouds for three layers using the Slingo algorithm (with AFGWC modifications). Following the Slingo subroutine, the next two subroutines spread the three layers of clouds to the appropriate layers and calculate the total cloud given the layer cloud amounts, using the maximum overlap method (refer back to Figure 3). Finally, the last subroutine saves the results to specified data files for importation into PV-WAVE[®]. Refer to Appendix F for the PV-WAVE[®] code used in this study.

Before the Slingo cloud output could be performed, RWM forecasts were stored on disk. The RWM forecast data were stored in one week blocks along with the corresponding RTNEPH data. Once the Slingo algorithm produced its cloud forecast, the results were evaluated using PV-WAVE[®]. The PV-WAVE[®] program was chosen for two reasons. First, AFGWC had initiated the development of a prototype program to perform a validation of the fixed RWM European Window, but the PV-WAVE[®] program was not yet completed. With the successful completion of the PV-WAVE[®] program in this study, AFGWC would then be able to exploit the completed code for further studies, as appropriate. Secondly, PV-WAVE[®] is widely used for analysis of meteorological and environmental data.

The PV-WAVE[®] program performed the physical breakdown of the RWM and RTNEPH domains, which included the grid transformation and nearest-neighbor interpolation (described in Section 3.3.3). Then, PV-WAVE[®] was programmed to build frequency count arrays for later statistical analysis, produce animated images for quality control, and output encapsulated postscript images.

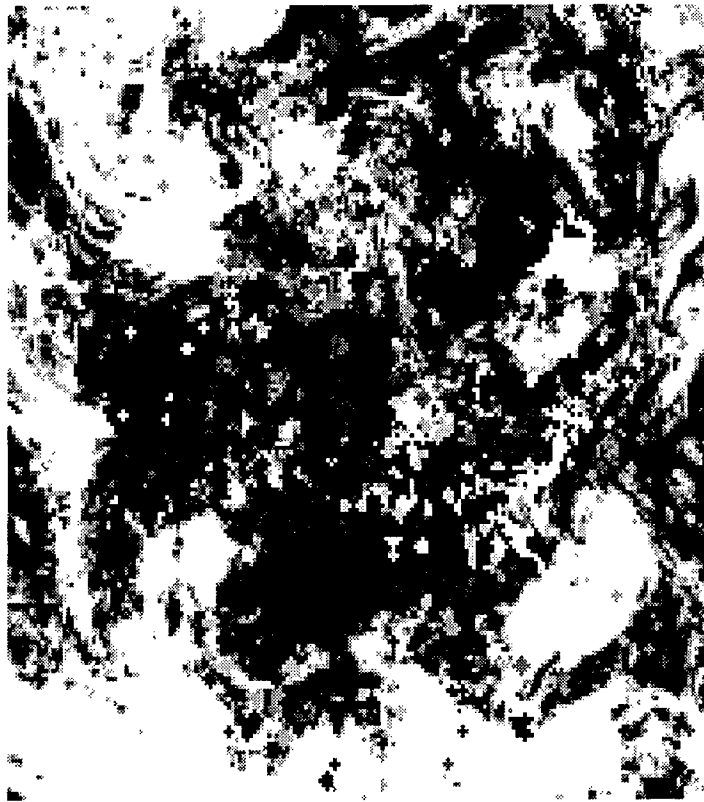


Figure 8: The untrimmed domain of the 3 x 3 RTNEPH boxes (192 x 192 grid points) of RTNEPH data for 1 July 1996 at 00 UTC, showing total cloud (represented from 0% (black) to 100% (white)).

3.3.3 *Grid Transformation and Quality Control*

The domains of the RTNEPH and the RWM had to be correctly matched and the RTNEPH data outside of the RWM window (associated with the larger RTNEPH domain (Figure 8)) had to be discarded. This resulted in a smaller RTNEPH domain consisting of 129 x 129 grid points (Figure 9) which coincided with the size of the RWM window. The RWM total cloud forecasts consisted of three vertical layers within the horizontal domain of the RWM (61 x 61 grid points), while the RTNEPH data consisted of four floating layers, all within a much larger horizontal domain (refer back to Figure 1). To extract RTNEPH data corresponding to the RWM, RTNEPH data in the area of interest (Figure 5) had to be properly removed from the intermediate 9-box domain (192 x 192, as seen in Figure 8). The resulting data was then quality controlled against satellite photos, surface analysis (Appendix G), upper-air charts, and also

against the RWM forecasts to ensure an appropriate match with date and time. The satellite comparison was coarse due to the limited availability of archived GOES data. Archived satellite data (when available) was retrieved for the satellite portion of quality control from the Purdue Weather Home Page at the URL of <http://wxp.atms.purdue.edu/archive.html>, as of 27 February 1997. In addition, RWM initial-hour forecasts were qualitatively compared to satellite imagery and to the corresponding RTNEPH data. This quality control step was also performed for the RWM total cloud forecasts to ensure the data was read properly. In addition, every date/time file header within the RWM and RTNEPH was manually checked for accuracy.

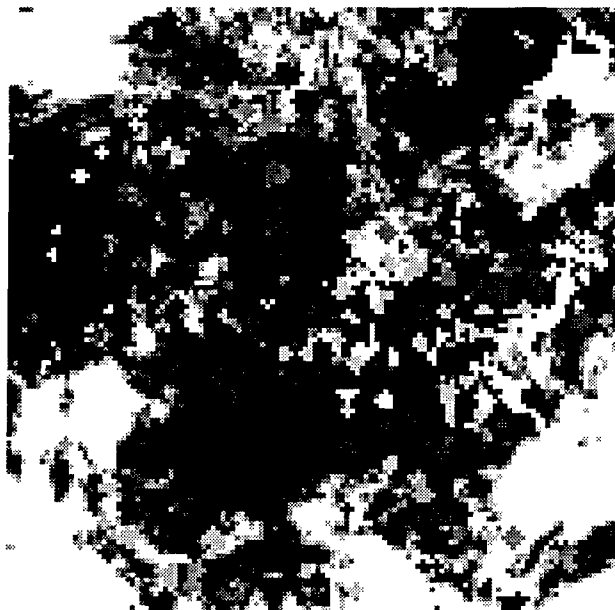


Figure 9: The trimmed RTNEPH for same date and time as Figure 8. Only the corresponding grid points (129 x 129) within the domain of the RWM are used (refer to Figure 1). Window proportions are different from Figure 8; now it covers the same region as the RWM domain.

By trimming the extra grid points, only the corresponding RTNEPH points within the domain of the RWM were used as a comparison against the RTNEPH.

Next, an interpolation was performed to properly match the RWM and RTNEPH grid points. The nearest-neighbor interpolation scheme was used, due to the discrete non-continuous nature of clouds. The higher resolution of the RTNEPH data was interpolated to match the coarser resolution of the RWM data. The interpolation scheme used in this study associated each RWM data point with the nearest RTNEPH data point in each RWM grid volume. This method assumed the RTNEPH data were representative of the entire RWM grid volume at each point. As a result, the RTNEPH data used for validation is lower resolution than the full RTNEPH grid, because it is discretized to match the lower resolution RWM data (Figure 10). Using the nearest-neighbor interpolation scheme avoided the creation of artificial partially cloudy forecast data points between regions of different cloud cover. This is appropriate because clouds are not continuous functions of space. The alternative method of interpolating the RWM forecasts to the RTNEPH analysis, at higher resolution, was determined to be less desirable. This alternative method would increase the RWM's poorer resolution to match the higher resolution of the RTNEPH by creating artificial RWM forecast data. For the above reasons, the RTNEPH data was interpolated to match the coarser resolution of the RWM data.

Additional quality control steps ensured the accuracy of the data analysis process. Images were animated to ensure the data were synoptically realistic. In this step, the seven (0-, 6-, 12-, 18-, 24-, 30-, 36-hour) successive images were visually checked for physical consistency and correctness (refer to Figures 12-18). For example, when viewing the images in an animation, general westerly flow in the mid-latitudes and easterly flow in the low-latitudes can be seen, along with growth and evolution of synoptically defined cloud patterns. While carefully viewing each animation using PV-WAVE[®], arrays of frequency counts were built. These arrays were saved as ASCII files and accounted for every value of cloud increment forecasted or observed,



Figure 10: The RTNEPH data after interpolation with the same data used in Figure 8 and Figure 9. The data is now displayed in the properly arranged 64 x 64 grid points to match the horizontal resolution of the RWM. RTNEPH data now has the same resolution as the RWM as described in the text.

from 0% to 100%, in 1% increments. An example of the 101 x 101 array is depicted in Table 1 for viewing purposes only, with the RWM (forecast) data along the left side (rows) of the array and the RTNEPH (observed) data along the top (columns). Table 1 is binned to 10% increments only to show the format and general appearance of the data; all statistics in this study were calculated using the full 101 x 101 array.

Table 1: An example of the initial RWM forecast array with the initial RTNEPH analysis, after binning from the original 101 x 101 array, to a 10 x 10 array. The rows are represented by the RWM values and the columns are represented by the RTNEPH values. Each array is binned into a 10 x 10 array with each row and column representing 10 data points except the final row and column which contains eleven values due to the odd size of the original array.

		RTNEPH Observed %									
		<u>0-9</u>	<u>10-19</u>	<u>20-29</u>	<u>30-39</u>	<u>40-49</u>	<u>50-59</u>	<u>60-69</u>	<u>70-79</u>	<u>80-89</u>	<u>90-100</u>
R	<u>0-9</u>	1106	99	272	67	63	87	78	239	121	793
W	<u>10-19</u>	17	3	12	2	1	10	1	26	6	84
M	<u>20-29</u>	21	2	13	1	2	2	1	17	2	84
	<u>30-39</u>	12	2	11	0	2	4	3	10	4	58
F	<u>40-49</u>	8	1	7	2	3	2	3	12	5	54
C	<u>50-59</u>	7	0	7	0	0	1	2	7	1	34
S	<u>60-69</u>	9	0	2	2	1	3	2	5	1	31
T	<u>70-79</u>	6	0	2	0	1	0	2	4	1	29
	<u>80-89</u>	0	0	1	0	0	1	1	6	1	23
%	<u>90-100</u>	4	0	6	0	1	1	1	25	3	52

An additional quality check was performed to ensure every array contained the correct number of data points (3,721).

Each of these 101 x 101 arrays were saved as frequency counts of the forecasted and observed occurrence of cloud amounts. In addition to the RWM forecast arrays, a "forecast" of the initial RTNEPH analysis hour was persisted through the analysis period, and its array was also calculated for statistical comparison with the forecast (refer to Table 2 for its binned-equivalent array). The persisted RTNEPH forecast values gave a minimal skill baseline for comparison to the RWM forecast. The persistence arrays were imaged and animated for quality control and qualitative analysis (refer to Figures 29-35). After the arrays were built, each array was imported into Mathcad PLUS 6.0 Professional Edition®, a product of MathSoft, Inc., and the statistical calculations were performed to quantify the results.

Table 2: An example of the initial Persistence “forecast” (rows) against the initial RTNEPH analysis (columns). A diagonal clearly exist, indicating a perfect correlation between the forecast and analysis data. Table format is the same as Table 1. This is an example of the initial (0) hour persistence forecast.

		RTNEPH Observed %									
P		<u>0-9</u>	<u>10-19</u>	<u>20-29</u>	<u>30-39</u>	<u>40-49</u>	<u>50-59</u>	<u>60-69</u>	<u>70-79</u>	<u>80-89</u>	<u>90-100</u>
E											
R	<u>0-9</u>	1190	0	0	0	0	0	0	0	0	0
S	<u>10-19</u>	0	107	0	0	0	0	0	0	0	0
I	<u>20-29</u>	0	0	333	0	0	0	0	0	0	0
S	<u>30-39</u>	0	0	0	74	0	0	0	0	0	0
T	<u>40-49</u>	0	0	0	0	74	0	0	0	0	0
E	<u>50-59</u>	0	0	0	0	0	111	0	0	0	0
N	<u>60-69</u>	0	0	0	0	0	0	94	0	0	0
C	<u>70-79</u>	0	0	0	0	0	0	0	351	0	0
E	<u>80-89</u>	0	0	0	0	0	0	0	0	145	0
	<u>90-100</u>	0	0	0	0	0	0	0	0	0	1242
%											

3.3.4 Validation Statistics

Statistics were calculated, using the Mathcad® software mentioned previously, to quantify Slingo’s performance within the RWM. As a reference state, the RWM’s performance was also compared to a persisted RTNEPH initial analysis.

In order to determine the bias of the model, the mean error (ME) was computed using the following formula:

$$ME \equiv \frac{\sum_{A=0}^{MA} \sum_{B=0}^{MB} ARRAY_{A,B} \cdot (A - B)}{3721}, \quad (9)$$

where A represents the rows and B represents the columns. The terms MA and MB represent the maximum values of the rows and columns, respectively, and ARRAY represents the 101 x 101 array. The number 3721 represents the number of counts in each 101 x 101 array used for the calculations.

A mean error score can reveal problems in a parameterization scheme which creates consistent errors in one direction. If the trend of the bias is known, a forecaster can account for that error when forecasting.

Three scalar measures of forecast accuracy were calculated: mean absolute error (MAE), mean square error (MSE), and root mean square error (RMSE). The three scalar measures of forecast accuracy were computed using the formulas:

$$MAE \equiv \frac{\sum_{A=0}^{MA} \sum_{B=0}^{MB} |ARRAY_{A,B} \cdot (A - B)|}{3721}, \quad (10)$$

$$MSE \equiv \frac{\sum_{A=0}^{MA} \sum_{B=0}^{MB} ARRAY_{A,B} \cdot (A - B)^2}{3721}, \quad (11)$$

and

$$RMSE \equiv \sqrt{MSE}. \quad (12)$$

These are the three best known scalar measures of forecast accuracy (Wilks, 1995) and are used in other studies including the PL study (Nehrkorn *et al.*, 1994). The scalar measure of RMSE does not reveal any information about a models bias; however, RMSE does provide an indication of the typical magnitude of the errors in a forecast. The RMSE does this without the canceling effects of regional positive and negative errors which would make the mean error misleading.

Another method of determining the model's forecast accuracy is by calculating the hit rate, or percentage forecast correct (PFC). This value is obtained by calculating the number of occurrences along the main diagonal and dividing by the total frequency count within the 101 x 101 array (3,721 points).

The PFC is defined as:

$$PFC \equiv \frac{\sum_A^{MA} ARRAY_{A,A}}{3721} \quad (13)$$

Calculating PFC using only 1% binning which counted forecasts as incorrect which were only off by 1%, is a very stringent test of a model's performance. However, this PFC value can be used as a benchmark for other, more precise forecast models during future studies. A significant number of 0% forecasted and 0% observed (referred to as (0,0)) values matched. This matching of the (0,0) points made the RWM's PFC unrealistically accurate; Table 1 shows a clearly defined diagonal is not present. The PFC was calculated with and without the (0,0) data point to quantify this reliance of PFC on the (0,0) point.

To account for the stringent method of determining the PFC, an alternate method was used to determine the PFC. This alternate method took the same approach (with and without the (0,0) array point), but used more forecast and observation bins by widening the diagonal to include the diagonal and five adjacent diagonals either side of the main diagonal, known as the $PFC \pm 5$. Increasing the number of bins for calculation of accuracy was done to roughly compare the quantitative value of the $PFC \pm 5$ with the two arrays and their diagonals which were calculated for each chosen forecast day and hour.

An additional measure of the model's forecast accuracy is its "sharpness." Sharpness identifies how often forecasts of extremes (clear or cloudy) are made, rather than forecast of the average. Sharpness was calculated using an adapted version of the USAF Trapnell (1992) 20/20 score. In this study, the 20/20 score quantifies the percentage of forecasts that are within 20% of either clear (<20% or from 0-19% inclusive) or cloudy (>80% or from 81-100% inclusive). The 20/20 score can be used to identify whether the forecast model gave forecasts with sharpness comparable to the analysis.

As another measure of accuracy, a Brier Score was calculated. Perfect forecasts have a Brier Score equal to zero, and a forecast with no accuracy has a Brier Score of one. The Brier Score is essentially the mean-square error of the probability forecasts (Wilks, 1995). The Brier Score averages the squared differences between pairs of forecast probabilities. From the 101 x 101 array, a probability mass function (a vector of probabilities) and a joint probability matrix is built for the calculation of this statistic.

In order to determine the linear relationship between the forecasted and observed values, the Pearson Correlation Coefficient (Devore, 1995) was computed. As an additional check for correlation, and comparison with the Pearson Correlation Coefficient, the Cramer Statistic was also computed (Wilks, 1995). The Cramer Statistic values range from zero (no correlation) to one (perfect correlation). However, to achieve a perfect score of one, the values must be on the diagonal and equally distributed, along the diagonal. A Cramer Statistic of one will only be achieved when all of the values (forecasted and observed) on the diagonal are the same.

To determine if any dependence existed between the RWM total cloud forecast and the RTNEPH analysis data, a Chi-square ($\chi^2_{\alpha,v}$, referred to as χ^2) test was used, as described in Appendix H. Results of the χ^2 test are also briefly shown in Appendix H.

Two additional skill scores were computed for the RWM forecasts. The first skill score compared RWM MSE against the MSE of persistence, and the second skill score compared the Brier Score of the RWM against the Brier Score of persistence. The skill score quantifies the degree of skill of a set of RWM forecasts, expressed with reference to the RTNEPH analysis and persistence (Wilks, 1995).

This concludes the methodology of the study. The next chapter shows the images, scatter plots, box and whisker plots, and descriptive statistics in tabular form for a representative validation day (1 July 1996). The next chapter also shows the RWM and persistence statistics

for all cases, and RWM and persistence statistics for all cases and all times (cumulative statistics).

IV. Results

4.1 RWM Validation for 1 July 1996

This section discusses the validation of the RWM total cloud forecast for 00 UTC on 1 July 1996.

4.1.1 RWM Images

This section presents the forecast images of the RWM total cloud forecast and the associated RTNEPH analyses (Figures 11-18). The images are in sequential order of the forecast (initial (0) hour through 36 hours). RWM performance on this day was representative of other days examined.

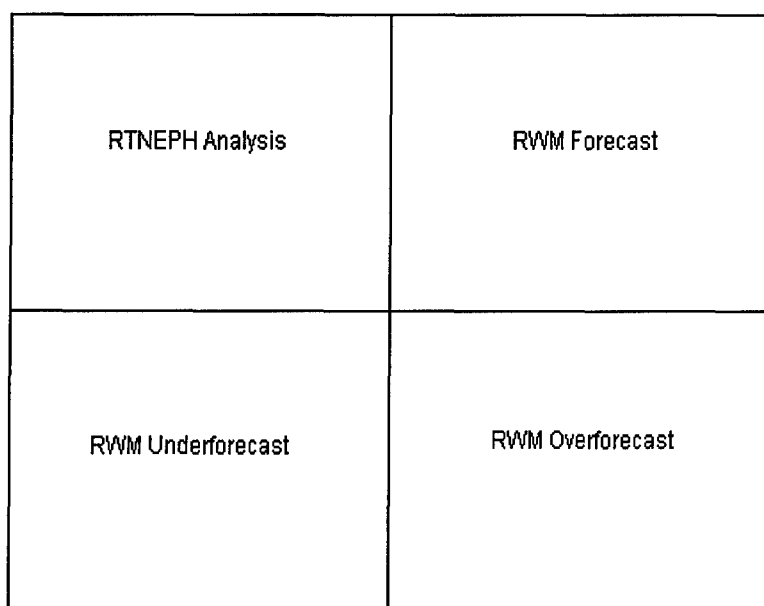


Figure 11: The top-right box represents the RWM forecast with the pixel values converted to bytescales. The magnitude of the individual pixel brightness represents percent of cloud occurrence. A value of zero is represented by a black pixel with brightness of zero, while a value of 100 is represented by a white pixel with brightness of 255. The top-left box represents the RTNEPH analysis for the corresponding time as the RWM forecast. The bottom-left box represents the amount and relative location of RWM total cloud underforecast, and the bottom-right box represents the amount and relative location of RWM total cloud overforecast. For the bottom two boxes, the brighter and more numerous the pixels, the more incorrect the forecast.

The images in this section were developed using PV-WAVE[®] and allow for an easy qualitative validation of the RWM. Underforecast is defined as the calculated positive difference in bytescale between the RTNEPH and RWM (RTNEPH minus RWM), and overforecast is defined as the negative difference in bytescale between the RTNEPH and RWM. The 0-hour RWM forecast (Figure 12), shows nearly complete absence of overforecast total clouds. The lack of clouds in the RWM forecast at 0 hours shows the poor quality of the initial RWM moisture data. The RWM forecast lacks the summertime convection which is often present and is seen in the RTNEPH analysis.

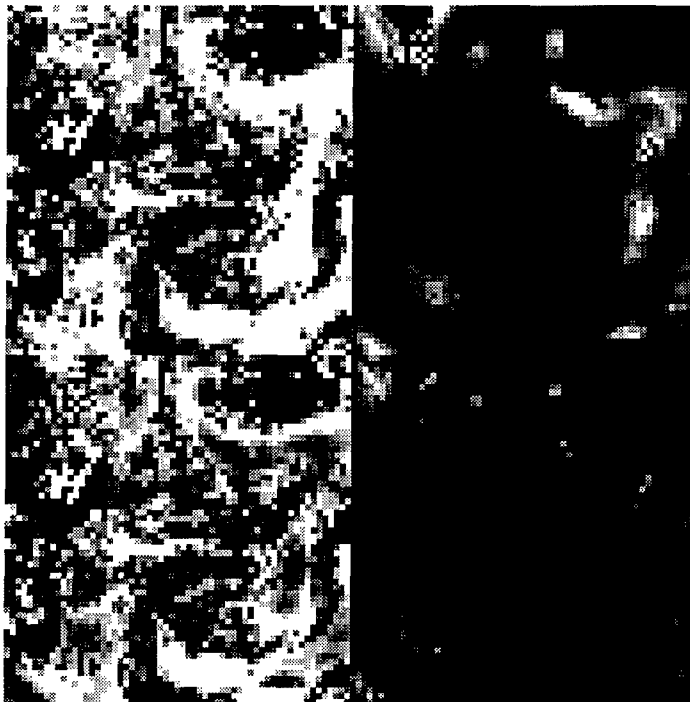


Figure 12: As Figure 11, for the initial (0) hour RWM forecast. The bottom-right box shows nearly complete absence of overforecast total clouds. Lack of clouds in the upper-right box shows the poor quality of initial RWM moisture data. The initial RWM field lacks convection, which can be seen in the upper-left box of the RTNEPH analysis.

Figure 13 shows a significant increase in RWM total cloud forecast from the initial (0) hour as the RWM moisture begins to increase.

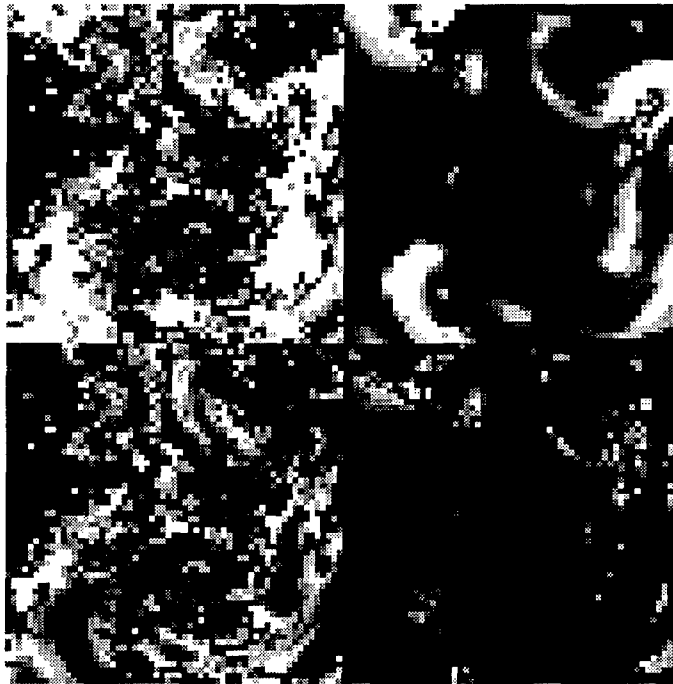


Figure 13: As Figure 11, for the 6-hour RWM forecast. There is a significant increase in total clouds from the initial hour as the RWM moisture begins to increase in the forecast model.

Figure 14 shows a continued increase in the RWM total cloud forecast at 12 hours. The RWM is predominately underforecasting total clouds. Small organized bands of clouds now appear overforecasted. The upper-right panel shows the RWM beginning to capture the general synoptic-scale cloudiness of the RTNEPH (except for the absence of convection).



Figure 14: As Figure 11, for the 12-hour RWM forecast.

Figure 15 shows the 18-hour forecast of the RWM and the corresponding RTNEPH analysis. The improved resolution of the RTNEPH is clear in these pictures. The regions of RWM underforecast nearly match the RTNEPH analysis. The underforecast also shows where much of the convection is located.



Figure 15: As Figure 11, for the 18-hour RWM forecast. The overforecast areas continue to increase, while the underforecast areas continue to remain relatively high.

Figure 16 shows the 24-hour forecast of the RWM. The underforecast image is, again, nearly identical to the RTNEPH image. Also, comparable total cloud synoptic patterns can be seen when comparing the top two images. This was another quality control step implemented during the study to ensure the data matched correctly.



Figure 16: As Figure 11, for the 24-hour RWM forecast.

Figure 17 shows the 30-hour forecast of the RWM. Organized areas of the RWM cloudiness match the RTNEPH analysis. This can also be seen by looking at the underforecast or overforecast images in the bottom-left and bottom-right boxes.



Figure 17: As Figure 11, for the 30-hour RWM forecast. The same general synoptic structure can be seen in both RWM and RTNEPH. Organized areas of the RWM forecast show clearly defined clear and cloudy areas. Although some areas within the images appear to have no cloud, a closer look at the data showed there are clouds with low coverage (very low brightness). For example, a cloud pixel with a 5% coverage will show up as a faint gray pixel (bytescale of approximately 25), which is barely visible.

Figure 18 shows the 36-hour forecast of the RWM. Fairly organized areas of overforecast clouds (bottom-right box) are seen. Bands of underforecast or overforecast cloudiness appear where the phase of the RWM forecast is faster or slower than the RTNEPH.



Figure 18: As Figure 11, for the 36-hour RWM forecast. Regions of organized underforecast and overforecast total clouds indicate the forecast is too slow or too fast.

4.1.2 RWM Total Cloud Forecast Statistics

This section provides statistical results for the RWM 00 UTC total cloud forecast for 1 July 1996. All plots in this section are scatter plots.

Table 3 is a key to interpret the other tables in this chapter. The tables within this section correspond to scatterplots, and display descriptive statistics for the plotted values.

Table 3: Statistical measures and abbreviations defined for the other tables in this section. Each table is a quantitative summary of its respective figure.

<u>Name of forecast method, analysis method or statistic used</u>	
N	Number of forecast and observation periods
MEAN	Average (mean) value of respective plot
SD	Standard Deviation of respective plot
MINIMUM	Minimum value of respective plot
MEDIAN	Median value of respective plot
MAXIMUM	Maximum value of respective plot

Figure 19 and Table 4 show the RWM mean error for 1 July 1996.

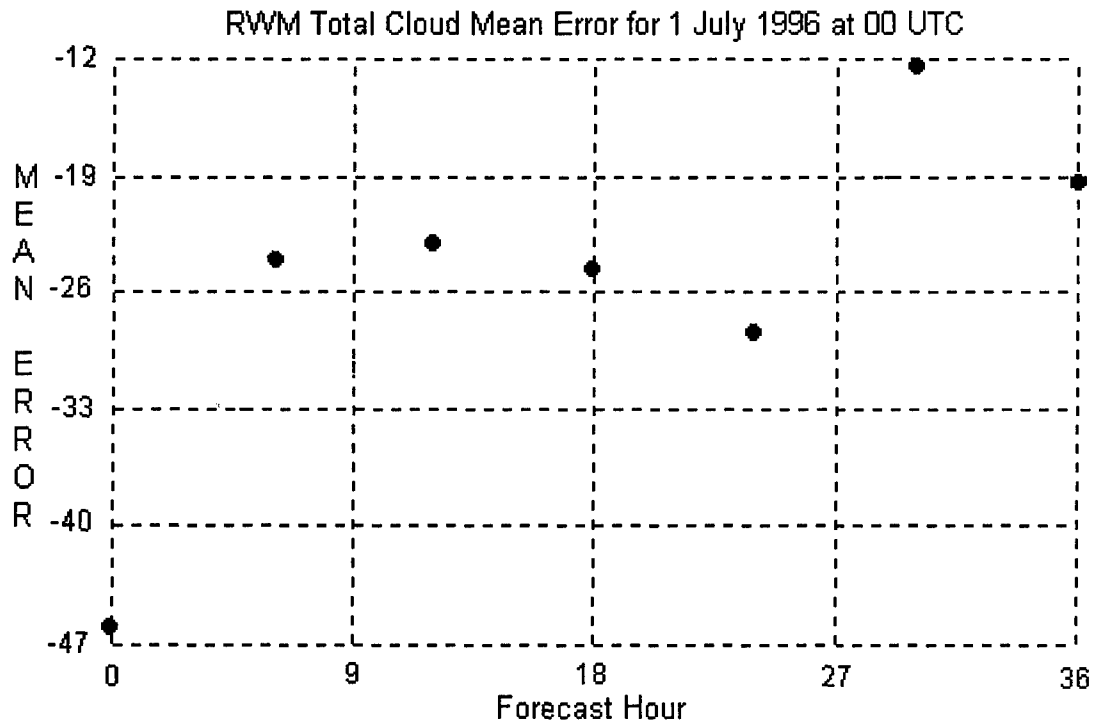


Figure 19: The RWM 00 UTC mean error scatter plot. Mean error value is steadily decreasing (improving). This indicates a negative bias throughout this forecast with a tendency to improve over time. Removing the initial (0) hour shows the tendency to slightly improve over time. Notice a big improvement between the 0- and 6-hour forecasts, with a slower change afterwards. The negative mean error value indicates the model's tendency to underforecast total clouds through the 36-hour period. For descriptive statistics, refer to Table 4.

Table 4: Descriptive statistics for Figure 19 for the RWM 00 UTC model forecast for 1 July 1996. The overall mean and median are negative.

<u>RWM Mean Error</u>	
N	7
MEAN	-25.450
SD	10.338
MINIMUM	-45.960
MEDIAN	-24.080
MAXIMUM	-12.600

Figure 20 and Table 5 show the RWM RMSE for 1 July 1996.

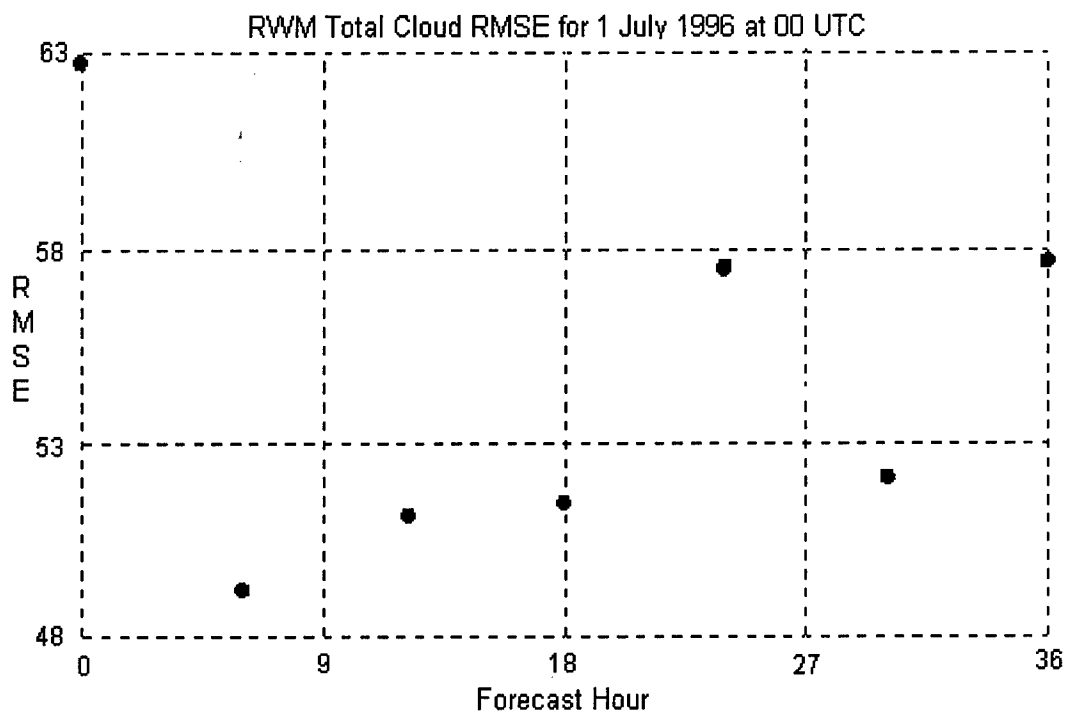


Figure 20: RWM total cloud forecast RMSE for 1 July 1996 at 00 UTC. The trend suggests slow improvement of the RWM forecast over time; however, the initial (0) hour of the RWM is so poor the trend of the RMSE values without the initial (0) hour (Figure 21) shows the forecast RMSE increases with time. For descriptive statistics, refer to Table 5 .

Table 5: Descriptive statistics for Figure 20 for RWM 00 UTC 1 July 1996 forecast.

<u>RWM RMSE</u>	
N	7
MEAN	54.567
SD	4.8431
MINIMUM	49.230
MEDIAN	52.170
MAXIMUM	62.700

Figure 21 shows the RWM RMSE for 1 July 1996 without the initial (0) hour.

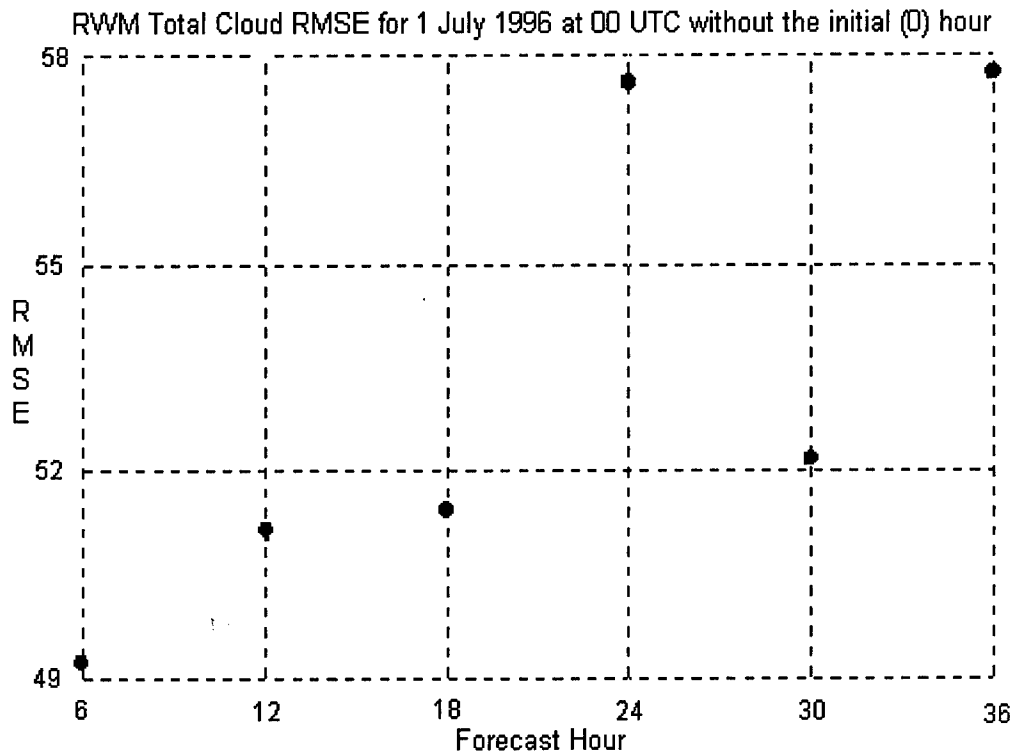


Figure 21: RWM total cloud forecast RMSE without the initial (0) hour. Without the initial hour, the scatter plot clearly shows a decrease in forecast performance through time. Refer to Table 5 for descriptive statistics.

Figure 22 and Table 6 show the RWM 0-19 score for 1 July 1996.

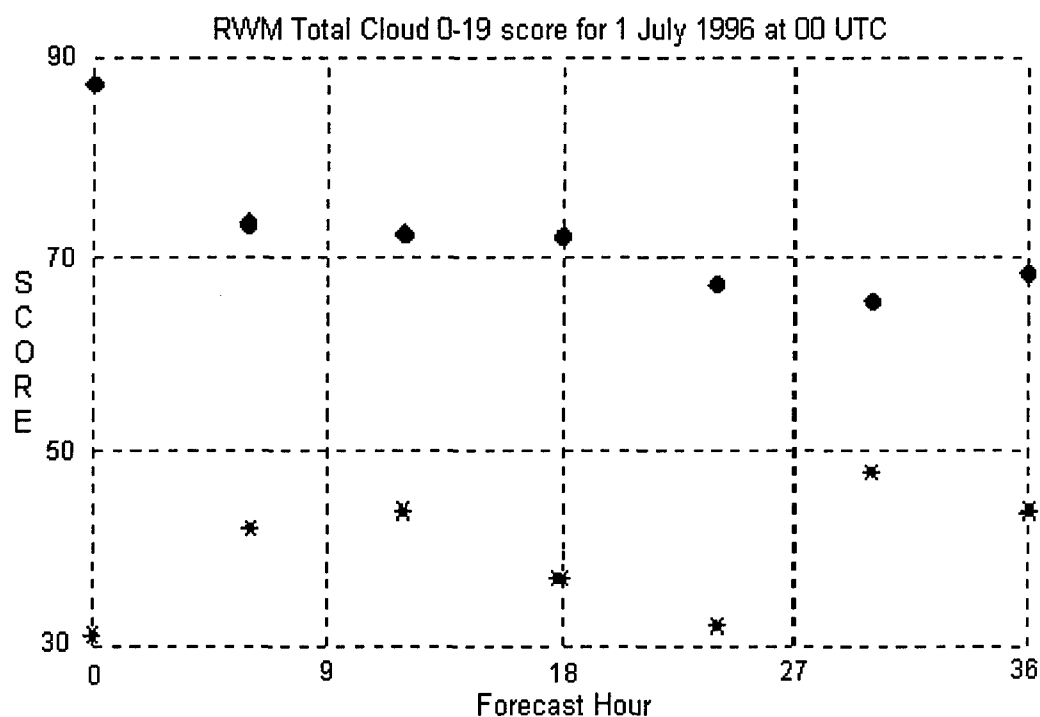


Figure 22: RWM total cloud forecast 0-19 score. Black dots depict RWM 0-19% clear forecast decreasing over time and asterisks depict RTNEPH. The 30-hour RWM forecast appears to be the closest to the true state of the RTNEPH 0-19 score. This plot, along with the values in Table 6 below, clearly shows the RWM overforecasts the clear (0-19) condition through 36 hours. Refer to Table 6 for descriptive statistics.

Table 6: Descriptive statistics for Figure 22. The statistics show the significant overforecast of clear conditions by the RWM.

	<u>0-19 score (clear)</u>	
	<u>RWM</u>	<u>RTNEPH</u>
N	7	7
MEAN	70.857	39.286
SD	7.3582	6.3170
MINIMUM	64.000	31.000
MEDIAN	71.000	41.000
MAXIMUM	86.000	47.000

Figure 23 and Table 7 show the RWM 81-100 score for 1 July 1996.

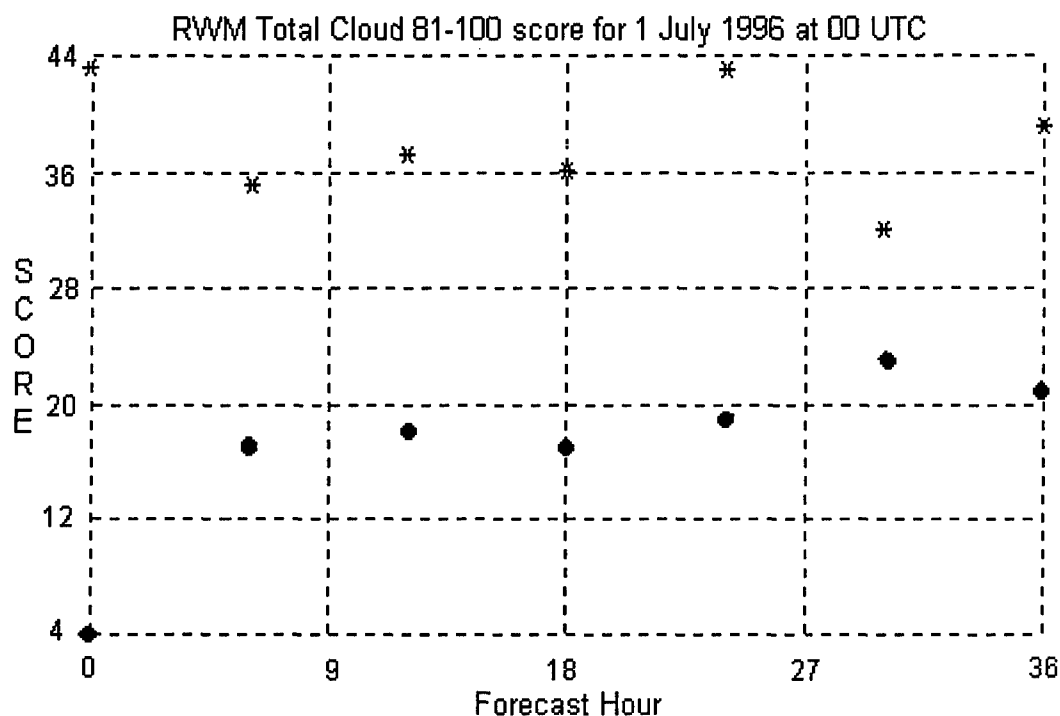


Figure 23: RWM 81-100 score (cloudy). Black dots show RWM 81-100% total cloud forecast, and asterisks show RTNEPH 81-100% total cloud analysis. As with Figure 22, the 30-hour forecast is the closest forecast to the true state. This plot indicates the RWM significantly underforecasts cloudy conditions with respect to the RTNEPH and shows moisture spin-up through 36 hours relatively steady after the 6-hour forecast. The RTNEPH analysis shows relatively little change. Refer to Table 7 for descriptive statistics.

Table 7: Descriptive statistics for Figure 23. This table shows the RWM underforecast cloudy conditions with a mean and median less than half of the RTNEPH.

	<u>81-100 score (cloudy)</u>	
	<u>RWM</u>	<u>RTNEPH</u>
N	7	7
MEAN	17.000	37.857
SD	6.1373	4.0999
MINIMUM	4.0000	32.000
MEDIAN	18.000	37.000
MAXIMUM	23.000	43.000

Figure 24 and Table 8 show the RWM PFC with and without point (0,0) for 1 July 1996.

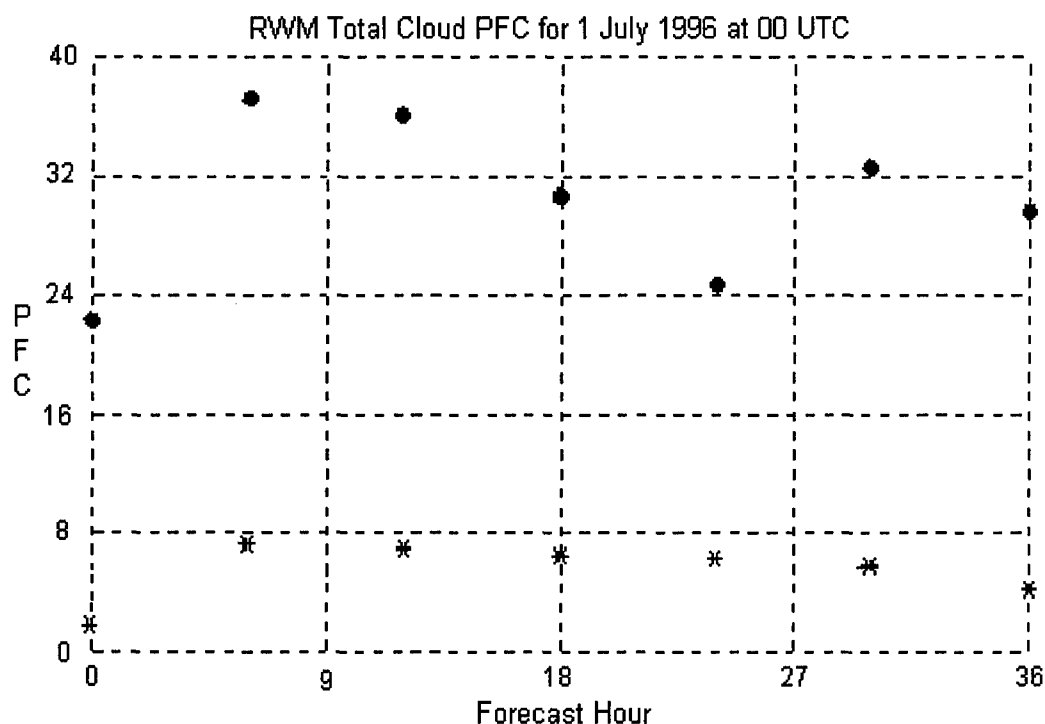


Figure 24: RWM PFC with and without point (0,0). Black dots represent the RWM total cloud forecast with point (0,0), while the asterisks represent the RWM total cloud forecast without point (0,0). The percentage forecast correct without the (0,0) point is very poor. For descriptive statistics, refer to Table 8.

Table 8: Descriptive statistics for Figure 24. Without the (0,0) point, the forecasts are very poor.

	<u>RWM PFC with and without point (0,0)</u>	
	<u>With (0,0)</u>	<u>Without (0,0)</u>
N	7	7
MEAN	30.376	5.4257
SD	5.4449	1.9822
MINIMUM	22.410	1.5600
MEDIAN	30.420	6.2100
MAXIMUM	37.030	7.3100

Figure 25 and Table 9 show the RWM PFC ± 5 with and without point (0,0) for 1 July 1996.

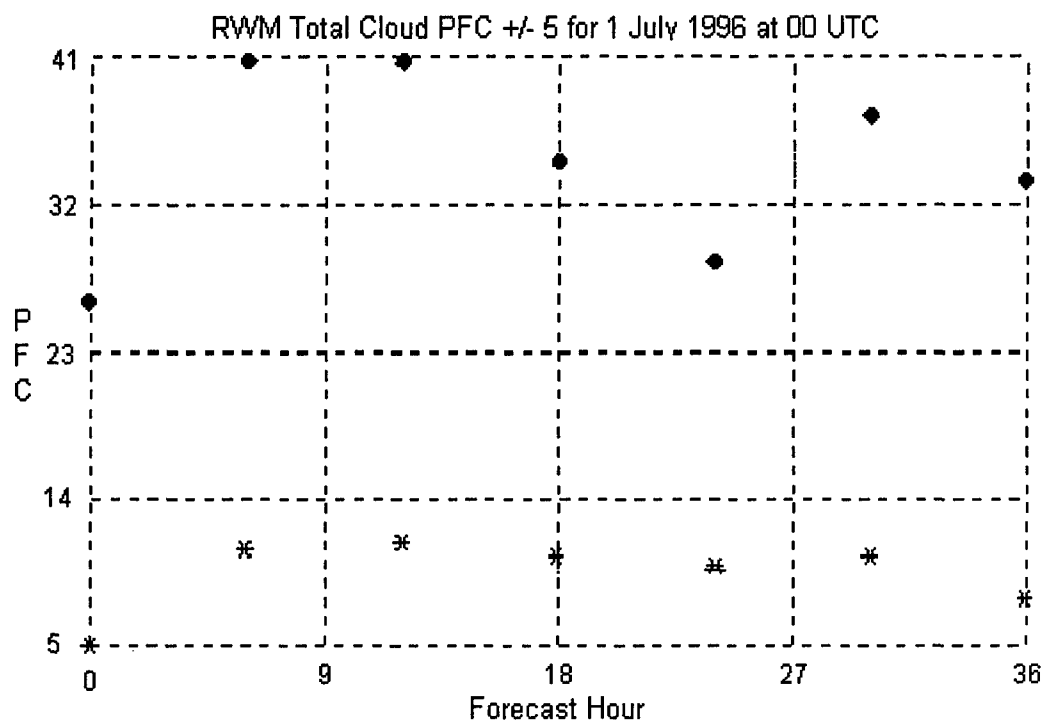


Figure 25: As Figure 24, except for PFC ± 5 with and without point (0,0). Without the point (0,0), the PFC is still poor, with a mean of less than 10% correct. For descriptive statistics, refer to Table 9.

Table 9: Descriptive statistics for Figure 25. Without the (0,0) point, the forecast would still have low PFC scores.

RWM PFC ± 5 with and without point (0,0)

	<u>With (0,0)</u>	<u>Without (0,0)</u>
N	7	7
MEAN	34.380	9.4286
SD	5.6757	2.2179
MINIMUM	25.910	5.0500
MEDIAN	34.480	10.350
MAXIMUM	40.550	11.340

Figure 26 and Table 10 show the Pearson Correlation Coefficient of the RWM against RTNEPH for 1 July 1996.

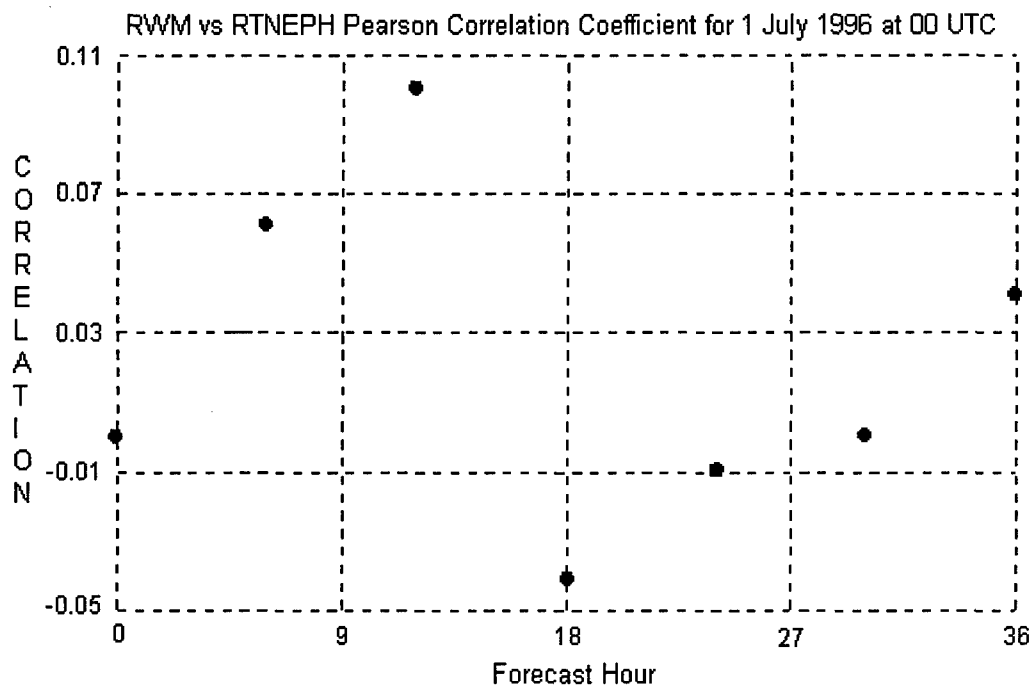


Figure 26: The RWM vs RTNEPH Pearson correlation coefficient for 1 July 1996 at 00 UTC. For descriptive statistics, refer to Table 10. Almost no correlation exists between the RWM and the RTNEPH.

Table 10: Descriptive statistics for Figure 26.

<u>RWM vs RTNEPH Pearson Correlation Coefficient</u>	
N	7
MEAN	0.0214
SD	0.0478
MINIMUM	-0.0400
MEDIAN	0.0000
MAXIMUM	0.1000

Figure 27 and Table 11 show the skill scores of the RWM MSE with respect to persistence MSE and the RWM Brier Score with respect to persistence Brier Score for 1 July 1996.

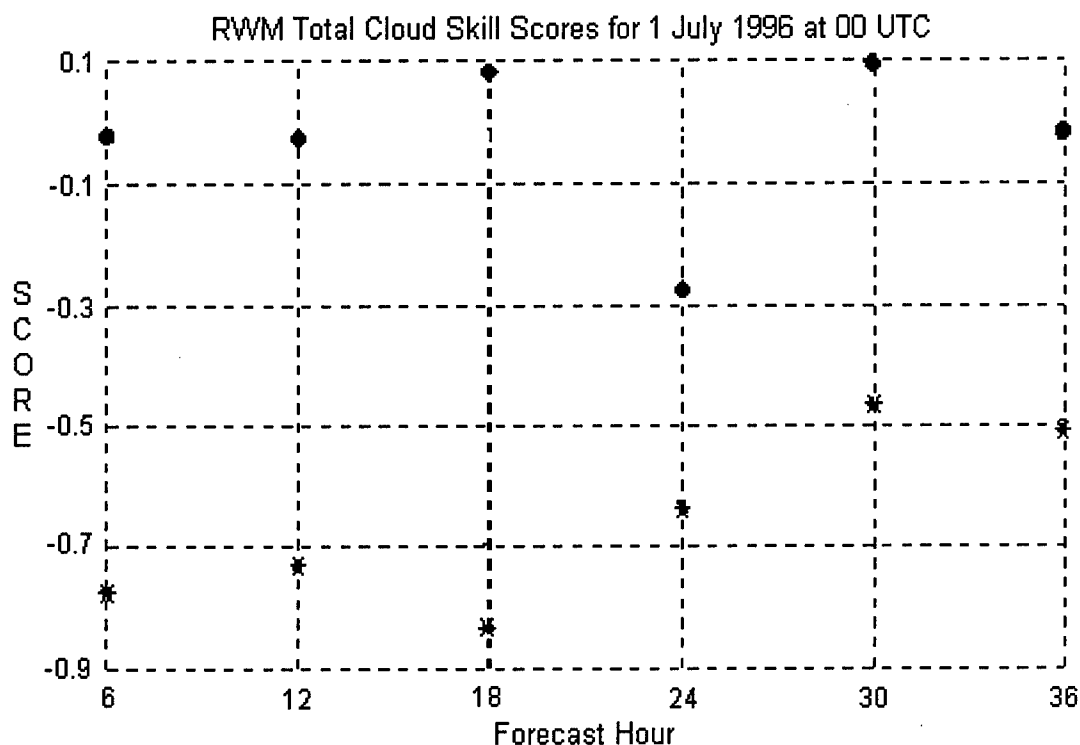


Figure 27: Skill scores of the RWM MSE with respect to persistence MSE and the skill score of RWM Brier Score with respect to persistence Brier Score. Black dots show RWM skill compared to persistence. The skill score is mostly negative, with no significant change through time. The asterisks show the RWM skill score with respect to Brier Score. RWM forecast skill is negative, indicating overall poor skill scores but skill improving over time. For descriptive statistics, refer to Table 11.

Table 11: Descriptive statistics for Figure 27. The initial (0) hour is not shown.

	<u>RWM Skill Score with respect to:</u>	
	<u>Persistence</u>	<u>Brier</u>
N	6	6
MEAN	-0.0283	-0.6600
SD	0.1298	0.1464
MINIMUM	-0.2700	-0.8300
MEDIAN	-0.0200	-0.6850
MAXIMUM	0.0900	-0.4700

4.2 Persistence Validation for 1 July 1996.

4.2.1 Persistence Images

This section presents the images of the RTNEPH persistence 00 UTC "forecast" for 1 July 1996. The images are in sequential order of their "forecast."

RTNEPH Analysis	Persisted RTNEPH "forecast"
Persistence Underforecast	Persistence Overforecast

Figure 28: As Figure 11, except top-right box represents the persisted initial (0) hour RTNEPH forecast.

The images in this section were developed using PV-WAVE[®] and allow for an easy qualitative assessment of the persistence forecast. Figure 29 shows the complete absence of underforecast and overforecast total clouds at the initial (0) hour.



Figure 29: As Figure 28, for the initial (0) hour of persistence “forecast.” Underforecast and overforecast, bottom left and bottom right, are empty because the “forecast” is perfect.

Figure 30 shows a rapid change from the initial (0) hour. The bottom two images show nearly evenly distributed forecast errors with no large regions of either under or overforecast total clouds. This suggests there are not large, organized areas of persisted data.



Figure 30: As Figure 28, this figure represents the 6-hour persistence "forecast." The qualitative underforecast and overforecast of persistence images. The two bottom images in this figure show nearly equal amount of error with the error fairly evenly distributed. There are no large regions of persisted data in the RTNEPH analysis; if there were, there would be large black areas.

Figure 31 depicts fairly even distribution of areas underforecast and overforecast total clouds for the 12-hour period.



Figure 31: As Figure 28. This figure represents the 12-hour persistence "forecast."

Figure 32 shows no large organized areas of persisted data for the 18-hour period.



Figure 32: As Figure 28, for the 18-hour persistence "forecast."

Figure 33 depicts the 24-hour persistence.



Figure 33: As Figure 28, for the 24-hour persistence "forecast."

Figure 34 shows the 30-hour persistence.



Figure 34: As Figure 28, for the 30-hour persistence "forecast."

Figure 35 shows the 36-hour persistence forecast.



Figure 35: As Figure 28, for the 36-hour persistence “forecast.”

4.2.2 Persistence Statistics

This section provides the statistical calculations and plots for the persistence 00 UTC “forecasts” for 1 July 1996. All plots in this section are scatter plots and the results are representative of results for persistence forecast of the other cases studied.

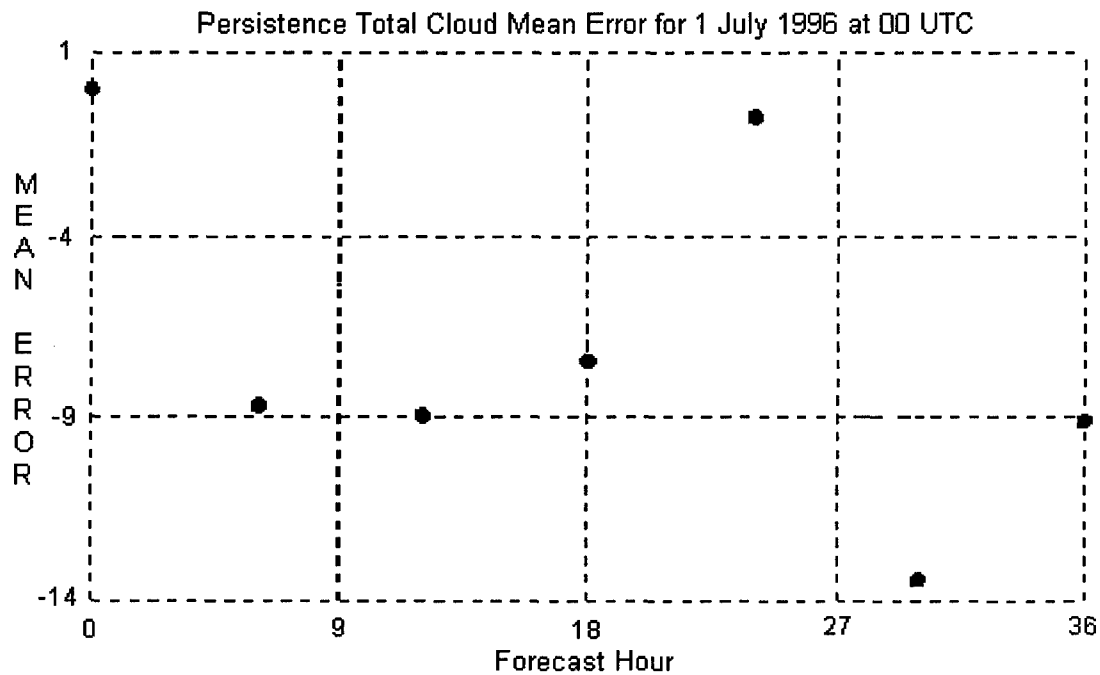


Figure 36: Persistence mean error is perfect at the initial hour, by definition. With the exception of the 24-hour “forecast,” persistence mean error decreases throughout the forecast period, indicating the “forecast” is becoming poorer. For descriptive statistics, refer to Table 12.

Table 12: Descriptive statistics for Figure 36.

Persistence Mean Error	
N	7
MEAN	-6.9271
SD	4.8298
MINIMUM	-13.480
MEDIAN	-8.6700
MAXIMUM	0.0000

Figure 37 shows the persistence RMSE for 1 July 1996.

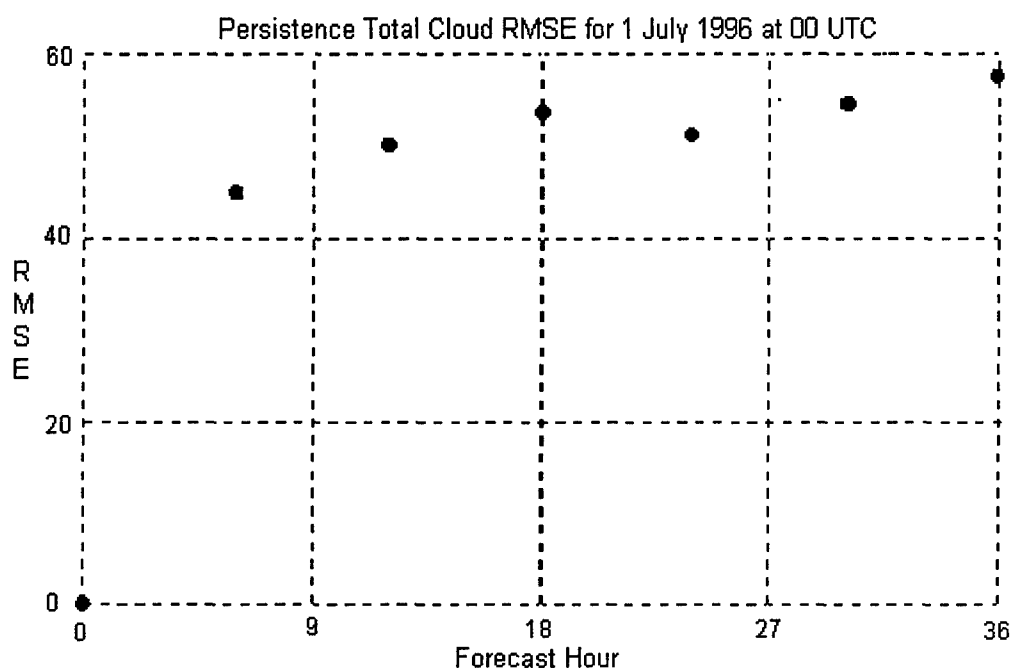


Figure 37: The initial (0) hour has a RMSE of zero, by definition. The RMSE increases rapidly over time, then remains relatively steady. Based on these results, persistence accuracy decreases over time. Without the initial (0) hour (Figure 38, next page), persistence forecasts show a gradual decrease in accuracy over time. For descriptive statistics, refer to Table 13.

Table 13: Descriptive statistics for Figure 37 and Figure 38.

<u>Persistence RMSE</u>	
N	7
MEAN	44.547
SD	20.024
MINIMUM	0.0000
MEDIAN	51.010
MAXIMUM	57.240

Figure 38 shows the persistence RMSE for 1 July 1996 without the initial (0) hour.

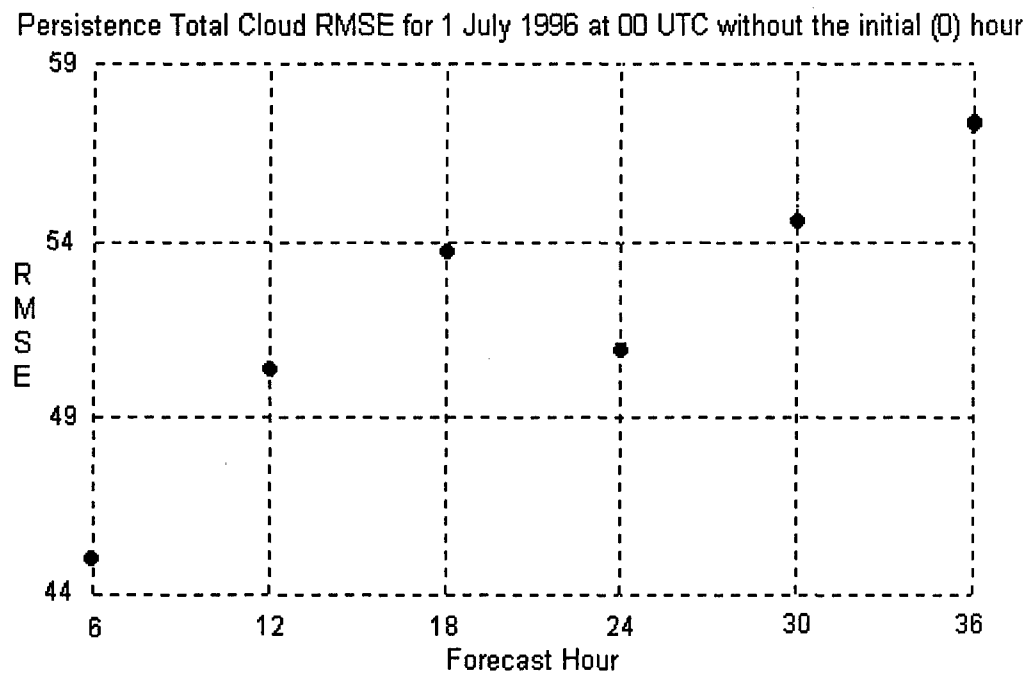


Figure 38: Same as Figure 37, without the initial (0) hour. This scatter plot now clearly shows a decrease in performance through time. For descriptive statistics, refer back to Table 13.

Figure 39 shows the persistence 0-19 score for 1 July 1996.

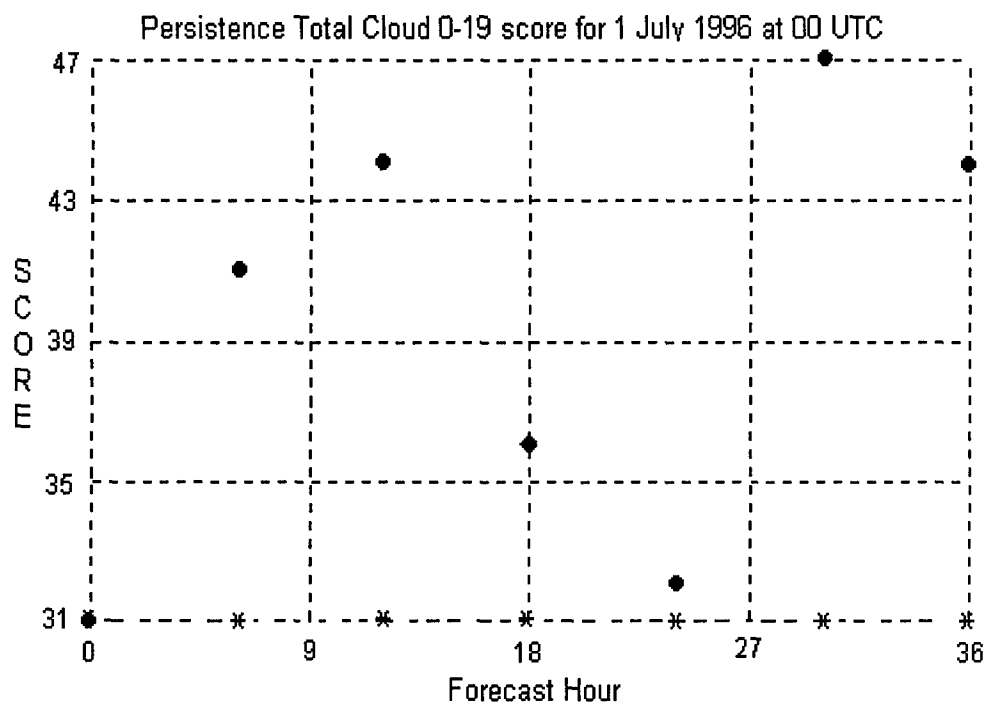


Figure 39: Persistence 0-19 score asterisks indicate persistence 0-19% cloud forecast remains the same over time against the RTNEPH (black dots). The best (perfect) score occurs at the initial (0) hour where they are both the same. The near match of the 24-hour forecast is an indication of the diurnal tendency in the persistence forecast. The RTNEPH 0-19 score is not constant, which indicates the lack of persistence in RTNEPH. For descriptive statistics, refer to Table 14.

Table 14: Descriptive statistics for Figure 39.

	<u>0-19 score (clear)</u>	
	<u>RTNEPH</u>	<u>Persistence</u>
N	7	7
MEAN	39.286	31.000
SD	6.3170	0.0000
MINIMUM	31.000	31.000
MEDIAN	41.000	31.000
MAXIMUM	47.000	31.000

Figure 40 shows the persistence 81-100 score for 1 July 1996.

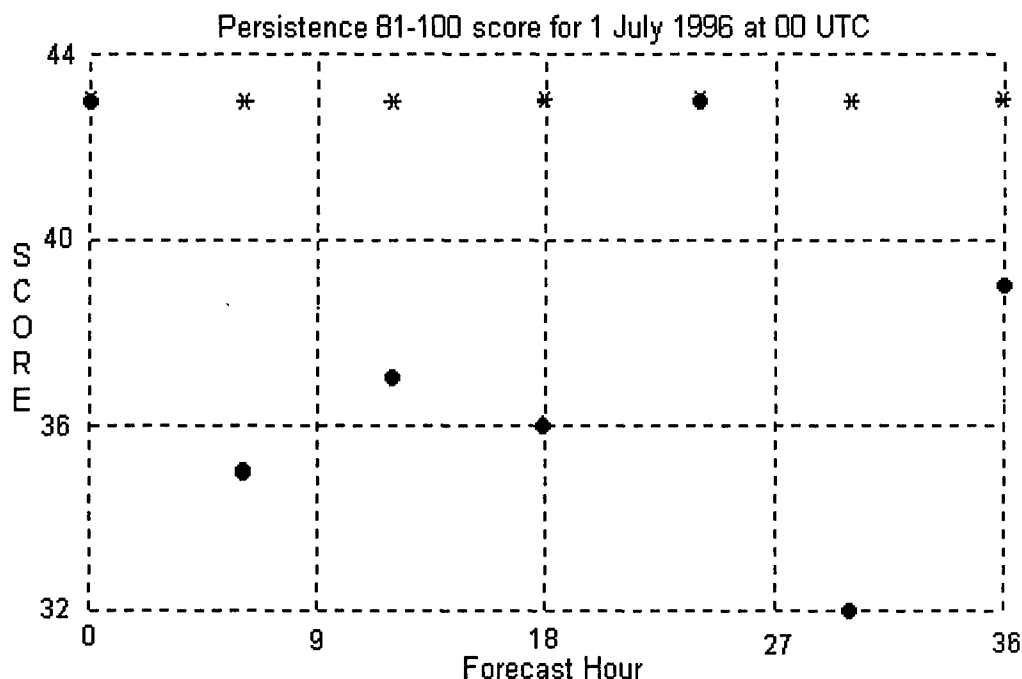


Figure 40: As Figure 39, except this figure shows the 81-100 score for persistence. The persistence 81-100 values, represented by asterisks, remain steady over time against the RTNEPH analysis. As in Figure 39, the 24-hour persistence for the 81-100% occurrence for total cloud is also similar. For descriptive statistics, refer to Table 15.

Table 15: Descriptive statistics for Figure 40.

	<u>81-100 score (cloudy)</u>	
	<u>RTNEPH</u>	<u>Persistence</u>
N	7	7
MEAN	37.857	43.000
SD	4.0999	0.0000
MINIMUM	32.000	43.000
MEDIAN	37.000	43.000
MAXIMUM	43.000	43.000

Figure 41 shows the persistence PFC with and without point (0,0) for 1 July 1996.

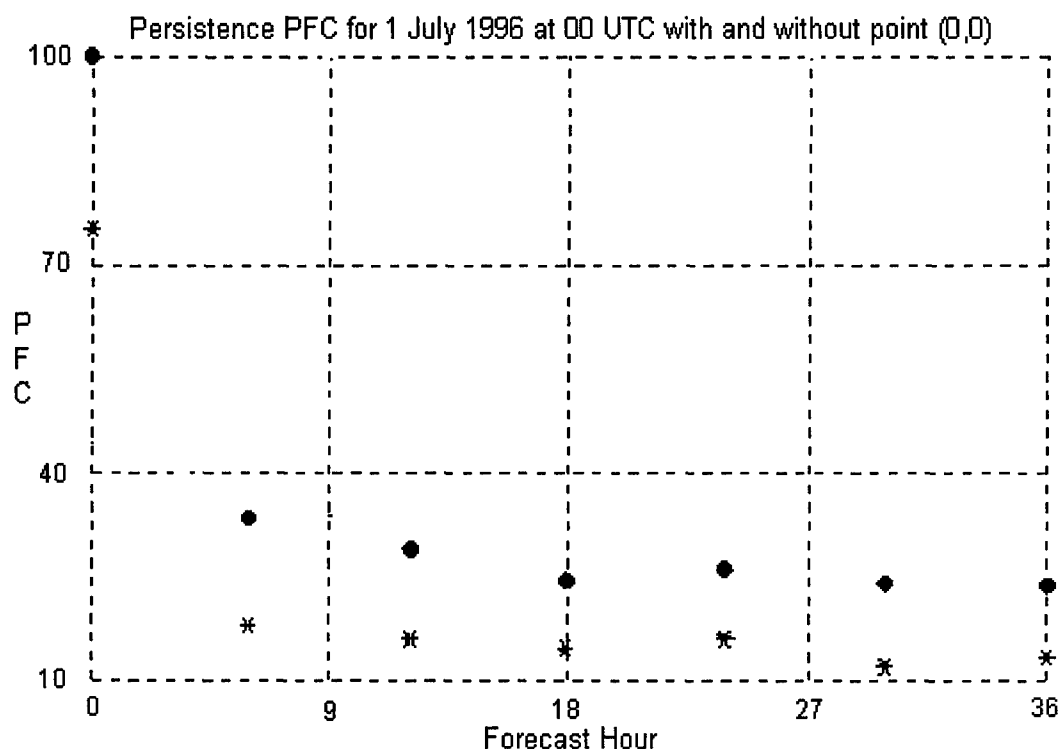


Figure 41: Black dots represent the persistence PFC with point (0,0), and the asterisks represent the persistence PFC without point (0,0). Without the initial (0) hour, the remaining points change little with time. For descriptive statistics, refer to Table 16.

Table 16: Descriptive statistics for Figure 41 and Figure 42. Even without the (0,0) point, persistence performs relatively well.

	<u>Persistence PFC</u>	
	<u>With (0,0)</u>	<u>Without (0,0)</u>
N	7	7
MEAN	37.290	23.456
SD	27.855	22.815
MINIMUM	23.860	11.800
MEDIAN	26.180	15.610
MAXIMUM	100.00	75.000

Figure 42 shows the persistence PFC with and without point (0,0) for 1 July 1996.

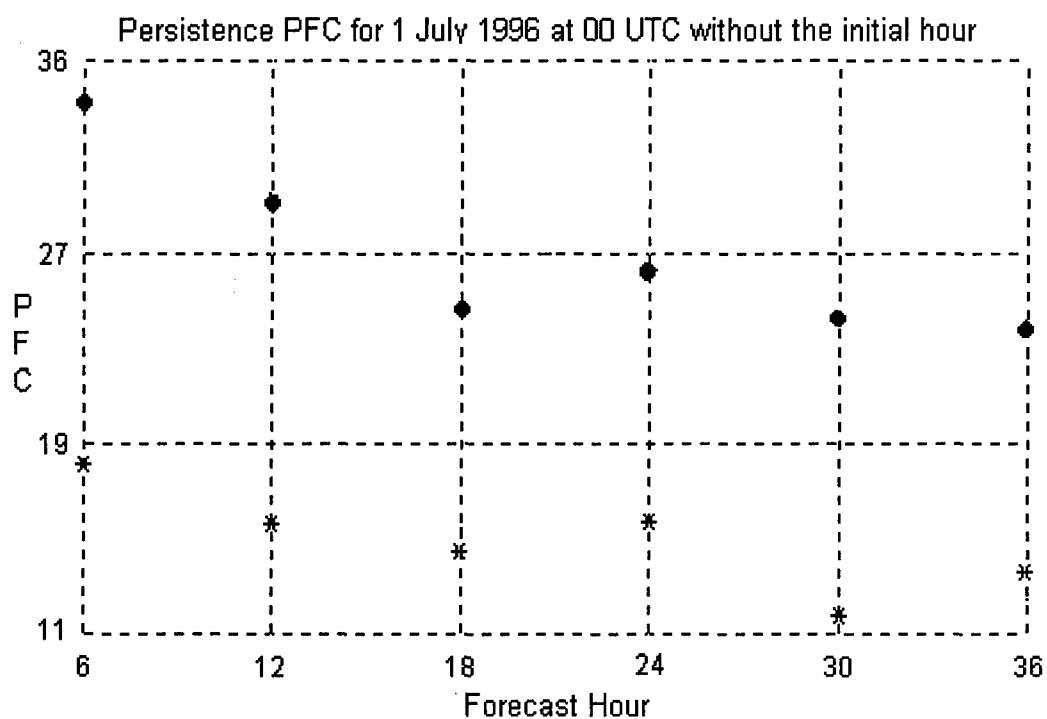


Figure 42: As Figure 41, except this figure shows persistence without the initial (0) hour. The persistence accuracy decreases through the forecast period. The persistence “forecast” performs consistently better than the RWM. For descriptive statistics, refer back to Table 16.

Figure 43 shows the persistence PFC ± 5 for 1 July 1996.

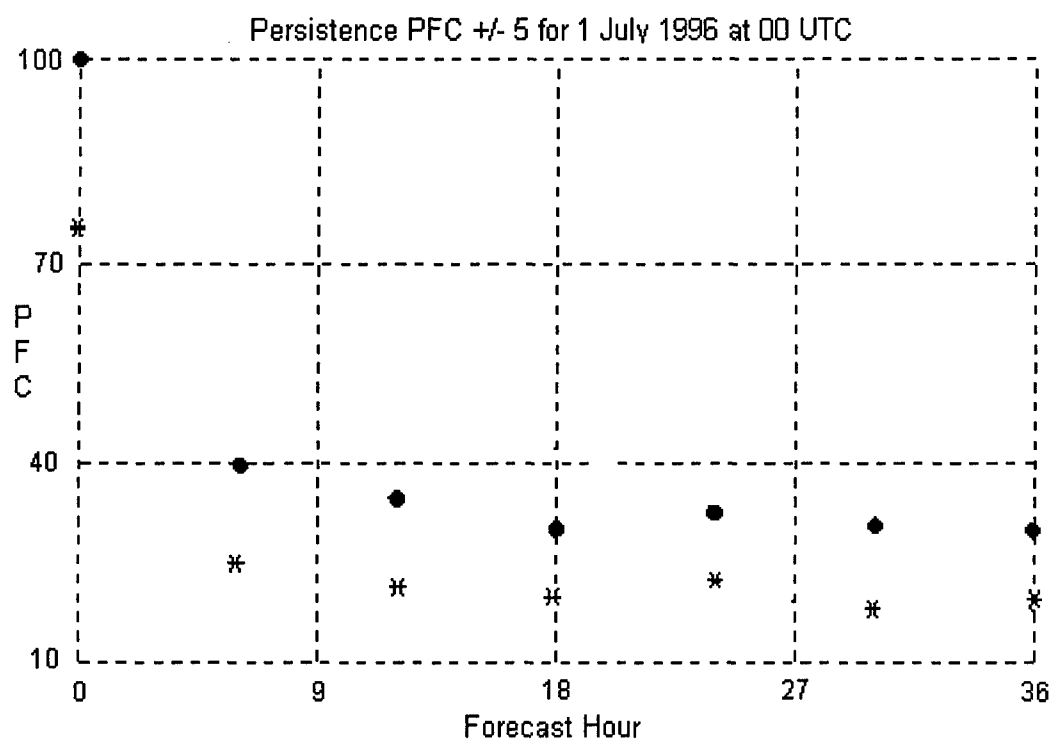


Figure 43: As Figure 41, except persistence PFC ± 5 with point (0,0) is represented by black dots, the persistence PFC ± 5 without point (0,0) is represented by asterisks. Without the initial (0) hour, the remaining points are similar. For descriptive statistics, refer to Table 17.

Table 17: Descriptive statistics for Figure 43 and Figure 44.

<u>PFC ± 5 with and without point (0,0)</u>		
	<u>Persistence with (0,0)</u>	<u>Persistence without (0,0)</u>
N	7	7
MEAN	42.313	28.480
SD	25.691	20.635
MINIMUM	29.430	17.740
MEDIAN	32.790	21.100
MAXIMUM	100.00	75.000

Figure 44 shows the persistence PFC ± 5 with and without point (0,0) for 1 July 1996.

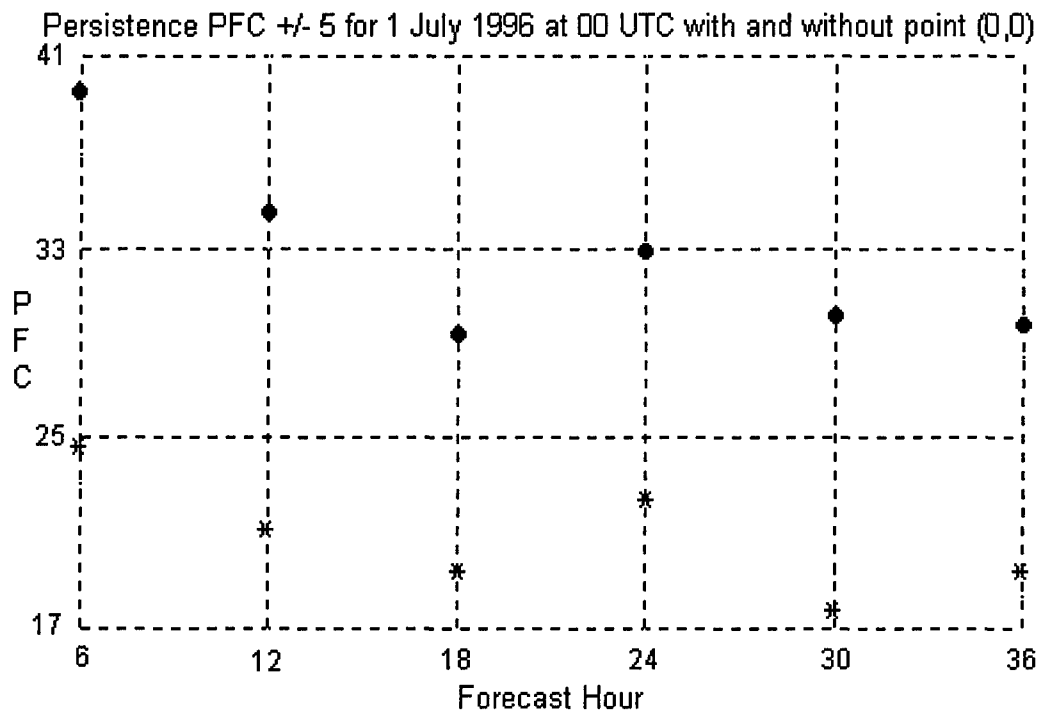


Figure 44: As Figure 43, except this figure shows persistence PFC ± 5 without the initial (0) hour. Persistence performs much better than the RWM. The performance does decrease through time, as would be expected. For descriptive statistics, refer back to Table 17.

Figure 45 shows the persistence Pearson Correlation Coefficient for 1 July 1996.

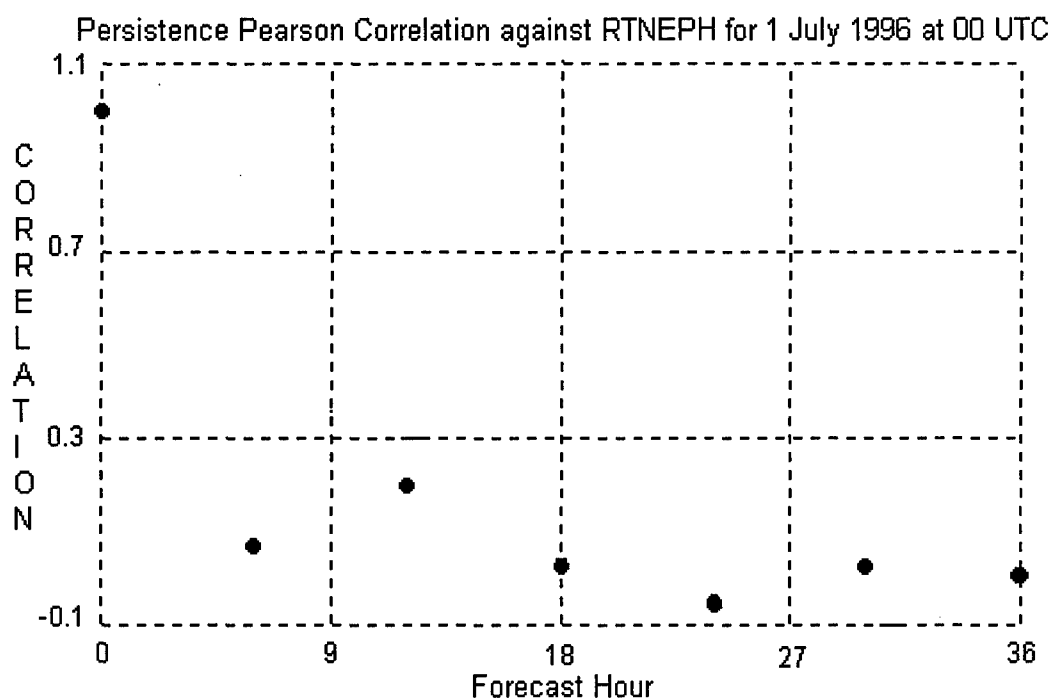


Figure 45: The Pearson Correlation Coefficient for persistence against RTNEPH. The mean correlation is just larger than zero except for the initial (0) hour. The persistence forecasts and RTNEPH analyses are poorly correlated. Relatively low correlation at 6 hours suggests many of the RTNEPH grid points are refreshed within 6 hours over the North American Window. For descriptive statistics, refer to Table 18.

Table 18: Descriptive statistics for Figure 45.

<u>Persistence vs RTNEPH Pearson Correlation Coefficient</u>	
N	7
MEAN	0.1814
SD	0.3693
MINIMUM	-0.0500
MEDIAN	0.0300
MAXIMUM	1.0000

4.3 RWM and Persistence Statistics for All Cases

This section presents cumulative statistics of each forecast hour and displays the results with box and whisker plots. Each forecast hour is represented by a box and two whiskers. The box encloses the middle half of the data, with the median represented by the horizontal line near the middle of each box. The vertical lines at the top and the bottom of the box are called whiskers, and they indicate the range of "typical" data values. Whiskers always end at the value of an actual data point and are not longer than $1\frac{1}{2}$ times the size of the box. Extreme values are displayed as "*" for possible outliers, and "o" for probable outliers. Possible outliers are values that are outside the box boundaries by more than $1\frac{1}{2}$ times the size of the box. Probable outliers are values that are outside the box boundaries by more than 3 times the size of the box.

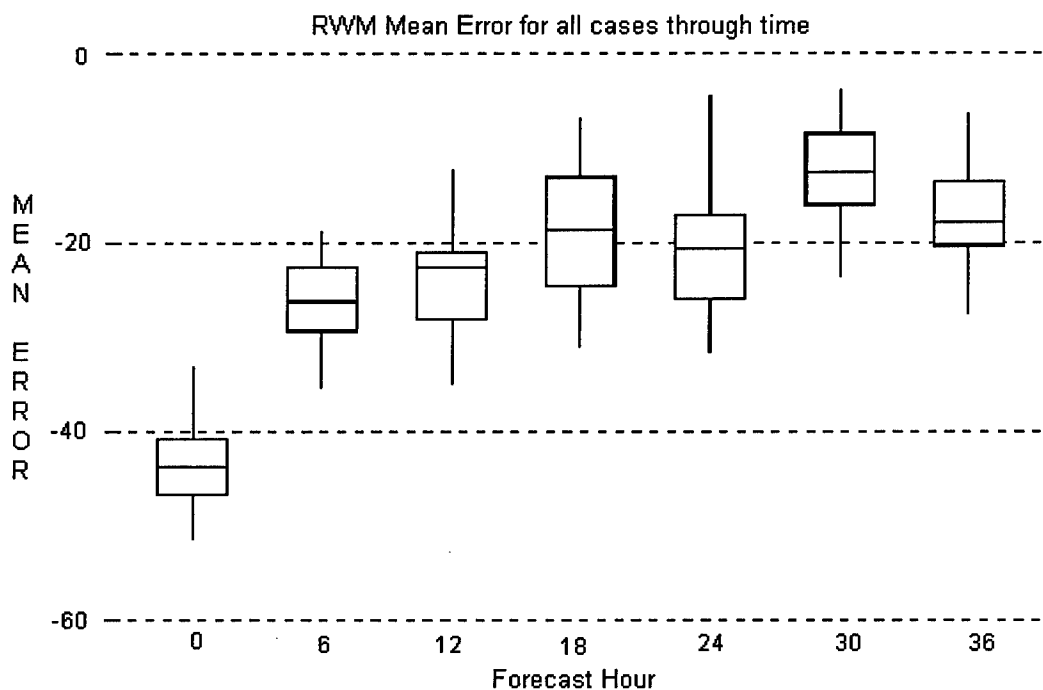


Figure 46: This plot shows a negative bias (underforecast of total clouds) through the entire forecast period. The RWM does show significant improvement over the first 6 hours with gradual improvement until the 36-hour forecast. A mean error of zero indicates a perfect forecast with respect to the RTNEPH. For descriptive statistics, refer to Table 19, next page.

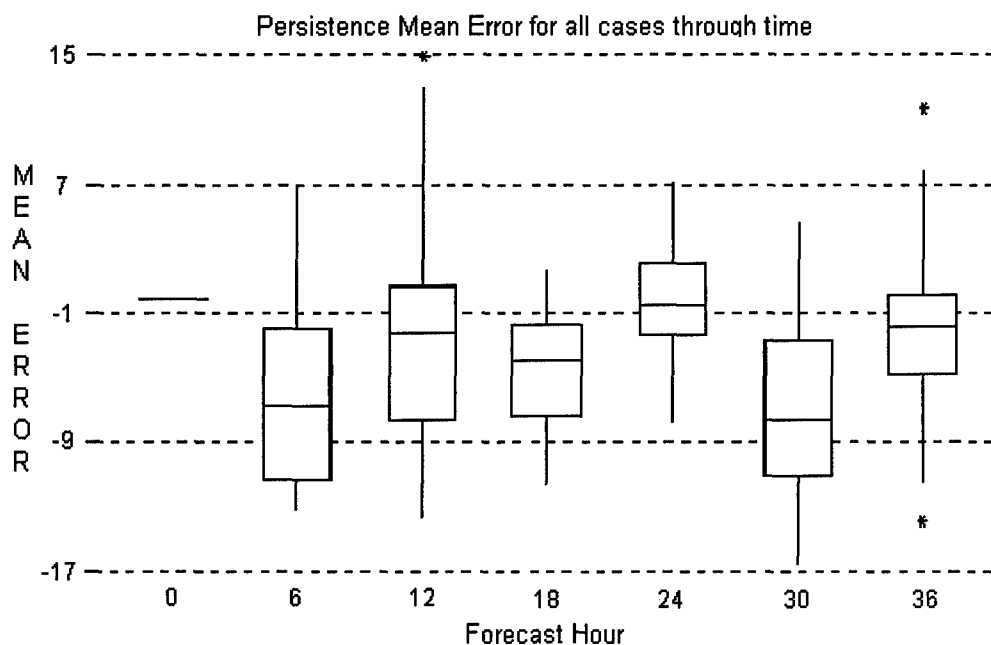


Figure 47: Persistence has a small negative bias tendency through time. However, the 24-hour persisted RTNEPH has a median bias of near zero. This can be expected with diurnal convective cloud changes during the late spring and early summer. For descriptive statistics, refer to Table 19.

Table 19: Descriptive statistics for Figures 46 and 47.

	<u>Mean Error</u>	
	<u>RWM</u>	<u>Persistence</u>
N	147	147
MEAN	-23.178	-3.3913
SD	10.876	5.9070
MINIMUM	-51.200	-16.440
MEDIAN	-21.210	-2.4900
MAXIMUM	-4.1000	14.810

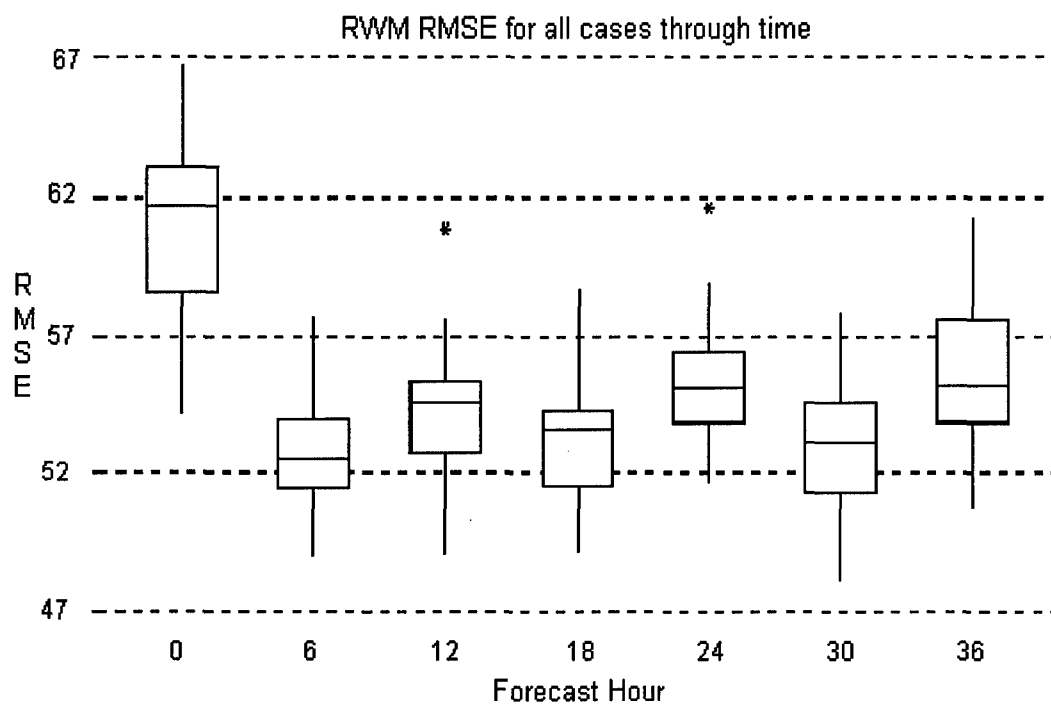


Figure 48: The RWM RMSE indicates the initial (0) hour is very inaccurate. The RWM total cloud forecast RMSE value decreases (improves) significantly at the 6-hour forecast, and oscillates slightly through the forecast period. An RMSE median value of more than 50 for all periods for the RWM indicates a very inaccurate forecast. For descriptive statistics, refer to Table 20, next page.

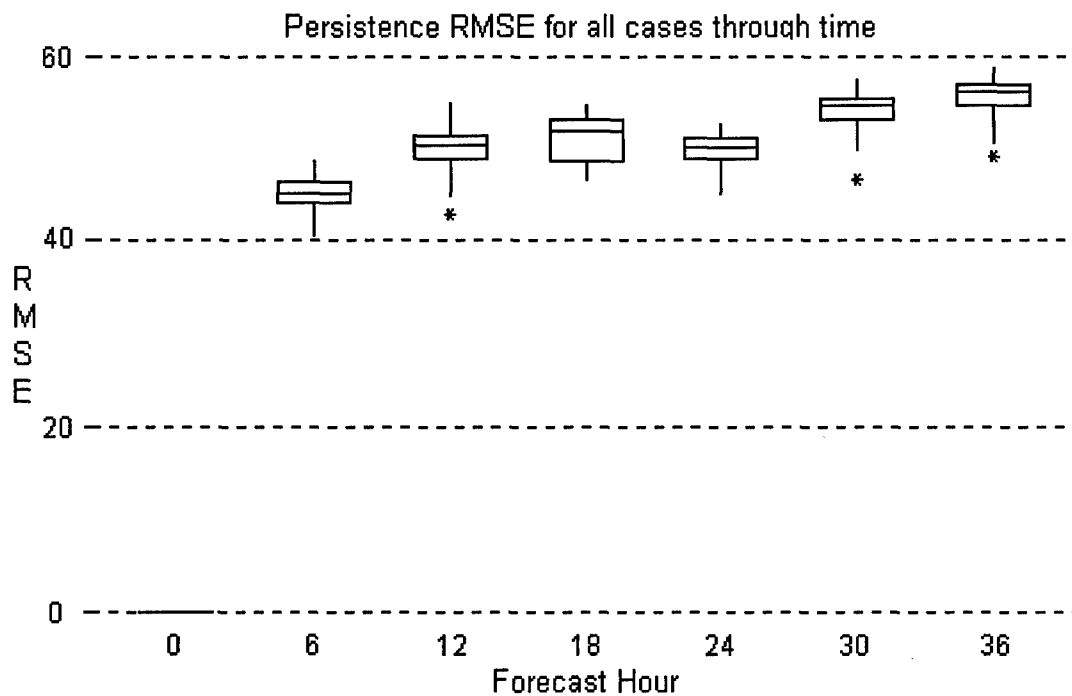


Figure 49: The persistence initial (0) hour is perfect, by definition. Persistence accuracy then rapidly decreases at the 6-hour forecast, slowly worsens through time, with a slight improvement at 24 hours. For descriptive statistics, refer to Table 20.

Table 20: Descriptive statistics for Figures 48 and 49.

	<u>RMSE</u>	
	<u>RWM</u>	<u>Persistence</u>
N	147	147
MEAN	55.016	48.184
SD	3.7305	12.097
MINIMUM	48.140	0.0000
MEDIAN	54.350	50.760
MAXIMUM	66.650	58.750

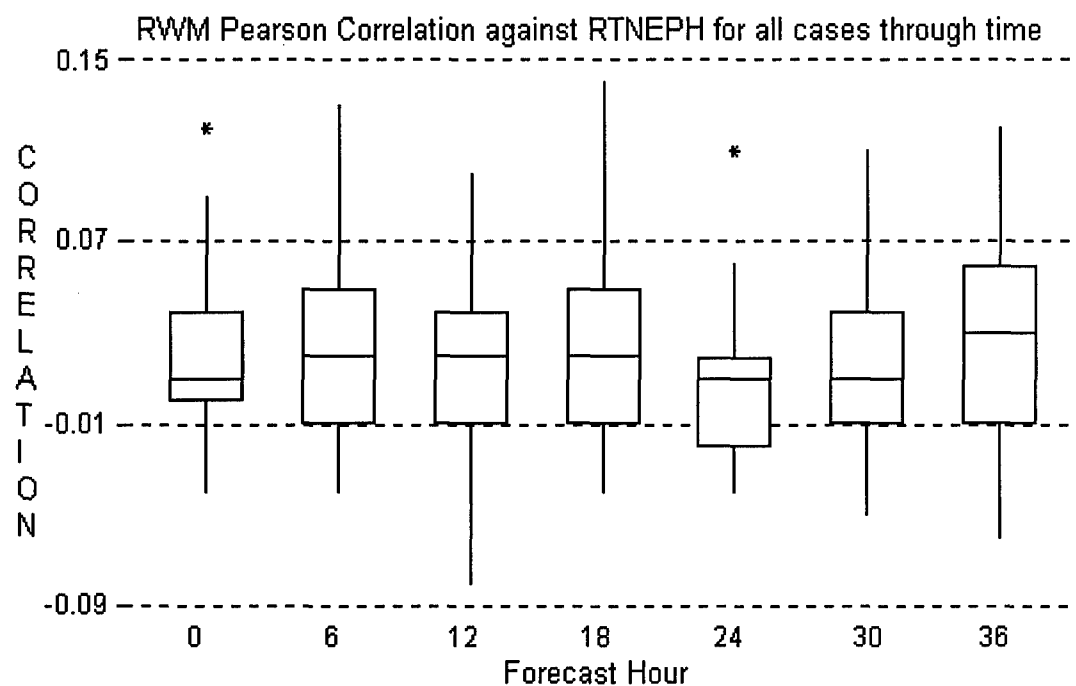


Figure 50: This figure shows the RWM total cloud forecast and the RTNEPH total cloud analysis is poorly correlated at all forecast times. For descriptive statistics, refer to Table 21, next page.

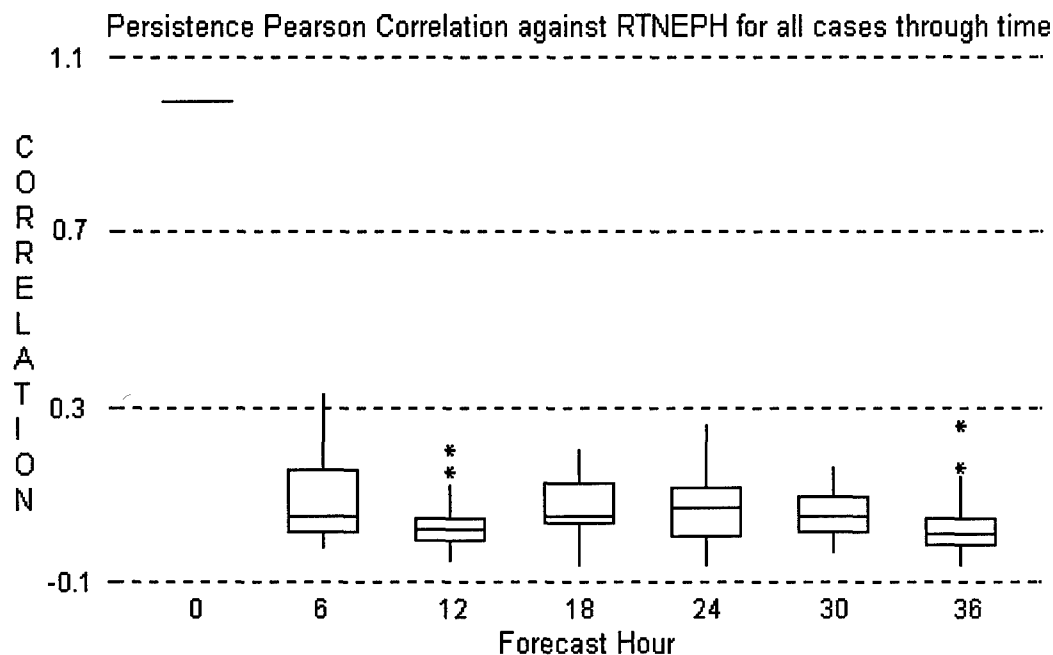


Figure 51: Persistence against RTNEPH shows perfect correlation at the 0 hour. The correlation then drops to near zero. The remaining persistence hours show a slightly higher correlation than the RWM (Figure 50). The low correlation at 6 hours suggests the RTNEPH is not highly persistent in the North American Window and does not bias the persistence measures of accuracy. For descriptive statistics, refer to Table 21.

Table 21: Descriptive statistics for Figures 50 and 51. This statistic is the RWM against the RTNEPH and persistence against the RTNEPH.

	<u>Pearson Correlation Coefficient against RTNEPH</u>	
	<u>RWM</u>	<u>Persistence</u>
N	147	147
MEAN	0.0191	0.1088
SD	0.0425	0.2250
MINIMUM	-0.0800	-0.0600
MEDIAN	0.0200	0.0400
MAXIMUM	0.1400	1.0000

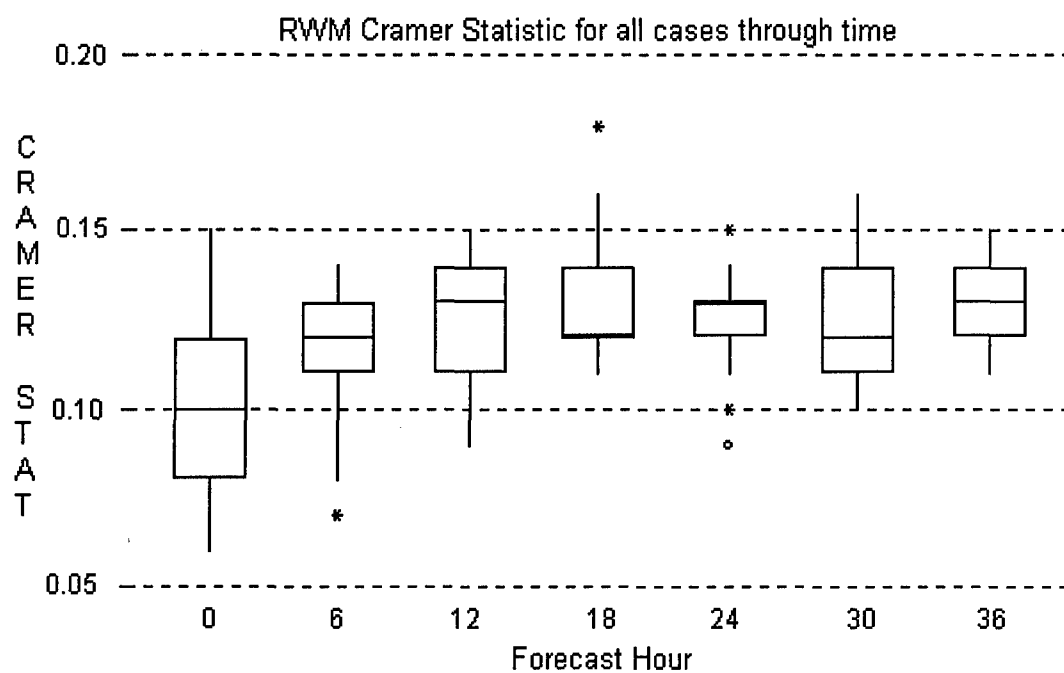


Figure 52: RWM Cramer Statistic indicates no linear relation between the RWM and RTNEPH. For descriptive statistics, refer to Table 22.

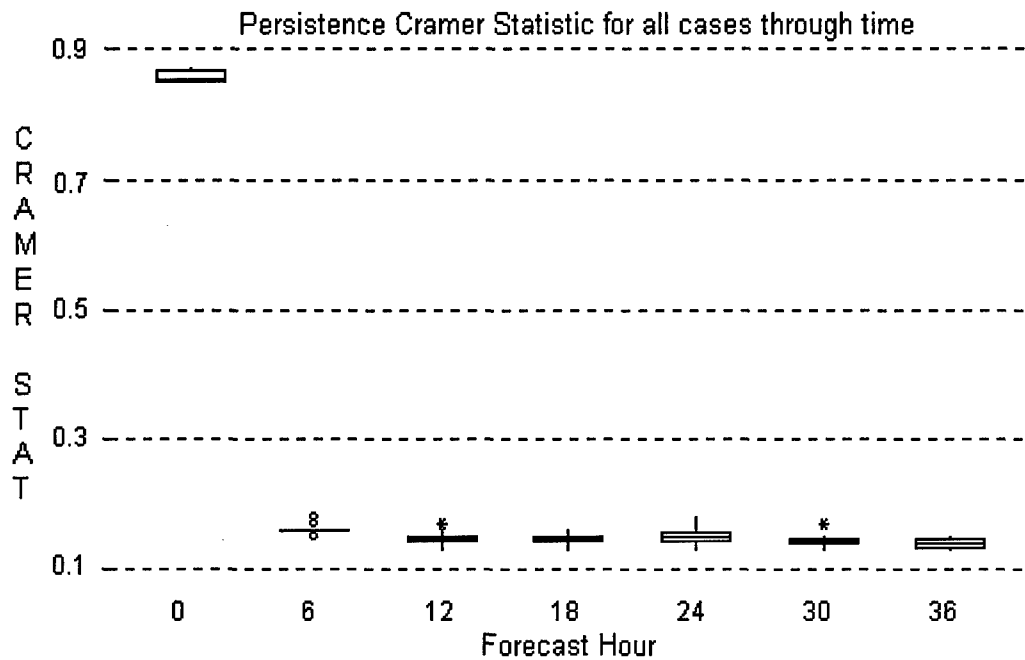


Figure 53: The Cramer Statistic for persistence begins as nearly perfect, then rapidly drops off at 6 hours. The Cramer Statistic then remains relatively steady through the remainder of the forecast period. For descriptive statistics, refer to Table 22.

Table 22: Descriptive statistics for Figures 52 and 53.

	<u>Cramer Statistic</u>	
	<u>RWM</u>	<u>Persistence</u>
N	147	147
MEAN	0.1209	0.1857
SD	0.0197	0.1596
MINIMUM	0.0600	0.1300
MEDIAN	0.1200	0.1500
MAXIMUM	0.1800	0.8700

4.4 RWM and Persistence Statistics for All Cases and All Times

This section presents the RWM and persistence statistical analysis composited from the individual statistics for each case and each forecast.

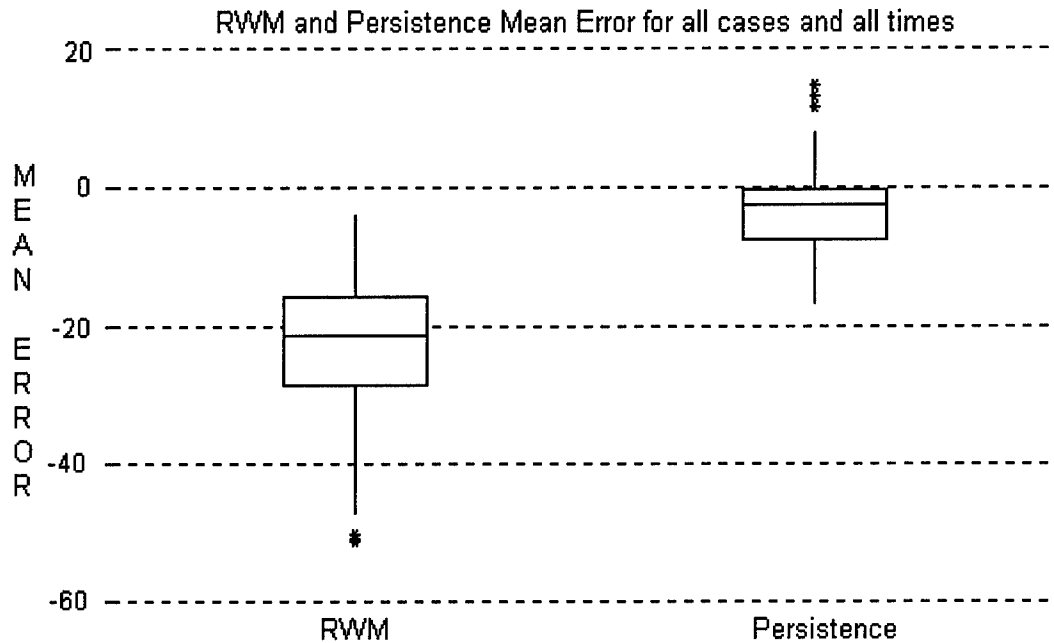


Figure 54: RWM and persistence mean error. This plot clearly shows the RWM has a negative bias. Refer to Table 23 for descriptive statistics.

Table 23: Descriptive statistics for Figure 54. The RWM clearly underforecasts total clouds with respect to the RTNEPH analysis data. Persistence has relatively little bias.

	Mean Error	
	RWM	Persistence
N	147	147
MEAN	-23.178	-3.3913
SD	10.876	5.9070
MINIMUM	-51.200	-16.440
MEDIAN	-21.210	-2.4900
MAXIMUM	-4.1000	14.810

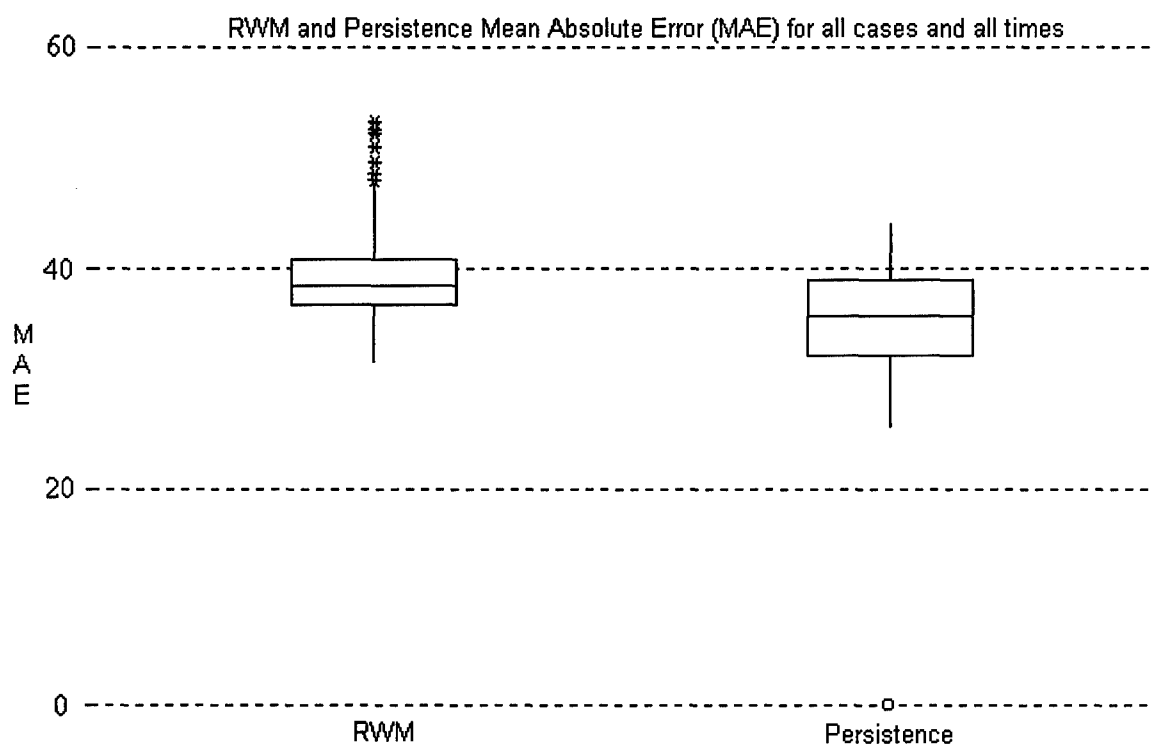


Figure 55: The RWM mean absolute error is greater than that of persistence. Refer to Table 24 for descriptive statistics.

Table 24: Descriptive statistics for Figure 55 for all cases and all times.

	<u>Mean Absolute Error</u>	
	<u>RWM</u>	<u>Persistence</u>
N	147	147
MEAN	39.256	33.990
SD	4.3187	9.0876
MINIMUM	31.540	0.0000
MEDIAN	38.580	35.750
MAXIMUM	53.260	44.040

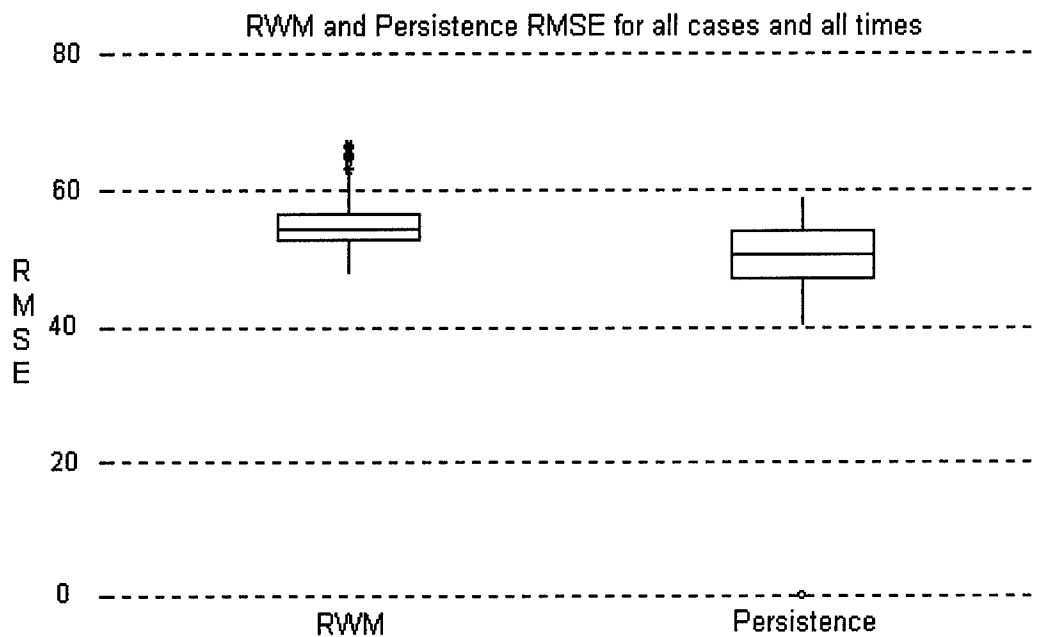


Figure 56: The RWM and persistence RMSE. This is another example of the RWM's total cloud forecast inaccuracy during the late spring and early summer. Refer to Table 25 for descriptive statistics.

Table 25: Descriptive statistics for Figure 56.

	<u>RMSE</u>	
	<u>RWM</u>	<u>Persistence</u>
N	147	147
MEAN	55.016	48.184
SD	3.7305	12.097
MINIMUM	48.140	0.0000
MEDIAN	54.350	50.760
MAXIMUM	66.650	58.750

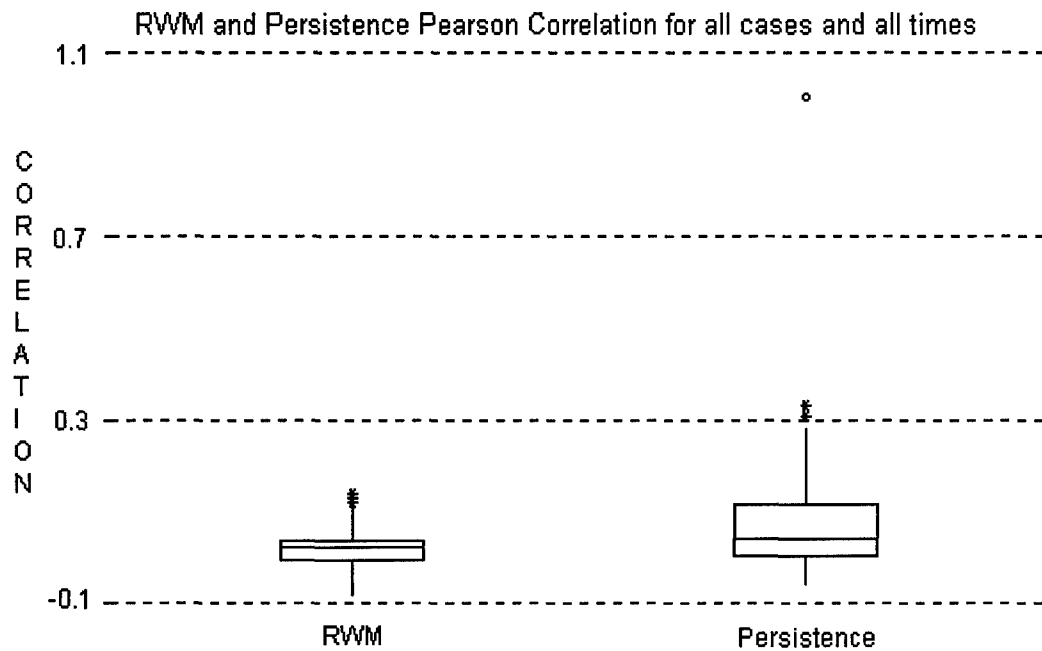


Figure 57: The RWM Pearson Correlation Coefficient for all cases and all times is lower than the correlation for persistence. For descriptive statistics, refer to Table 26.

Table 26: Descriptive statistics for Figure 57.

	<u>Pearson Correlation Coefficient</u>	
	<u>RWM</u>	<u>Persistence</u>
N	147	147
MEAN	0.0191	0.1088
SD	0.0425	0.2250
MINIMUM	-0.0800	-0.0600
MEDIAN	0.0200	0.0400
MAXIMUM	0.1400	1.0000

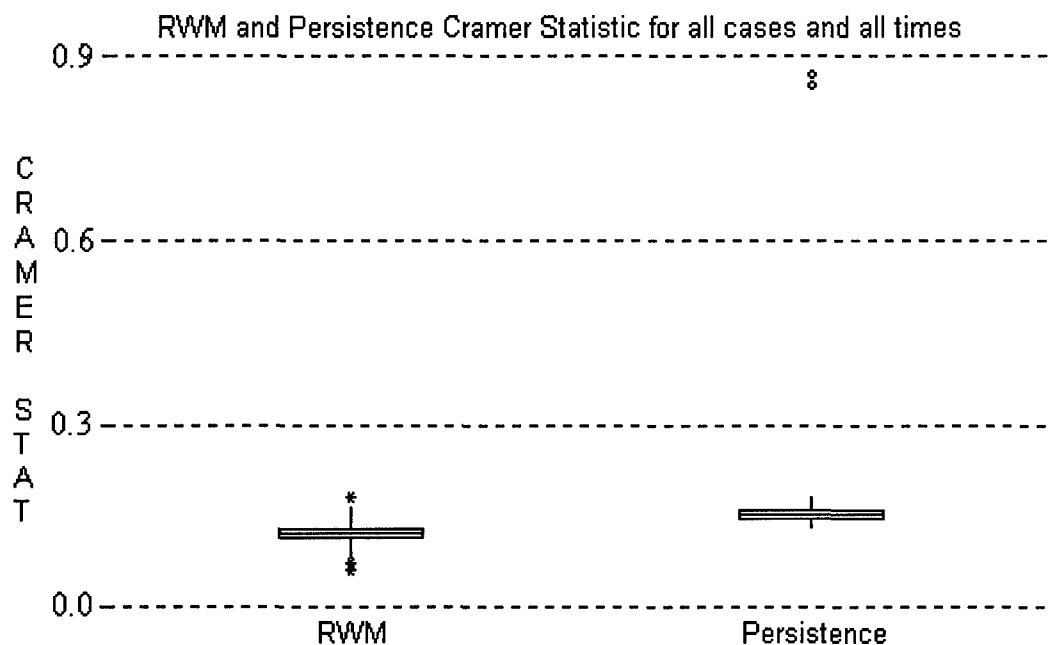


Figure 58: RWM and persistence Cramer Statistic for all cases and all times. The RWM shows no linear relation to the RTNEPH, while persistence is slightly higher. For descriptive statistics, refer to Table 27.

Table 27: Descriptive statistics for Figure 58.

	<u>Cramer Statistic</u>	
	<u>RWM</u>	<u>Persistence</u>
N	147	147
MEAN	0.1209	0.1857
SD	0.0197	0.1596
MINIMUM	0.0600	0.1300
MEDIAN	0.1200	0.1500
MAXIMUM	0.1800	0.8700

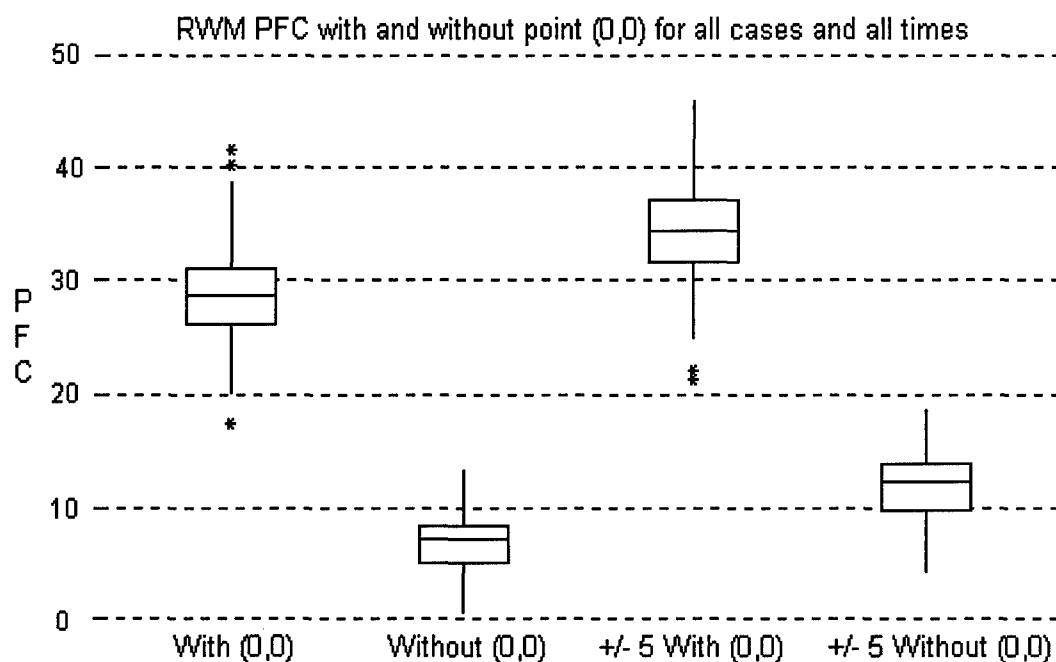


Figure 59: RWM PFC without point (0,0) and including the five diagonals either side of the main diagonal. This figure indicates poor performance of the RWM in forecasting total clouds with a heavy reliance on the point (0,0). Only a slight improvement in percentage forecast correct is seen when including the additional 10 diagonals. This figure shows most of the RWM's skill comes from forecasting 0% total cloud. For descriptive statistics, refer to Table 28.

Table 28: Descriptive statistics for Figure 59.

	<u>RWM PFC (Percentage Forecast Correct)</u>			
	<u>With (0,0)</u>	<u>Without (0,0)</u>	<u>± 5 with (0,0)</u>	<u>± 5 without (0,0)</u>
N	147	147	147	147
MEAN	28.638	6.6931	34.045	11.664
SD	4.3781	2.9048	4.9598	3.3455
MINIMUM	17.360	0.5900	21.230	4.3800
MEDIAN	28.620	7.2800	34.320	12.360
MAXIMUM	41.520	13.250	45.900	18.600

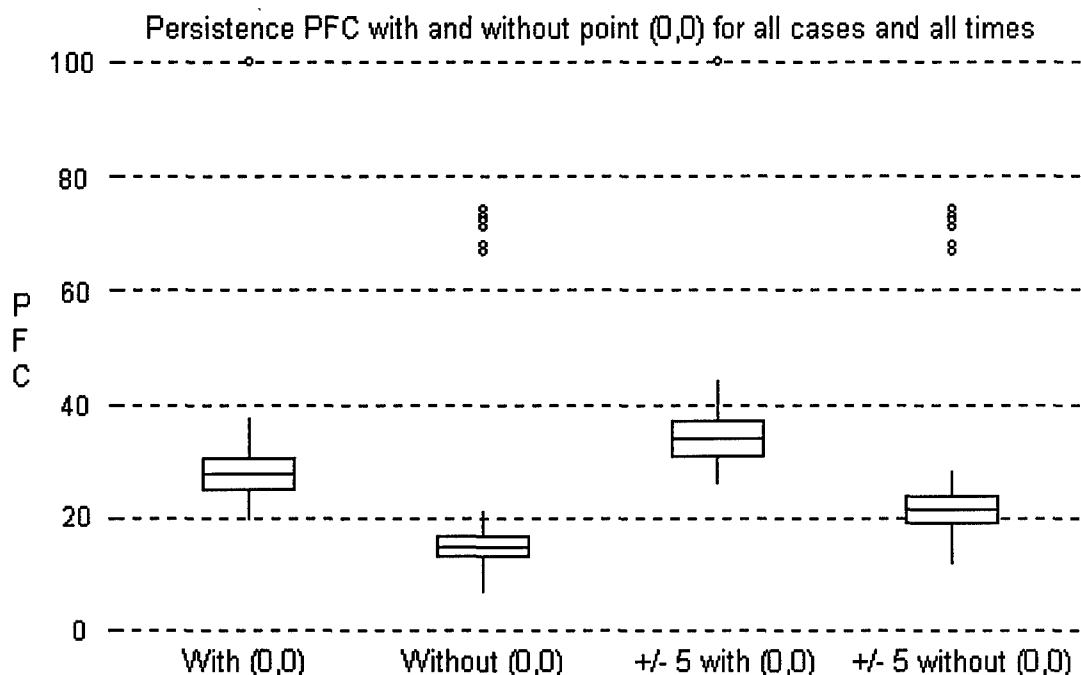


Figure 60: As Figure 59, except Figure 60 shows persistence PFC. There is less of a difference from the persisted "forecast" and RTNEPH when including the point (0,0). This figure shows less of the persistence "forecast" skill comes from forecasting 0% total cloud. For descriptive statistics, refer to Table 29.

Table 29: Descriptive statistics for Figure 60.

	<u>Persistence PFC (Percentage Forecast Correct)</u>			
	<u>With (0,0)</u>	<u>Without (0,0)</u>	<u>± 5 with (0,0)</u>	<u>± 5 without (0,0)</u>
N	147	147	147	147
MEAN	31.339	17.580	37.362	23.597
SD	16.743	12.801	15.424	11.523
MINIMUM	19.860	6.9100	26.070	12.150
MEDIAN	27.710	14.650	34.100	21.420
MAXIMUM	100.00	74.070	100.00	74.070

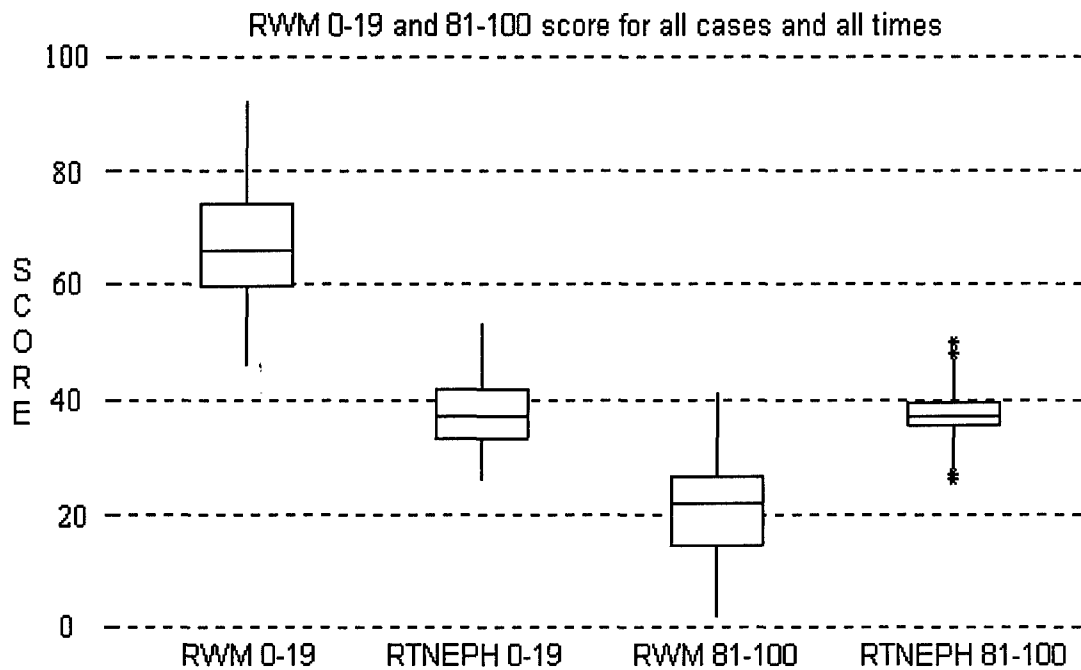


Figure 61: The RWM significantly overforecasts clear conditions (0-19) by approximately 30% and underforecasts the cloudy conditions (81-100) by approximately 17%. For descriptive statistics refer to Table 30.

Table 30: Descriptive statistics for Figure 61.

<u>RWM 0-19 and 81-100 score for all cases and times</u>				
	<u>RWM 0-19</u>	<u>RTNEPH 0-19</u>	<u>RWM 81-100</u>	<u>RTNEPH 81-100</u>
N	147	147	147	147
MEAN	67.796	37.592	20.327	37.605
SD	10.981	5.9677	9.3429	4.4284
MINIMUM	46.000	26.000	2.0000	26.000
MEDIAN	66.000	37.000	22.000	37.000
MAXIMUM	92.000	53.000	41.000	50.000

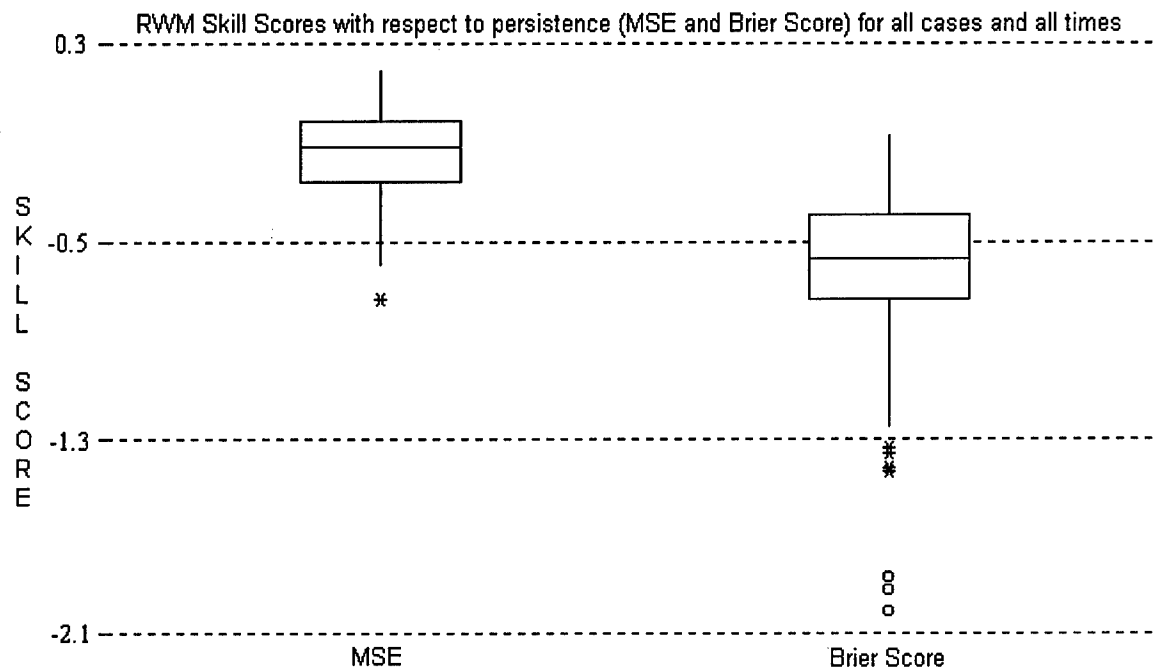


Figure 62: Cumulative Skill Score of the RWM. For descriptive statistics, refer to Table 31.

Table 31: Descriptive statistics for Figure 62.

	<u>RWM Skill Scores</u>	
	<u>MSE</u>	<u>Brier Score</u>
N	147	147
MEAN	-0.1435	-0.6326
SD	0.1863	0.3499
MINIMUM	-0.7300	-2.0100
MEDIAN	-0.1150	-0.5700
MAXIMUM	0.1900	-0.0700

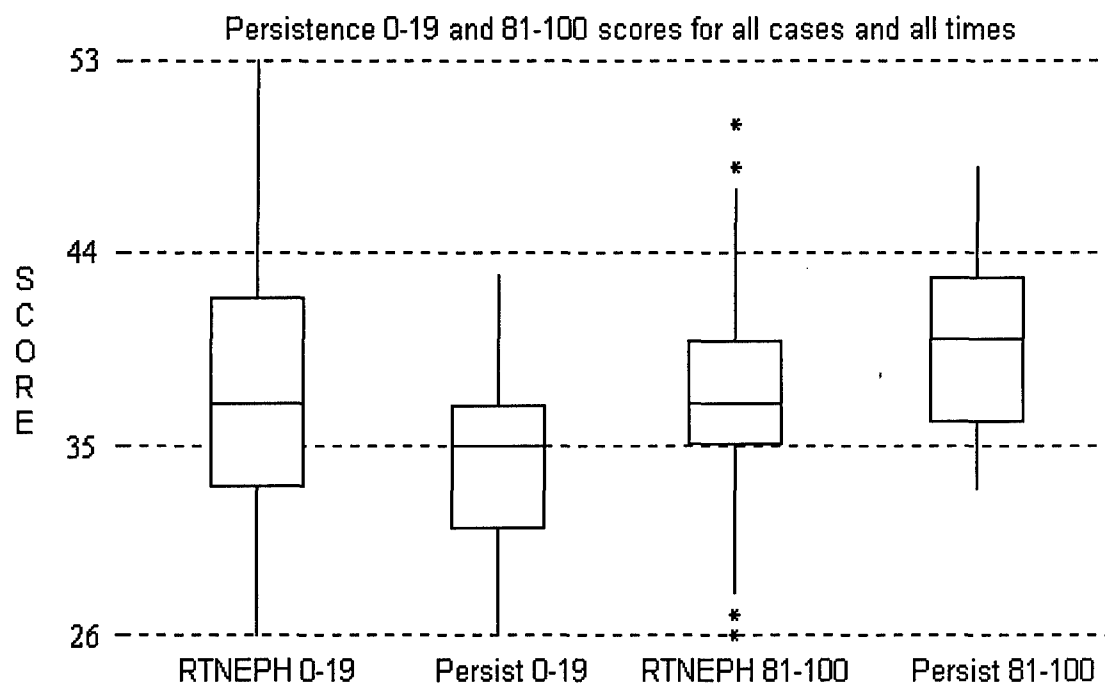


Figure 63: Persistence closely resembles the RTNEPH total cloud amount. Persistence and RTNEPH scores differ by only 3%. For descriptive statistics, refer to Table 32.

Table 32: Descriptive statistics for Figure 63.

<u>Persistence 0-19 and 81-100 scores</u>				
	<u>Persis 0-19</u>	<u>RTNEPH 0-19</u>	<u>Persis 81-100</u>	<u>RTNEPH 81-100</u>
N	147	147	147	147
MEAN	34.476	37.592	40.286	37.605
SD	4.8531	5.9677	4.3808	4.4284
MINIMUM	26.000	26.000	33.000	26.000
MEDIAN	35.000	37.000	40.000	37.000
MAXIMUM	43.000	53.000	48.000	50.000

V. Conclusions and Recommendations

5.1 Validation Summary

This chapter presents conclusions and recommendations based on the results shown in Chapter 4.

This study evaluated the bias, accuracy, sharpness, and skill of the RWM total cloud forecasts for selected days in May, June, and July 1996. The following six considerations must be taken into account when analyzing the results.

1. The RWM forecasts and RTNEPH analysis data are assumed to be independent data sets.

This is appropriate because of the chi-square test which was performed on the RWM forecast data and the RTNEPH analysis data. The results of the chi-square test strongly suggest independence (Appendix H).

2. In order for the RWM to be considered useful to a forecaster, the RWM should be able to significantly outperform persistence, both qualitatively and quantitatively. Persistence is used in this study as a minimal skill baseline for comparison with the RWM.
3. No attempt was made to tune the Slingo algorithm. The algorithm was tested as implemented at AFGWC.
4. The RWM European Window study, performed by AFGWC, suggests the RWM has a tendency to overforecast clouds, especially in the middle and high levels.
5. The method of maximum overlap used to sum individual cloud layers within the Slingo algorithm should overforecast total clouds, if the layers are forecast accurately. This method of overlap is not a very realistic method of summing total cloud cover but is very simple computationally.

6. The Slingo algorithm was originally designed for forecasts of the global scale radiation budget. The Slingo algorithm was not originally intended for accurate, small-scale cloud forecasting.

With those considerations in mind, the conclusions can now be discussed.

5.2 *Conclusions*

This section includes the conclusions drawn from the results in Chapter 4.

5.2.1 *Bias*

The results of this study suggest the RWM total cloud forecasts have a negative bias (mean error) in all cases and for all forecast times. A negative bias indicates the RWM consistently underforecasts total cloud amounts, which contradicts the results of the fourth consideration (previous page). Because of the poor initial RWM moisture fields, cloud forecasts at the initial stages are very error-prone, making the persistence “forecast” very competitive. The RWM had 36 hours to spin-up the three-dimensional moisture field and failed in outperforming persistence. Throughout the entire forecast period, the RWM continued to maintain a negative bias. The underforecast of the RWM is greatest at the initial (0) hour and improves significantly for the 6-hour forecast. Finally, for all cases and all forecast times, the RWM exhibited no cases of positive bias (no overforecasting).

The persistence results show a much lower bias for all cases and forecast times. Although the overall persistence bias is negative, the magnitude is much less than that of the RWM. In fact, the persistence bias is nearly an order of magnitude better than that of the RWM. The persistence underforecasting shows a negative bias through time, but the box and whisker plots suggest a diurnal tendency. The 24-hour forecast closely resembles the initial (0) hour, as would be expected with persistence during the summer, with convective clouds.

5.2.2 Accuracy

The results of the RMSE scores suggest the RWM is very inaccurate at the initial hour with some improvement at the 6-hour forecast. The 6-hour forecast is relatively the most accurate of the forecast period, but is absolutely inaccurate.

Persistence RMSE scores were slightly better than the RWM RMSE scores. The persistence RMSE score was zero at the initial hour, with the RMSE score rapidly increasing over the first 6 hours. The accuracy of persistence continued to decline through the forecast period, with a slight improvement at the 24-hour forecast, due in part to diurnal persistence in the cloud fields. Overall, persistence is more accurate than RWM, based on RMSE. This suggests the RWM is not an accurate forecast of total cloud.

5.2.3 Correlation

The Pearson Correlation Coefficient was calculated for both the RWM and persistence against the RTNEPH. The mean and median correlation coefficient values of the RWM were nearly identical. The equivalent values of persistence were 0.11 and 0.04, a slight improvement over RWM, and indicate a very weak linear relationship with the RTNEPH. The low correlation of persistence suggests the RTNEPH does have a fairly high refresh rate every six hours, and suggests the RTNEPH persistence forecasts were not strongly biased by persistence in the analysis. If a three-hour analysis was performed, the results may indicate a higher correlation due to the RTNEPH's persisting data on the three-hour interval.

The results of the Cramer Statistic suggest the RWM's performance was worse than that of persistence. The Cramer Statistic for the RWM increases over time, while the Cramer Statistic for persistence decreases over time. The lack of correlation between persistence and RTNEPH again suggests the persistence scores are not strongly biased in favor of accuracy due to

persistence within the RTNEPH. If RTNEPH widely persisted due to missing data, the expected correlation and Cramer Statistic would suggest a higher correlation.

5.2.4 Sharpness

Sharpness is a measure of how often a forecast method produces extreme (clear or cloudy) forecasts. However, a sharp forecast is not necessarily a skillful forecast. The results of the 0-19 (clear) and 81-100 (cloudy) scores suggest the RWM overforecasts the clear conditions and underforecasts the cloudy conditions. The RWM overforecasted the clear conditions for all cases and forecast times by approximately 30% and underforecasted the cloudy conditions by approximately 15%. This finding is important for operational forecasters who use the RWM as their primary guidance in formulating forecasts for operational purposes.

Previous studies show the RTNEPH has tendencies to overanalyze clear and cloudy conditions (i.e., Hamill *et al.*, 1992). With this in mind, the RWM's performance for clear conditions (0-19) would be worse, but the RWM's performance for cloudy conditions (81-100) would be better. Also, the maximum overlap method of the Slingo algorithm should have a tendency to overforecast total clouds. Even with these considerations, the RWM's sharpness was still poor. A significant reason why the RWM clearly overforecasts the clear conditions and underforecasts the cloudy conditions is due to the absence of convection within the Slingo algorithm. No clouds such as cumulus, cumulonimbus, cirrus clouds associated with cumulonimbus, cirrus from dissipated cumulus clouds, and precipitating and non-precipitating cumulus will be produced in the forecasts.

Persistence has a much improved sharpness over the RWM, as expected during the late spring and early summer, when viewing the animated images using PV-WAVE®. The persisted clear condition "overforecasts" and differs by only 2%. On the other hand, the cloudy condition

“underforecasts” and differs by only 3%. This is reasonable since the RTNEPH 20/20 score is relatively constant over 36 hours.

When qualitatively viewing the images of underforecast and overforecast total clouds, areas of organized cloud cover are present in both the underforecast or overforecast images. This indicates possible phase errors with the RWM forecast and the RTNEPH analysis. However, the poor 0-19 and 81-100 scores suggest the poor accuracy of RWM total cloud forecast is not entirely due to phase errors in the forecast fields, but is also due to amplitude errors and the missing convection. An otherwise accurate, but out of phase forecast should show better 0-19 and 81-100 scores.

5.2.5 RWM Overall Total Cloud Forecast Skill

The results of the study suggests the RWM is a much poorer performer than persistence through 36 hours during the late spring and early summer. One measure of skill was determined using the percentage forecast correct (PFC), or hit rate. The RWM PFC relied heavily on the forecasted and observed values of 0% total cloud cover (referred to as point (0,0)). The RWM and persistence results were nearly identical for the forecasts of the PFC and the PFC $\pm 5\%$. However, when PFC and the PFC $\pm 5\%$ were modified by omitting the (0,0) point, the RWM skill was half of persistence. The RWM skill was inflated by including the (0,0) point due to the high frequency of no cloud forecasts, because the RWM severely overforecasts clear conditions as shown by the 0-19 scores.

Other measures of RWM skill were also measured. The RWM total cloud forecast skill was calculated using RWM MSE with respect to persistence MSE, and the RWM Brier Score with respect to persistence Brier Score. Brier Score results suggests the performance of the RWM and persistence as nearly perfect. This unrealistically high skill score of the RWM is due to the fact that there are so many matches (ties) of the points (0,0) and (100,100). In both instances, the

RWM cloud forecasts did not outperform persistence cloud "forecasts," but the RWM Brier Score did show improvement over the forecast period. The RWM MSE skill score with respect to persistence MSE indicates a near zero skill and no change with time of the skill over the forecast period.

In summary, for all cases and forecast times, both skill scores suggest the RWM did not outperform persistence in forecasting total clouds through 36 hours during the late spring and early summer.

5.2.6 Summary of Conclusions

The results suggest the RWM showed no areas, subjectively or objectively, in which its total cloud forecasts for the North American Window during the late spring and early summer performed better than persistence through the entire 36-hours forecast period. In terms of the RWM's bias, accuracy, sharpness and skill, the RWM performed poorly with respect to persistence. The results of this study suggest the RWM, as tested, is not capable of accurately fulfilling the total cloud forecasting needs of the Air Force during the late spring and early summer over the North American Window.

However, the results of this study are dependent upon the RWM and the RTNEPH resolved total cloud cover and the inherent limitations of the simple diagnostic relationships between atmospheric parameters and total cloud cover resolvable on the scale of the RWM, which has gross simplifications of the important physical processes. The results are also dependent upon the accuracy of the RWM forecasts and RTNEPH cloud analysis.

The results of this study suggest the RWM total cloud forecasts are also not useful for the operational forecaster unless the known characteristic, strengths, and weaknesses of the RWM total cloud forecasts are understood.

Despite the poor performance of the RWM, a biased model forecast can provide useful guidance. If a model's bias is known, a forecaster can correct for this and adjust the forecast appropriately. In this study, the bias of the RWM could be reduced by simply incorporating the convective parameterization. Including solar and terrestrial radiation would also improve the bias. In addition to the bias, poor RMSE scores do not necessarily indicate a useless forecast. Accurate forecasts with phase or amplitude errors would have a high RMSE, but might provide useful guidance to a skilled forecaster. Conversely, a useless forecast (for example, a consistent 50% total cloud forecast) may have a lower RMSE than demonstrated by the RWM in this study, but also may be useless to the customer. High RMSE values suggests the forecasts could be inaccurate due to phase or amplitude errors (or both). Therefore, the forecasts require skillful interpolation to be useful, and the user must be careful in applying the output without modifications.

5.3 Recommendations

The recommendations are centered upon two approaches to solving the suggested deficiencies. The first approach focuses on short-term recommendations and suggests ways of meeting the needs of today's operational forecast community. The second approach focuses on the long-term recommendations and suggests ways of meeting the future needs of the operational forecast community.

5.3.1 Short-term Recommendations

A similar study should be performed for the late spring and early summer which incorporates the convective parameterization in the Slingo algorithm and with the RWM using NOGAPS as the initial fields and boundary conditions. Once the convective parameterization is included, manually tuning the convective parameterization and the critical RH can be tested. If

the results show improved performance, then validation of each layer or ceiling vs no-ceiling can be performed. However, until the total cloud forecasts improve, the more thorough validation of model forecast of individual cloud layers should not be performed.

Second, other seasons should be tested to determine the RWM cloud forecast skill and quantify its performance characteristics. The RWM may also be determined to serve as an interim method until other more accurate models are incorporated into AFGWC. If the RWM is retained as an interim solution, the 80% critical RH could be replaced, or tweaked, by a set of relationships which would account for seasonal, land vs sea, or even latitudinal variations. The critical RH value of 80% is a very crude estimate of the diagnosis of total cloud cover over such a large geographical region, and modifications to the critical RH should be considered.

Third, studies including the adjustment of the convective parameterization should be undertaken when convection does not play such a large role in the models output, such as during the other seasons. This is especially true during the autumn and winter seasons where large-scale condensation replaces the diabatic heating normally occurring in the subtropics associated with cumulus convection during the summer months.

Fourth, validation statistics can be computed only for the grid points within the RTNEPH which prove more timely, using the RTNEPH time flag in the RTNEPH data. In the data provided, the RTNEPH time flag was not included and could not be used. Including the time flag would ensure a more fair comparison between the forecast schemes and persistence and the use of 3-hourly RTNEPH data could be used to validate the 3-hourly RWM total cloud forecast.

Finally, the results should be communicated to the field. Educating the forecasters on the known characteristics, strengths, and weaknesses of a forecast model is critical in making the model forecasts useful to operational forecasters. Communicating the results may be the most simple means of improving the forecast support for today's operational forecasters.

5.3.2 Long-term Recommendations

The forecast models of the future should have high horizontal and vertical resolutions, improved planetary boundary layer physics, non-hydrostatic physics, explicit three-dimensional moisture physics, and improved data assimilation. The more advanced data assimilation techniques should also be implemented in the model over the next several years and incorporate all satellite data, including GOES. The extratropical regions have a greater number of gridpoints with updated cloud amounts due to the higher frequency of polar-orbiting satellites, while the tropics have less frequent satellite refreshed data. This is a primary reason why GOES data should be included in the analysis. In addition to the conventional satellite data, multispectral analysis should also be performed to identify clouds in regions where cloud identification has demonstrated to be a problem.

In summary, as computers become more powerful, the Air Force should seriously consider deterministic cloud forecasting in the future. Cloud forecast studies should be performed to determine at what forecast hour (cross-over point) during the forecast period the deterministic cloud forecast outperforms the diagnostic cloud forecast. From the cross-over point and beyond, the deterministic cloud forecast approach should provide a significant improvement over today's diagnostic cloud forecast approach. Deterministic cloud forecasts should be capable of providing more accurate, very high spatial resolution long-range cloud forecasts required to support new DoD requirements in virtually all mission areas.

Appendices

Appendix A: GSM Discussion.

The GSM was developed by the NMC in 1980, and AFGWC implemented the GSM in 1984. For this study, the GSM was used as a first-guess model for HIRAS. The first-guess model is an R30-wave, 12-layer vertical resolution of the GSM. The GSM produces 0-, 6-, and 12-hour forecasts of winds, temperatures and heights from the surface to 100 mb and moisture from the surface to 300 mb. In this study, HIRAS used the GSM six-hour forecast as its first guess input. The GSM data was stored as spectral coefficients on a $2.5^\circ \times 2.5^\circ$ latitude/longitude grid. The GSM input fields include monthly sea surface temperature climatology, surface roughness, and terrain.

The primary forecast model of the GSM was an R40-wave, and also included 12-layer vertical resolution. The forecast model produced forecasts of heights, temperatures, winds, and vertical velocity from the surface to 100 mb with forecasts out to 96 hours, with three-hour intervals out to 48 hours.

The GSM strengths include its high dependability and its ability to handle long waves well. Its original design was for flight-level wind forecasting.

The GSM weaknesses include poor horizontal and vertical resolution. The GSM first guess model (R30-wave) is only able to resolve 30 waves around the globe. This is an equivalent longitudinal resolution of 350 km and a latitudinal resolution of 270 km, true at 35°N . Another weakness is the GSM's overall inaccuracy. This inaccuracy is due to the lack of physics parameterizations, the climatological use of sea surface temperatures, and the lack of moisture at all layers. The GSM also forecasts geopotential heights (a function of temperature) too high because the GSM temperatures are too warm in the troposphere (Neel *et al.*, 1993).

Appendix B: High Resolution Analysis System (HIRAS) Description.

The HIRAS is the primary analysis system which is used in the Advanced Weather Analysis and Prediction System (AWAPS). The HIRAS database (used as input into the RWM) uses ship reports, surface observations, buoys reports, aircraft reports, satellite photos, satellite soundings from the Defense Meteorological Satellite Program (DMSP) Microwave Temperature Sounder (SSM/T-1) and Radiosonde Observations (RAOB) data. The HIRAS includes an Optimum Interpolation (OI) objective analysis method, and a 30-wave GSM to produce a 6-hour and 12-hour forecast used as a first guess for the RWM (Neel *et al.*, 1993). The OI method uses a combination of observations and the first-guess routine. The better the first-guess, the less weight is given to the individual observations. The HIRAS analyzes five variables: heights, u and v wind components, temperature and relative humidity. Inherent to all observations, are errors, and the HIRAS is manually and automatically quality controlled. Manually through bogusing, and automatically through gross checks and buddy checks. Bogusing is referred to as having an analyst identify and manually correct, discard, or add meteorological information to the analysis data. Gross checks are comparisons of adjacent gridpoint data from the first-guess model output. If the comparison is questionable the buddy check is initiated, where the observation in question is compared to nearby stations. If the observation is drastically different, the observation is discarded (Conklin, 1992).

Appendix C: Sigma (σ) Coordinate System Description.

A sigma (σ) coordinate system, or "terrain-following" coordinate system, is a system in which the ground is always at the same level in the vertical, and is defined as:

$$\sigma \equiv \frac{p}{p_o}$$

where p_o is the surface pressure, and p is the pressure at the height under consideration.

The seventeen valid RWM σ levels include:

- 00 - Surface
- 01 - 1.000 - .965
- 02 - .965 - .922
- 03 - .922 - .872
- 04 - .872 - .816
- 05 - .816 - .754
- 06 - .754 - .688
- 07 - .688 - .618
- 08 - .618 - .546
- 09 - .546 - .472
- 10 - .472 - .397
- 11 - .397 - .323
- 12 - .323 - .250
- 13 - .250 - .180
- 14 - .180 - .114
- 15 - .114 - .054
- 16 - .054 - .000

Appendix D: The 12 Mandatory Pressure Levels used by RWM.

The twelve mandatory levels include:

- 01 - 1000 mb
- 02 - 850 mb
- 03 - 700 mb
- 04 - 500 mb
- 05 - 400 mb
- 06 - 300 mb
- 07 - 250 mb
- 08 - 200 mb
- 09 - 150 mb
- 10 - 100 mb
- 11 - 50 mb
- 12 - 10 mb

Appendix E: Slingo FORTRAN Cloud Algorithm.

(Purpose: diagnose clouds for three layers of clouds using the Slingo method plus our modifications.)

(Method: loop down from top of atmosphere and set the cloud amount for each layer using the Slingo parameterizations. Return the low, mid, high cloud layer, base, top, and amount.)

(Inputs: RHBASE, RHCRIT, CNVAMT, CNVTOP, RHX , LOLAPS, OMEGAX, MISING, IJMAX , KLXA , KLXM7 , KLOW , KMID, CONV , LAPLEV)

(Outputs: CDAMT, CDBAS, CDTOP, CDLEV, CAMT)

(Variables:

CAMT	INTERIM LAYER CLOUD AMOUNTS AT EACH POINT
CDAMT	LOW, MID, HIGH CLOUD AMOUNTS
CDLEV	LOW, MID, HIGH CLOUD LEVELS
CLDAMT	FINAL LAYER CLOUD AMOUNTS
CNVAMT	CONVECTIVE CLOUD AMOUNT
CNVTOP	CONVECTIVD CLOUD TOP
CONV	NUMBER OF CLOUD TYPES (4)
FINHI	LOGICAL FINISH FLAG FOR HIGH CLOUD SEARCH
HI	HIGH CLOUD LAYER NUMBER
IJMAX	MAX NUMBER OF GRID POINTS IN HORIZONTAL PLANE
K	VERTICAL SIGMA LEVEL INDEX
KLOW	SIGMA LEVEL BELOW WHICH LOW CLOUDS OCCUR
KMID	SIGMA LEVEL BELOW WHICH MID CLOUDS OCCUR
KLXA	TOTAL EXPANDED VERTICAL LEVELS
KLXM7	KLXA MINUS 7
LAPLEV	LAPSE RATE AT EACH SIGMA LEVEL
LOLAPS	SIGMA LEVEL CONTAINING MOST STABLE LAPSE RATE
LOPM1	FIRST COEFFICIENT IN SLINGO'S EQN 8
LOPM2	SECOND COEFFICIENT IN SLINGO'S EQN 8
LOPRIM	INTERIM LOW CLOUD CALCULATION
LOW	LOW CLOUD LAYER NUMBER
MID	MID CLOUD LAYER NUMBER
MISING	MISSING FLAG
OMEGAX	OMEGA AT EXPANDED VERTICAL RESOLUTION
RHBASE	RH AT BASE OF INVERSION
RHC	CRITICAL RELATIVE HUMIDITY
RHCRIT	CRITICAL RELATIVE HUMIDITY LEVELS ARRAY
RHMOD	FUNCTION - CONVECTION MODIFIED RH
RHX	RH AT EXPANDED VERTICAL RESOLUTION)

(Updates: MAR95 INITIAL VERSION.....MR KIESS/SYSM

27Feb96 Added comments, changed high cloud convective parameter
to 400mb from 500mb, changed low level cloud with
inversion statement to remove cloud with RH < 60%,

removed code duplicated in SPDCLD.F....Capt Cantrell/SYSM)

(Parameter statements)

```
INTEGER  CONV
INTEGER  HI
INTEGER  IJMAX
INTEGER  KLXA
INTEGER  LOW
INTEGER  MID
REAL     LOPM1
REAL     LOPM2
```

(Set parameter values)

```
PARAMETER (HI = 3)
PARAMETER (MID = 2)
PARAMETER (LOW = 1)
PARAMETER (LOPM1 = -6.67)
PARAMETER (LOPM2 = 0.667)
```

(Variable declarations)

```
INTEGER  CDLEV (IJMAX,CONV)
INTEGER  CNVTOP (IJMAX)
INTEGER  IJ
INTEGER  K
INTEGER  KLOW
INTEGER  KLXM7
INTEGER  KMID
INTEGER  LAPLEV (IJMAX)
LOGICAL  FINHI
REAL     CAMT (IJMAX,KLXA)
REAL     CDAMT (IJMAX,CONV)
REAL     CLDAMT
REAL     CNVAMT (IJMAX)
REAL     LOLAPS (IJMAX)
REAL     LOPRIM
REAL     MISING
REAL     OMEGAX (IJMAX,KLXA)
REAL     RHX (IJMAX,KLXA)
REAL     RHBASE (IJMAX)
REAL     RHC
REAL     RHCRIT (HI)
REAL     RHMOD
```

(Statement functions: RHMOD \Rightarrow RH modified by convective cloud amount)

$$\text{RHMOD}(\text{IJ},\text{K}) = \text{RHX}(\text{IJ},\text{K}) * (1. - (\text{CNVAMT}(\text{IJ}) / 4.))$$

(Loop through the layers starting at the top of the moist layers and set the cloud amounts, the hi, mid, low determination, and the max cloud amount layer. (restrict cloud production from 980mb to 215mb))

```
DO 200 IJ = 1, IJMAX  
FINHI = .FALSE.  
DO 100 K = KLXM7, 3, -1
```

(Find the cloud level and calculate the cloud)

```
IF (K .GT. KMID) THEN  
RHC = RHCRIT (HI)
```

(Set high cloud amount: algorithm differentiates between convective blow off and frontal cirrus. Check for convection by convective cloud amount greater than 40% and convective top above 400 mb. Since convective cloud parameterization require just one pass, jump to next k index if already through once.)

```
IF (FINHI) GO TO 100  
IF ((CNVAMT(IJ) .GT. 0.4) .AND. (CNVTOP(IJ) .GT. 21)) THEN
```

(Use the convective cloud parameterization to set amount)

```
CDAMT (IJ,HI) = 2. * (CNVAMT(IJ) - 0.3)  
CDLEV (IJ,HI) = CNVTOP(IJ)  
FINHI = .TRUE.  
ELSE
```

(Use the frontal cirrus parameterization)

```
CLDAMT = AMAX1 ( ( (RHX(IJ,K)-RHC)/(1.0-RHC) ), 0.0)  
CAMT (IJ,K) = CLDAMT * CLDAMT  
END IF
```

(Set the initial amount, level, top, and base)

```
IF (CAMT(IJ,K) .GT. CDAMT(IJ,HI)) THEN  
CDAMT(IJ,HI) = CAMT (IJ,K)  
CDLEV(IJ,HI) = K  
END IF
```

(Check for middle level cloud, one parameterization used)

```
ELSE IF (K .GT. KLOW) THEN  
RHC = RHCRIT (MID)  
CLDAMT = AMAX1( ((RHMOD(IJ,K)-RHC) / (1.0-RHC)), 0.0)  
CAMT (IJ,K) = CLDAMT * CLDAMT  
IF (CAMT(IJ,K) .GT. CDAMT(IJ,MID)) THEN  
CDAMT(IJ,MID) = CAMT (IJ,K)  
CDLEV(IJ,MID) = K  
END IF
```

(Low cloud parameterization uses two forms which are mutually exclusive: the first is associated with boundary layer clouds and must have an inversion in the lowest layer. If there is not an inversion, then parameterization associated with fronts and tropical disturbances is used.)

```

ELSE
RHC = RHCRT (LOW)
IF (LOLAPS(IJ) .NE. MISING) THEN

```

(If an inversion exists, use boundary layer parameterization calculate an initial low cloud amount, loprim. then use the relative humidity at the base of the inversion to determine how to modify loprim.)

```

LOPRIM = LOPM1 * LOLAPS(IJ) - LOPM2
IF ((RHBASE(IJ) .GE. 0.6) .AND.
&(RHBASE(IJ) .LE. 0.8)) THEN
CAMT(IJ,LAPLEV(IJ)) = LOPRIM *
&(1. - (RHC - RHBASE(IJ)) / (1. - RHC))
ELSE IF (RHBASE(IJ) .GT. 0.8) THEN
CAMT(IJ,LAPLEV(IJ)) = LOPRIM
ELSE
CAMT(IJ,LAPLEV(IJ)) = 0.0
END IF

```

(Update the output arrays. Since only one pass is needed and no more layers need to be checked, jump out of the level loop.)

```

CDAMT(IJ,LOW) = CAMT (IJ,LAPLEV(IJ))
IF (CDAMT(IJ,LOW) .GT. 0.) THEN
CDLEV(IJ,LOW) = LAPLEV(IJ)
ELSE
CDLEV(IJ,LOW) = 0
END IF
GO TO 110
ELSE

```

(Use the frontal parameterization: check for subsidence, if there, then no low cloud. For rising air, diagnose cloud using the standard RH diagnosis and then modify by vertical motion.)

```

IF (OMEGAX(IJ,K) .GE. 0) THEN
CAMT(IJ,K) = 0.0
ELSE
CLDAMT = AMAX1( (RHMOD(IJ,K)-RHC) / (1.0-RHC), 0.0)
LOPRIM = CLDAMT * CLDAMT
IF (OMEGAX(IJ,K) .GT. -0.1) THEN
CAMT(IJ,K) = -10.0 * OMEGAX(IJ,K) * LOPRIM
ELSE
CAMT(IJ,K) = LOPRIM
END IF
END IF
IF (CAMT(IJ,K) .GT. CDAMT(IJ,LOW)) THEN
CDAMT(IJ,LOW) = CAMT (IJ,K)
CDLEV(IJ,LOW) = K
END IF
END IF
END IF

```



```
100 CONTINUE
110 CONTINUE
```

(Make sure cloud amounts are between 0.0 and 1.0)

```
DO 150 K = LOW, HI
  CDAMT(IJ,K) = MAX(CDAMT(IJ,K), 0.0)
  CDAMT(IJ,K) = MIN(CDAMT(IJ,K), 1.0)
150 CONTINUE
200 CONTINUE
  RETURN
  END
```

Appendix F: PV-WAVE Code.

PRO nn

```

;*****
; NAME: SLINGO VERIFICATION (MAIN DRIVER)
;
; PURPOSE: TO VERIFY RWM (WITH SLINGO DIAGNOSTICS) AGAINST RTNEPH
;
; VARIABLES
; =====
; BOX      NEPH BOX
; CLDAMT    RWM GRID LOW, MID, HIGH, CONV CLOUD AMOUNTS
; CNT(#)    TEMPORARY COUNT OF INDEX(#) ELEMENTS
; CRTOTL    CEILING ARRAY FOR RWM TOTAL CLOUD AMOUNT (1=YES, 0=NO)
; CRHAMT    CEILING ARRAY FOR RWM HIGH CLOUD AMOUNT (1=YES, 0=NO)
; CRMAMT    CEILING ARRAY FOR RWM MIDDLE CLOUD AMOUNT (1=YES, 0=NO)
; CRLAMT    CEILING ARRAY FOR RWM LOW CLOUD AMOUNT (1=YES, 0=NO)
; CVTOTL    CEILING ARRAY FOR VER TOTAL CLOUD AMOUNT (1=YES, 0=NO)
; CVHAMT    CEILING ARRAY FOR VER HIGH CLOUD AMOUNT (1=YES, 0=NO)
; CVMAMT    CEILING ARRAY FOR VER MIDDLE CLOUD AMOUNT (1=YES, 0=NO)
; CVLAMT    CEILING ARRAY FOR VER LOW CLOUD AMOUNT (1=YES, 0=NO)
; DTOTL     DIFFERENCE OF TOTAL ARRAYS (VERIFICATION - FORECAST)
; DHAMT     DIFFERENCE OF HIGH ARRAYS (VERIFICATION - FORECAST)
; DMAMT     DIFFERENCE OF MIDDLE ARRAYS (VERIFICATION - FORECAST)
; DLAMT     DIFFERENCE OF LOW ARRAYS (VERIFICATION - FORECAST)
; FILENAME  DATA FILE NAME
; H         LOOP INDEX
; I         LOOP INDEX
; IEND      I-INDEX END
; INDEX(#)  TEMPORARY ARRAY INDEX
; ISRT      I-INDEX
; JEND      J-INDEX END
; JSRT      J-INDEX START
; LAYR(#)   LAYER-1,2,3, or 4 1/8 MESH CLOUD DATA (BIT PACKED)
; L(#)AMT   LAYER-1,2,3, or 4 1/8 MESH CLOUD AMOUNT (ENCODED %)
; L(#)BSE   LAYER-1,2,3, or 4 1/8 MESH CLOUD BASE (ENCODED)
; L(#)TOP   LAYER-1,2,3, or 4 1/8 MESH CLOUD TOP (ENCODED)
; L(#)TYP   LAYER-1,2,3, or 4 1/8 MESH CLOUD TYPE (ENCODED)
; NOE       NUMBER OF ELEMENTS ON A LEVEL AT A GIVEN FORECAST HOUR
; PGCAFH    PERCENT GOOD CLOUD AMOUNT FCST FOR HIGH AMOUNTS
; PGCAFL    PERCENT GOOD CLOUD AMOUNT FCST FOR LOW AMOUNTS
; PGCAFM    PERCENT GOOD CLOUD AMOUNT FCST FOR MIDDLE AMOUNTS
; PERCENT GOOD CLOUD AMOUNT FORECAST FOR TOTAL AMOUNTS
; PYNFTOTL  PERCENT YES/NO FORECAST TOTAL CEILING
; PYNFHAMT  PERCENT YES/NO FORECAST HIGH CEILING
; PYNFMAMT  PERCENT YES/NO FORECAST MIDDLE CEILING
; PYNFLAMT  PERCENT YES/NO FORECAST HIGH CEILING

```

```

; PNFTOTL      PERCENT RWM UNDER FORECAST TOTAL CEILING
; PNFHAMT      PERCENT RWM UNDER FORECAST HIGH CEILING
; PNFAMT       PERCENT RWM UNDER FORECAST MIDDLE CEILING
; PNFLAMT      PERCENT RWM UNDER FORECAST HIGH CEILING
; PYFTOTL      PERCENT RWM OVER FORECAST TOTAL CEILING
; PYFHAMT      PERCENT RWM OVER FORECAST HIGH CEILING
; PYFMAMT      PERCENT RWM OVER FORECAST MIDDLE CEILING
; PYFLAMT      PERCENT RWM OVER FORECAST HIGH CEILING
; RCAMT        RTNEPH GRID CONVECTIVE CLOUD AMOUNT
; RHAMT        RTNEPH GRID RWM HIGH CLOUD AMOUNTS
; RLAMT        RTNEPH GRID RWM LOW CLOUD AMOUNTS
; RMAMT        RTNEPH GRID RWM MID CLOUD AMOUNTS
; RMSET        RMSE OF TOTAL
; RMSEH        RMSE OF HIGH LEVEL
; RMSEM        RMSE OF MIDDLE LEVEL
; RMSEL        RMSE OF LOW LEVEL
; RTOTL        RTNEPH GRID RWM TOTAL CLOUD AMOUNTS
; SQT          SUM OF SQUARE OF TOTAL DIFFERENCE AMOUNTS
; SQH          SUM OF SQUARE OF HIGH DIFFERENCE AMOUNTS
; SQM          SUM OF SQUARE OF MIDDLE DIFFERENCE AMOUNTS
; SQL          SUM OF SQUARE OF LOW DIFFERENCE AMOUNTS
; STHOUR       STRING EQUIVALENT OF INTEGER HOUR
; TOTL8        TOTAL 1/8 MESH CLOUD COVERAGE (%)
; TOTLB        BYTE VERSION OF TOTL8 ARRAY
; TOTCLD_US    RWM GRID TOTAL CLOUD AMOUNTS
; S(#)AMT      SUPER GRID 1/8 MESH AMOUNT FOR LAYER-1,2,3, or 4 (ENCODED)
; S(#)BSE      SUPER GRID 1/8 MESH BASE FOR LAYER-1,2,3, or 4 (ENCODED)
; S(#)TOP      SUPER GRID 1/8 MESH TOP FOR LAYER-1,2,3, or 4 (ENCODED)
; S(#)TYP      SUPER GRID 1/8 MESH TYPE FOR LAYER-1,2,3, or 4 (ENCODED)
; STOTL        SUPER GRID TOTAL 1/8 MESH CLOUD COVERAGE (%)
; TEMPORARY    TEMP ARRAY TO RESIZE RTNEPH VERIFICATION ARRAYS
; UNIT1        LOGICAL UNIT NUMBER FOR EXTERNAL FILE
; UNIT2        LOGICAL UNIT NUMBER FOR EXTERNAL FILE
; VHAMT        VERIFICATION HIGH CLOUD AMOUNT
; VLAMT        VERIFICATION LOW CLOUD AMOUNT
; VMAMT        VERIFICATION MIDDLE CLOUD AMOUNT
;
; UPDATES
; =====
; AUG 96 ORIGINAL VERSION.....CAPT CANTRELL/SYSM
; DEC 96 Changed for the North American region .....LT HARRIS/AFIT
;
; *****
; BYTARR - returns a byte array
; FLTARR - returns a single-precision floating-point array
; INTARR - returns an integer array
; LONARR - returns a longword integer array

```

```

; INFO, /Device

DEVICE, PSEUDO_COLOR=8
; DEVICE, TRUE_COLOR=24

; Transfers images from top to bottom
!ORDER = 1

; "box" sets up the 9 RTNEPH grid boxes in order from top left to bottom right
box=[35,36,37,43,44,45,51,52,53]

; The layers of the RTNEPH grids follow:
; The LONARR function returns a longword integer vector or array
totl8 = LONARR(64,64)
layr1 = LONARR(64,64)
layr2 = LONARR(64,64)
layr3 = LONARR(64,64)
layr4 = LONARR(64,64)
l1amt = BYTARR(64,64)
l1bse = BYTARR(64,64)
l1top = BYTARR(64,64)
l1typ = BYTARR(64,64)
l2amt = BYTARR(64,64)
l2bse = BYTARR(64,64)
l2top = BYTARR(64,64)
l2typ = BYTARR(64,64)
l3amt = BYTARR(64,64)
l3bse = BYTARR(64,64)
l3top = BYTARR(64,64)
l3typ = BYTARR(64,64)
l4amt = BYTARR(64,64)
l4bse = BYTARR(64,64)
l4top = BYTARR(64,64)
l4typ = BYTARR(64,64)

; The RTNEPH 3x3 (192x192) grid for 8 time steps 0,3,6,9,12,15,18,21
stotl = BYTARR(64*3,64*3,8)
s1amt = BYTARR(64*3,64*3,8)
s1bse = BYTARR(64*3,64*3,8)
s1top = BYTARR(64*3,64*3,8)
s1typ = BYTARR(64*3,64*3,8)
s2amt = BYTARR(64*3,64*3,8)
s2bse = BYTARR(64*3,64*3,8)
s2top = BYTARR(64*3,64*3,8)
s2typ = BYTARR(64*3,64*3,8)
s3amt = BYTARR(64*3,64*3,8)
s3bse = BYTARR(64*3,64*3,8)

```

```

s3top = BYTARR(64*3,64*3,8)
s3typ = BYTARR(64*3,64*3,8)
s4amt = BYTARR(64*3,64*3,8)
s4bse = BYTARR(64*3,64*3,8)
s4top = BYTARR(64*3,64*3,8)
s4typ = BYTARR(64*3,64*3,8)

;----- Begin Interactive -----\
;
; day: 1 1 1 1 2 2 2
; If (FORECAST eq 00) then, hour: 00, 06, 12, 18, 00, 06, 12
; or FORECAST (looping) h: 0, 1, 2, 3, 4, 5, 6

; THEN ANALYSIS is: hour: 00, 06, 12, 18, 00, 06, 12
; or ANALYSIS (looping): h: 0, 1, 2, 3, 0, 1, 2

;
; day: 1 1 2 2 2 2 3
; If (FORECAST eq 12) then, hour: 12, 18, 00, 06, 12, 18, 00
; or FORECAST (looping): h: 0, 1, 2, 3, 4, 5, 6

; THEN ANALYSIS is: hour: 12, 18, 00, 06, 12, 18, 00
; or ANALYSIS (looping): h: 0, 1, 0, 1, 2, 3, 0

;*****
;
bgn = 0
fin = 6
;*****

FCST=0
Read,'Enter the RWM Forecast hour (00 or 12):',FCST

IF (FCST EQ 0) THEN BEGIN
monda1=""
Read,'Enter RTNEPH verification numerical month and day (0728):96',monda1
monda2=""
Read,'Enter RTNEPH verification numerical month and day (0729):96',monda2
ENDIF ELSE BEGIN
monda3=""
Read,'Enter RTNEPH verification numerical month and day (0728):96',monda3
monda4=""
Read,'Enter RTNEPH verification numerical month and day (0729):96',monda4
monda5=""
Read,'Enter RTNEPH verification numerical month and day (0730):96',monda5
ENDELSE
;----- Begin to account for corrupt data or data which does not match up -----\
; If the analysis data does not contain all values (0-6) continue building
; the arrays but only build the files which exist.
; The analysis data will more than likely be present and not be garbled
; but may not necessarily matchup with the Forecast data.

```

```

; If an hour within a Forecast file or Analysis file is corrupt,
; don't build the file but keep building the other "good" files.

; The case where there's garbled/corrupt data in the Forecast
ON_IOERROR, BADOBS
Start=0

; Each place corresponds to a value of h
VALIDOBS=[0,0,0,0,0,0,0]

;\----- End Account for data not always matching up perfectly -----/

FOR h=bgn,fin DO BEGIN

IF (FCST EQ 0) THEN BEGIN
  IF (h LE 3) THEN BEGIN
    day=1
    hour=6*h
  ENDIF ELSE BEGIN
    day=2
    hour=6*(h-4)
  ENDELSE
ENDIF ELSE BEGIN
IF (h LE 1) THEN BEGIN
  day=1
  hour=12+(h*6)
ENDIF ELSE IF(h LE 5) THEN BEGIN
  day=2
  hour=6*(h-2)
ENDIF ELSE BEGIN
  day=3
  hour=0
ENDELSE
ENDELSE

PRINT,'RWM FCST=',FCST,'      Day=',day,'      h=',h,'      Hour=',hour

IF (hour LT 10) THEN BEGIN
  sthour = '0' + STRCOMPRESS(STRING(hour),/REMOVE_ALL)
ENDIF ELSE BEGIN
  sthour = STRCOMPRESS(STRING(hour),/REMOVE_ALL)
ENDELSE

; Do for all 9 boxes
FOR i = 0, 8 DO BEGIN

; 00 hour forecast:
IF (FCST EQ 0) THEN BEGIN

```

```

IF (day EQ 1) THEN BEGIN
    filename = '~/rtnephdata/rtneph_96'+monda1+'/b' +
    STRCOMPRESS(box(i),/REMOVE_ALL) + $
    '_' + sthour + 'hr'
ENDIF ELSE BEGIN
    filename = '~/rtnephdata/rtneph_96'+monda2+'/b' +
    STRCOMPRESS(box(i),/REMOVE_ALL) + $
    '_' + sthour + 'hr'
ENDELSE
ENDIF ELSE BEGIN

IF (day EQ 1) THEN BEGIN
    filename = '~/rtnephdata/rtneph_96'+monda3+'/b' +
    STRCOMPRESS(box(i),/REMOVE_ALL) + $
    '_' + sthour + 'hr'
ENDIF ELSE IF (day EQ 2) THEN BEGIN
    filename = '~/rtnephdata/rtneph_96'+monda4+'/b' +
    STRCOMPRESS(box(i),/REMOVE_ALL) + $
    '_' + sthour + 'hr'
ENDIF ELSE BEGIN
    filename = '~/rtnephdata/rtneph_96'+monda5+'/b' +
    STRCOMPRESS(box(i),/REMOVE_ALL) + $
    '_' + sthour + 'hr'
ENDELSE
ENDELSE

;\----- End Interactive -----/
; open the RTNEPH file / Get a unique file unit and open the file
;   OPENR, /Get_Lun; unit1, filename
;   OPENR, unit1, filename, /Get_Lun

Start=1

;PRINT, 'Reading cloud amounts from RTNEPH data files'
    READU, unit1, totl8, layr1, layr2, layr3, layr4

; unpack the layer-1 amount, type, base, and top of the RTNEPH
    l1amt = BYTE(layr1,0,64,64)
    l1typ = BYTE(layr1,1,64,64)
    l1bse = BYTE(layr1,2,64,64)
    l1top = BYTE(layr1,3,64,64)

; unpack the layer-2 amount, type, base, and top of the RTNEPH
    l2amt = BYTE(layr2,0,64,64)
    l2typ = BYTE(layr2,1,64,64)
    l2bse = BYTE(layr2,2,64,64)
    l2top = BYTE(layr2,3,64,64)

```

```

; unpack the layer-3 amount, type, base, and top of the RTNEPH
  l3amt = BYTE(layr3,0,64,64)
  l3typ = BYTE(layr3,1,64,64)
  l3bse = BYTE(layr3,2,64,64)
  l3top = BYTE(layr3,3,64,64)

; unpack the layer-4 amount, type, base, and top of the RTNEPH
  l4amt = BYTE(layr4,0,64,64)
  l4typ = BYTE(layr4,1,64,64)
  l4bse = BYTE(layr4,2,64,64)
  l4top = BYTE(layr4,3,64,64)

; unpack the total amount
  totlb = BYTE(totl8)

; Get the index range of the super grid for the RTNEPH North American box.
; These are the i and j start and end coordinates of the 3x3 RTNEPH
CASE i OF
0: BEGIN
  isrt = 0
  iend = 63
  jsrt = 0
  jend = 63
END
1: BEGIN
  isrt = 64
  iend = 127
  jsrt = 0
  jend = 63
END
2: BEGIN
  isrt = 128
  iend = 191
  jsrt = 0
  jend = 63
END
3: BEGIN
  isrt = 0
  iend = 63
  jsrt = 64
  jend = 127
END
4: BEGIN
  isrt = 64
  iend = 127
  jsrt = 64
  jend = 127
END

```



```

5: BEGIN
  isrt = 128
  iend = 191
  jsrt = 64
  jend = 127
  END
6: BEGIN
  isrt = 0
  iend = 63
  jsrt = 128
  jend = 191
  END
7: BEGIN
  isrt = 64
  iend = 127
  jsrt = 128
  jend = 191
  END
ELSE: BEGIN
  isrt = 128
  iend = 191
  jsrt = 128
  jend = 191
  END
ENDCASE

```

```

; write the data to the supergrids
  stotl(isrt:iend, jsrt:jend, h) = totlb(*,*)

```

```

set_plot,'ps'

```

```

; Save in results subdirectory *****

```

```

device,filename= '/workspace/eharris/results/untrimmed.eps',/encapsulated
tv, BYTSCL(stotl(*,*,5))
DEVICE,/Close_file
SET_PLOT,'X'

```

```

;PRINT, 'stotl array is: ', stotl
  s1amt(isrt:iend, jsrt:jend, h) = l1amt(*,*)
  s2amt(isrt:iend, jsrt:jend, h) = l2amt(*,*)
  s3amt(isrt:iend, jsrt:jend, h) = l3amt(*,*)
  s4amt(isrt:iend, jsrt:jend, h) = l4amt(*,*)
  s1bse(isrt:iend, jsrt:jend, h) = l1bse(*,*)
  s2bse(isrt:iend, jsrt:jend, h) = l2bse(*,*)
  s3bse(isrt:iend, jsrt:jend, h) = l3bse(*,*)
  s4bse(isrt:iend, jsrt:jend, h) = l4bse(*,*)
  s1top(isrt:iend, jsrt:jend, h) = l1top(*,*)
  s2top(isrt:iend, jsrt:jend, h) = l2top(*,*)

```

```

s3top(isrt:iend, jsrt:jend, h) = l3top(*,*)
s4top(isrt:iend, jsrt:jend, h) = l4top(*,*)
s1typ(isrt:iend, jsrt:jend, h) = l1typ(*,*)
s2typ(isrt:iend, jsrt:jend, h) = l2typ(*,*)
s3typ(isrt:iend, jsrt:jend, h) = l3typ(*,*)
s4typ(isrt:iend, jsrt:jend, h) = l4typ(*,*)

GOTO, DONEOBS
BADOBS: PRINT, 'Corrupt data in Slingo/RWM', h
; Mark the data as "not valid"
VALIDOBS(h) = -1
DONEOBS:

IF (Start EQ 1) THEN BEGIN
  FSLUN1 = FSTAT(unit1)
  IF (FSLUN1.OPEN EQ 1) THEN BEGIN
    FREE_LUN, unit1
  ENDIF
ENDIF

ENDFOR
ENDFOR

; Cancels the ON_IOERROR, BADOBS "prompt"
ON_IOERROR, null

; Free all useless arrays
totl8 = 0
layr1 = 0
layr2 = 0
layr3 = 0
layr4 = 0
l1amt = 0
l1bse = 0
l1top = 0
l1typ = 0
l2amt = 0
l2bse = 0
l2top = 0
l2typ = 0
l3amt = 0
l3bse = 0
l3top = 0
l3typ = 0
l4amt = 0
l4bse = 0
l4top = 0
l4typ = 0

```

```

;/-----\
; PROCESS SLINGO OUTPUT CLOUDS
;\-----/

; Reinitialize the grids to the North American RWM
; Forecast times are: 0, 6, 12, 18, 24, 30, 36

      big_cldamt = FLTARR(61,61,4,8)

      TOTCLD_US  = FLTARR(61,61,8)
      cldamt     = FLTARR(61,61,4,8)

; Open the rwm total cloud and cloud amount files
; change the files to match what the Slingo code puts out

;/-----\
      OPENR, unit1, '~/rwmdata/TOTCLD_US', /GET_LUN
;\-----/
      tempread = 0.0

ON_IOERROR, BADFCST
VALIDFCST=[0,0,0,0,0,0,0]

FOR h = bgn, fin DO BEGIN
  FOR j = 0,60 DO BEGIN
    FOR i = 0,60 DO BEGIN
      READU, unit1, tempread
      ; Rearranges the order of the RWM array to correspond to the RTNEPH
      ; array with point (0,0) in the upper left corner for both arrays
      ; Change the array to a new "j-inverted" array:
      ; From: TOTCLD_US(i,j,h) = tempread To:
      TOTCLD_US(i,60-j,h) = tempread

      GOTO,DONEFCST
    BADFCST: PRINT,'Bad Forecast data',h
    VALIDFCST(h)=-1
    DONEFCST:

      ENDFOR
    ENDFOR
  ENDFOR

; Encapsulate the RWM Forecast data "TOTCLD_US" after it's correctly inverted
set_plot,'ps'
; Save in results subdirectory *****

device,filename= '/workspace/eharris/results/correctrwm.eps',/encapsulated

```

```

tv, BYTSCL(TOTCLD_US(*,*,5))
DEVICE,/Close_file
SET_PLOT,'X'

; Cancels the ON_IOERROR, BADFCST "prompt"
ON_IOERROR,null

    tempread = 0.0

FOR h = bgn, fin DO BEGIN
    FOR k = 0,3 DO BEGIN
        FOR j = 0,60 DO BEGIN
            FOR i = 0,60 DO BEGIN

; This is the RWM 61 x 61 x 4 x 8
big_cldamt(i,j,k,h) = tempread

                ENDFOR ; i
            ENDFOR ; j
        ENDFOR ; k
    ENDFOR ; h

; close data files and free LUN's
    FREE_LUN,unit1

    cldamt(0:60,0:60,0:3,0:7) = big_cldamt(0:60,0:60,0:3,0:7)

; free useless arrays
    big_cldamt = 0.0

; /-----Begin Diagnostic code for the RWM -----\
; result = BYTSCL(array) where array is the array to be scaled and
; converted to byte data type. The result is a copy of array whose
; values have been scaled and converted to bytes.
;   WINDOW,3, XS=244,YS=244, Xpos=5, Ypos=5, Title='RWM'
;   WSET,3

;   abd=bytscl(congrid(TOTCLD_US(*,*,4),61*4,61*4))
;   tv, abd

; /---- Begin Enable mouse to display pixel values ---\
;   RDPIX, abd
; \---- End Enable mouse to display pixel values ----/

; \-----End Diagnostic code for the RWM -----/

; PRINT, 'Converting floating RTNEPH data to low, mid, and high amounts'
; These are the trimmed RTNEPH size values which corresponds to the North

```

```

; American supergrid and RWM similar corner points.
; Where: rtxsize: 162-34+1=129, rysize: 174-46+1=129
      rtxsize = 129
      rysize = 129

; These are the trimmed sizes for North America
; Subtract 1 to get the arrays to zero (0) for PVWave
      rtxsizem1 = rtxsize - 1
      rtrysizem1 = rysize - 1

; PRINT, 'Trimming RTNEPH "supergrid" data to match RWM data and window'
      temporary = BYTARR(rtxsize,rysize,8)

; PRINT,'Keeping only the corresponding RTNEPH data which matches the RWM window'
; ... and call it stotl
      temporary(0:rtxsizem1,0:rtrysizem1,0:7) = stotl(34:162,46:174,0:7)
      stotl = temporary
      temporary(0:rtxsizem1,0:rtrysizem1,0:7) = slamt(34:162,46:174,0:7)
      slamt = temporary
      temporary(0:rtxsizem1,0:rtrysizem1,0:7) = slbse(34:162,46:174,0:7)
      slbse = temporary
      temporary(0:rtxsizem1,0:rtrysizem1,0:7) = sltop(34:162,46:174,0:7)
      sltop = temporary
      temporary(0:rtxsizem1,0:rtrysizem1,0:7) = sltyp(34:162,46:174,0:7)
      sltyp = temporary
      temporary(0:rtxsizem1,0:rtrysizem1,0:7) = s2amt(34:162,46:174,0:7)
      s2amt = temporary
      temporary(0:rtxsizem1,0:rtrysizem1,0:7) = s2bse(34:162,46:174,0:7)
      s2bse = temporary
      temporary(0:rtxsizem1,0:rtrysizem1,0:7) = s2top(34:162,46:174,0:7)
      s2top = temporary
      temporary(0:rtxsizem1,0:rtrysizem1,0:7) = s2typ(34:162,46:174,0:7)
      s2typ = temporary
      temporary(0:rtxsizem1,0:rtrysizem1,0:7) = s3amt(34:162,46:174,0:7)
      s3amt = temporary
      temporary(0:rtxsizem1,0:rtrysizem1,0:7) = s3bse(34:162,46:174,0:7)
      s3bse = temporary
      temporary(0:rtxsizem1,0:rtrysizem1,0:7) = s3top(34:162,46:174,0:7)
      s3top = temporary
      temporary(0:rtxsizem1,0:rtrysizem1,0:7) = s3typ(34:162,46:174,0:7)
      s3typ = temporary
      temporary(0:rtxsizem1,0:rtrysizem1,0:7) = s4amt(34:162,46:174,0:7)
      s4amt = temporary
      temporary(0:rtxsizem1,0:rtrysizem1,0:7) = s4bse(34:162,46:174,0:7)
      s4bse = temporary
      temporary(0:rtxsizem1,0:rtrysizem1,0:7) = s4top(34:162,46:174,0:7)
      s4top = temporary
      temporary(0:rtxsizem1,0:rtrysizem1,0:7) = s4typ(34:162,46:174,0:7)

```

```

s4typ = temporary

;----- Begin Diagnostic code - for RTNEPH -----\
; congrid says stotl array will be resampled to 244,244 to match the size
; and pixel resolution of the RWM 61x61 output.
; /Interp - specifies the interpolation method to be used in the resampling
; If zero, uses the nearest neighbor method
; If you want nearest neighbor, don't put /interp in code (UG-141)
; If nonzero, uses the bilinear interpolation method
; RTNEPH to include: 00, 06, 12, 18, 24, 30, 36
; or another way: 0, 1, 2, 3, 0, 1, 2

; WINDOW,5,XS=244,YS=244, XPos=269, Ypos=5, Title='RTNEPH'
; WSET,5

stotltrim=BYTARR(61,61,8)

FOR h= bgn, fin DO BEGIN
  stotltrim(*,*,h)=congrid(stotl(*,*,h),61,61)
ENDFOR

abc=bytsc1(congrid(stotltrim(*,*,2),61*4,61*4))

; Plot the stotl trimmed image for comparison to the untrimmed image
set_plot,'ps'
; Save in results subdirectory *****

device,filename= '/workspace/eharris/results/trimmed.eps',/encapsulated, Scale_factor=.667
tv, bytsc1(stotl(*,*,5))
DEVICE,/Close_file
SET_PLOT,'X'

;tv, bytsc1(stotl(*,*,5))
; WINDOW,4,XS=244,YS=244, Xpos=5, Ypos=5, Title='RTNEPH & RWM Domains'

; Plot the stotl image for comparison to the untrimmed image
set_plot,'ps'
; Save in results subdirectory *****

device,filename= '/workspace/eharris/results/stotltrimmed.eps',/encapsulated
tv, bytsc1(congrid(stotltrim(*,*,5),61*4,61*4))
DEVICE,/Close_file
SET_PLOT,'X'

;\----- End Diagnostic code - for RTNEPH -----/

;----- Begin Plot the domains of RTNEPH and RWM grids -----\
; MAP, Projection=7, Range = [-150.4, 10.3, -40.6, 70.7], Gridstyle=0, $

```

```

; Gridlines=0,/gridlines, Gridcolor='0000ff'x,/NoErase

; WINDOW,4,XS=244,YS=244, Xpos=152, Ypos=293, Title='Grid Domains'

;abc=WINDOW,4,XS=244,YS=244, Xpos=5, Ypos=5, Title='NEPH & RWM Domains'
;device,filename= 'domain.eps',/encapsulated
;tv, abc
;WINDOW,4,XS=244,YS=244, Xpos=5, Ypos=5, Title='NEPH & RWM Domains'
;DEVICE,/Close_file
;SET_PLOT,'X'

;WINDOW,4,XS=244,YS=244, Xpos=5, Ypos=5, Title='RTNEPH & RWM Domains'
;set_plot,'ps'

; Uncomment the line below when you want to save to a postscript file

; map,center=[-95,50],zoom=3,Gridlines='00ff00'x,Gridstyle=0,Projection=7, $
; Gridcolor='00007f'x

;WINDOW,7,XS=244,YS=244, Title='Domain2'
;WSET,7
;map,center=[-95,50],zoom=1,/gridlines,Gridstyle=1,Projection=1
; MAP, Projection=7, Range = [-160.0, -20.0, 120.0, 80.0], $
; Gridlines=3, Gridcolor='00ffff'x,/NoErase

;MAP, Range = [-108.8, 13.3, -44.6 , 64.7], $
; Gridlines=3, Gridcolor=9,/NoErase

; Color 'B G R' 0-255, 0-255, 0-255
; 0-9,a-f = hex digits, using base 16
; i.e., Blue 'ff0000'x , Red '0000ff'x , Green '00ff00'x ,
; Medium grey '7f7f7f'x , Yellow '00ffff'x

; The RWM border with straight lines and no great circle lines plotted
; UL and UR
; MAP_PLOTS, [-144.4, -44.6],[44.2, 64.7], Linestyle=0, $
; Psym=0, Thick=2, /NoCircle
; LR and UR
; MAP_PLOTS, [-69.4, -44.6],[19.6, 64.7], Linestyle=0, $
; Psym=0, Thick=2, /NoCircle
; LR and LL
; MAP_PLOTS, [-108.8, -69.4],[13.3, 19.6], Linestyle=0, $
; Psym=0, Thick=2, /NoCircle
; UL and LL
; MAP_PLOTS, [-144.4, -108.8],[44.2, 13.3], Linestyle=0, $
; Psym=0, Thick=2, /NoCircle
;
;
; Border the RTNEPH window

```

```

; UL and UR
;   MAP_PLOTS, [-170.0, 10.0],[35.707, 61.672], Color='00ff00'x, Linestyle=0, $
;       Psym=0, Thick=2, /NoCircle
; LR and UR
;   MAP_PLOTS, [-61.745, 10.0],[12.285, 61.672], Color='00ff00'x, Linestyle=0, $
;       Psym=0, Thick=2, /NoCircle
; LR and LL
;   MAP_PLOTS, [-61.745, -113.828],[12.285, 4.707], Color='00ff00'x, Linestyle=0, $
;       Psym=0, Thick=2, /NoCircle
; UL and LL
;   MAP_PLOTS, [-170.0, -113.828],[35.707, 4.707], Color='00ff00'x, Linestyle=0, $
;       Psym=0, Thick=2, /NoCircle
;
; \----- End Plot the domains of RTNEPH and RWM grids -----/

```

```

rtotl = FLTARR(61,61,8)
rcamt = FLTARR(61,61,8)
rhamt = FLTARR(61,61,8)
rmamt = FLTARR(61,61,8)
rlamt = FLTARR(61,61,8)
rtotlt = FLTARR(61,61,8)

```

```

rcamtt = FLTARR(61,61)
rhamtt = FLTARR(61,61)
rmamtt = FLTARR(61,61)
rlamtt = FLTARR(61,61)

```

```

totcldt = FLTARR(61,61)
cldamt3 = FLTARR(61,61)
cldamt2 = FLTARR(61,61)
cldamt1 = FLTARR(61,61)
cldamt0 = FLTARR(61,61)

```

```

rtotltt= FLTARR(rtxsize,rtysize,h)

```

```

FOR h = bgn, fin DO BEGIN
  FOR i = 0,60 DO BEGIN
    FOR J = 0,60 DO BEGIN
      totcldt(i,j)=TOTCLD_US(i,j,h)
      cldamt3(i,j)=cldamt(i,j,3,h)
      cldamt2(i,j)=cldamt(i,j,2,h)
      cldamt1(i,j)=cldamt(i,j,1,h)
      cldamt0(i,j)=cldamt(i,j,0,h)
    ENDFOR
  ENDFOR
ENDFOR

```

```

; Use congrid to get RWM and RTNEPH to match up the grid sizes
; to match up with the icombo

```



```

; NEPH(0:60,0:60,h) = congrid(stotl(*,*,h), 61, 61)

rtotltt(0:60,0:60,h) = congrid(stotl(*,*,h), 61, 61)
rtotlt(0:60,0:60,h) = congrid(TOTCLD_US(*,*,h),61,61)

; WSET,3
; tv,bytsc1(congrid(TOTCLD_US(*,*,0),61*4,61*4))

rcamt(0:60,0:60)=congrid(cldamt3(*,*),61,61)
rhamt(0:60,0:60)=congrid(cldamt2(*,*),61,61)
rhamt(0:60,0:60)=congrid(cldamt1(*,*),61,61)
rlamt(0:60,0:60)=congrid(cldamt0(*,*),61,61)

ENDFOR

; initialize verification low, mid, and high and total amount arrays
vhamt = BYTARR(rtxsize, rtysize, 8)
vmamt = BYTARR(rtxsize, rtysize, 8)
vlamt = BYTARR(rtxsize, rtysize, 8)
vtotl = BYTARR(rtxsize, rtysize, 8)

; print,'Evaluating 4 layers of supergrid rtneph data to 3 layers of RWM'
print,'
print, '    This will take a minute . . . '

; for each point in the verification grid
FOR h = bgn, fin DO BEGIN
FOR i = 0,rtxsizem1 DO BEGIN
FOR j = 0,rtysizem1 DO BEGIN

; evaluate layer 1 super grid rtneph data to low, mid, and high amounts.
IF (s1typ(i,j,h) EQ 01 OR s1typ(i,j,h) EQ 11) THEN BEGIN
vhamt(i,j,h) = slamt(i,j,h)
vmamt(i,j,h) = slamt(i,j,h)
vlamt(i,j,h) = slamt(i,j,h)
ENDIF
IF (s1typ(i,j,h) EQ 02 OR s1typ(i,j,h) EQ 12 OR $
s1typ(i,j,h) EQ 03 OR s1typ(i,j,h) EQ 13 OR $
s1typ(i,j,h) EQ 04 OR s1typ(i,j,h) EQ 14 OR $
s1typ(i,j,h) EQ 06 OR s1typ(i,j,h) EQ 16 ) THEN BEGIN
vlamt(i,j,h) = slamt(i,j,h)
ENDIF
IF (s1typ(i,j,h) EQ 05 OR s1typ(i,j,h) EQ 15 OR $
s1typ(i,j,h) EQ 07 OR s1typ(i,j,h) EQ 17 ) THEN BEGIN
vmamt(i,j,h) = slamt(i,j,h)
IF (s1bse(i,j,h) LT 77) THEN vlamt(i,j,h) = slamt(i,j,h)
ENDIF
IF (s1typ(i,j,h) EQ 08 OR s1typ(i,j,h) EQ 18 OR $

```

```

      s1typ(i,j,h) EQ 09 OR s1typ(i,j,h) EQ 19 OR $
      s1typ(i,j,h) EQ 10 OR s1typ(i,j,h) EQ 20 ) THEN BEGIN
      vhamt(i,j,h) = s1amt(i,j,h)
      IF (s1bse(i,j,h) LT 197) THEN vmamt(i,j,h) = s1amt(i,j,h)
      IF (s1bse(i,j,h) LT 77) THEN vlamt(i,j,h) = s1amt(i,j,h)
    ENDIF

```

;evaluate layer 2 super grid rtneph data to low, mid, and high amounts.

```

    IF (s2typ(i,j,h) EQ 01 OR s2typ(i,j,h) EQ 11) THEN BEGIN
      vhamt(i,j,h) = MAX([s2amt(i,j,h),vhamt(i,j,h)])
      vmamt(i,j,h) = MAX([s2amt(i,j,h),vmamt(i,j,h)])
      vlamt(i,j,h) = MAX([s2amt(i,j,h),vlamt(i,j,h)])
    ENDIF
    IF (s2typ(i,j,h) EQ 02 OR s2typ(i,j,h) EQ 12 OR $
      s2typ(i,j,h) EQ 03 OR s2typ(i,j,h) EQ 13 OR $
      s2typ(i,j,h) EQ 04 OR s2typ(i,j,h) EQ 14 OR $
      s2typ(i,j,h) EQ 06 OR s2typ(i,j,h) EQ 16 ) THEN BEGIN
      vlamt(i,j,h) = MAX([s2amt(i,j,h),vlamt(i,j,h)])
    ENDIF
    IF (s2typ(i,j,h) EQ 05 OR s2typ(i,j,h) EQ 15 OR $
      s2typ(i,j,h) EQ 07 OR s2typ(i,j,h) EQ 17 ) THEN BEGIN
      vmamt(i,j,h) = MAX([s2amt(i,j,h),vmamt(i,j,h)])
      IF (s2bse(i,j,h) LT 77) THEN vlamt(i,j,h) = $
        MAX([s2amt(i,j,h),vlamt(i,j,h)])
    ENDIF
    IF (s2typ(i,j,h) EQ 08 OR s2typ(i,j,h) EQ 18 OR $
      s2typ(i,j,h) EQ 09 OR s2typ(i,j,h) EQ 19 OR $
      s2typ(i,j,h) EQ 10 OR s2typ(i,j,h) EQ 20 ) THEN BEGIN
      vhamt(i,j,h) = MAX([s2amt(i,j,h),vhamt(i,j,h)])
      IF (s2bse(i,j,h) LT 197) THEN vmamt(i,j,h) = $
        MAX([s2amt(i,j,h),vmamt(i,j,h)])
    ENDIF

```

;evaluate layer 3 super grid rtneph data to low, mid, and high amounts.

```

    IF (s3typ(i,j,h) EQ 01 OR s3typ(i,j,h) EQ 11) THEN BEGIN
      vhamt(i,j,h) = MAX([s3amt(i,j,h),vhamt(i,j,h)])
      vmamt(i,j,h) = MAX([s3amt(i,j,h),vmamt(i,j,h)])
      vlamt(i,j,h) = MAX([s3amt(i,j,h),vlamt(i,j,h)])
    ENDIF
    IF (s3typ(i,j,h) EQ 02 OR s3typ(i,j,h) EQ 12 OR $
      s3typ(i,j,h) EQ 03 OR s3typ(i,j,h) EQ 13 OR $
      s3typ(i,j,h) EQ 04 OR s3typ(i,j,h) EQ 14 OR $
      s3typ(i,j,h) EQ 06 OR s3typ(i,j,h) EQ 16 ) THEN BEGIN
      vlamt(i,j,h) = MAX([s3amt(i,j,h),vlamt(i,j,h)])
    ENDIF
    IF (s3typ(i,j,h) EQ 05 OR s3typ(i,j,h) EQ 15 OR $
      s3typ(i,j,h) EQ 07 OR s3typ(i,j,h) EQ 17 ) THEN BEGIN
      vmamt(i,j,h) = MAX([s3amt(i,j,h),vmamt(i,j,h)])

```

```

      IF (s3bse(i,j,h) LT 77) THEN vlamt(i,j,h) = $
        MAX([s3amt(i,j,h), vlamt(i,j,h)])
    ENDIF
    IF (s3typ(i,j,h) EQ 08 OR s3typ(i,j,h) EQ 18 OR $
      s3typ(i,j,h) EQ 09 OR s3typ(i,j,h) EQ 19 OR $
      s3typ(i,j,h) EQ 10 OR s3typ(i,j,h) EQ 20 ) THEN BEGIN
      vhamt(i,j,h) = MAX([s3amt(i,j,h), vhamt(i,j,h)])
      IF (s3bse(i,j,h) LT 197) THEN vmamt(i,j,h) = $
        MAX([s3amt(i,j,h), vmamt(i,j,h)])
      IF (s3bse(i,j,h) LT 77) THEN vlamt(i,j,h) = $
        MAX([s3amt(i,j,h), vlamt(i,j,h)])
    ENDIF

```

;evaluate layer 4 super grid rtneph data to low, mid, and high amounts.

```

    IF (s4typ(i,j,h) EQ 01 OR s4typ(i,j,h) EQ 11) THEN BEGIN
      vhamt(i,j,h) = MAX([s4amt(i,j,h), vhamt(i,j,h)])
      vmamt(i,j,h) = MAX([s4amt(i,j,h), vmamt(i,j,h)])
      vlamt(i,j,h) = MAX([s4amt(i,j,h), vlamt(i,j,h)])
    ENDIF
    IF (s4typ(i,j,h) EQ 02 OR s4typ(i,j,h) EQ 12 OR $
      s4typ(i,j,h) EQ 03 OR s4typ(i,j,h) EQ 13 OR $
      s4typ(i,j,h) EQ 04 OR s4typ(i,j,h) EQ 14 OR $
      s4typ(i,j,h) EQ 06 OR s4typ(i,j,h) EQ 16 ) THEN BEGIN
      vlamt(i,j,h) = MAX([s4amt(i,j,h), vlamt(i,j,h)])
    ENDIF
    IF (s4typ(i,j,h) EQ 05 OR s4typ(i,j,h) EQ 15 OR $
      s4typ(i,j,h) EQ 07 OR s4typ(i,j,h) EQ 17 ) THEN BEGIN
      vmamt(i,j,h) = MAX([s4amt(i,j,h), vmamt(i,j,h)])
      IF (s4bse(i,j,h) LT 77) THEN vlamt(i,j,h) = $
        MAX([s4amt(i,j,h), vlamt(i,j,h)])
    ENDIF
    IF (s4typ(i,j,h) EQ 08 OR s4typ(i,j,h) EQ 18 OR $
      s4typ(i,j,h) EQ 09 OR s4typ(i,j,h) EQ 19 OR $
      s4typ(i,j,h) EQ 10 OR s4typ(i,j,h) EQ 20 ) THEN BEGIN
      vhamt(i,j,h) = MAX([s4amt(i,j,h), vhamt(i,j,h)])
      IF (s4bse(i,j,h) LT 197) THEN vmamt(i,j,h) = $
        MAX([s4amt(i,j,h), vmamt(i,j,h)])
      IF (s4bse(i,j,h) LT 77) THEN vlamt(i,j,h) = $
        MAX([s4amt(i,j,h), vlamt(i,j,h)])
    ENDIF

```

```

  ENDFOR ; j
  ENDFOR ; i
  ENDFOR ; h

```

; Find the total cloud amount for verification array
 vtotl = ((vhamt + vmamt + vlamt) < 100)

```

; Free useless arrays
    temporary = 0
    stotl = 0
    s1amt = 0
    s1bse = 0
    s1top = 0
    s1typ = 0
    s2amt = 0
    s2bse = 0
    s2top = 0
    s2typ = 0
    s3amt = 0
    s3bse = 0
    s3top = 0
    s3typ = 0
    s4amt = 0
    s4bse = 0
    s4top = 0
    s4typ = 0

; /----- Begin Build contingency table ----- \

IF (FCST EQ 0) THEN BEGIN
    Forecast = '00_'
ENDIF ELSE BEGIN
    Forecast = '12_'
ENDELSE

PRINT, 'Max Neph Table Value = ',max(stotltrim)
PRINT, 'Min Neph Table Value = ',min(stotltrim)

PRINT, 'Max RWM Table Value = ',max(100*TOTCLD_US)
PRINT, 'Min RWM Table Value = ',min(100*TOTCLD_US)

FOR h=bgn,fin DO BEGIN

; Check to see is the value of h is any good?
; The value of 0 represents "true" and -1 represents "false"

IF ((VALIDFCST(h) EQ 0) AND (VALIDOBS(h) EQ 0)) THEN BEGIN

IF (FCST EQ 0) THEN BEGIN
    IF (h LE 3) THEN BEGIN
        day=1
        hour=6*h
    ENDIF ELSE BEGIN
        day=2
        hour=6*(h-4)
    ENDIF
ENDIF
ENDIF

```

```

    ENDELSE
ENDIF ELSE BEGIN
IF (h LE 1) THEN BEGIN
    day=1
    hour=12+(h*6)
ENDIF ELSE IF(h LE 5) THEN BEGIN
    day=2
    hour=6*(h-2)
ENDIF ELSE BEGIN
    day=3
    hour=0
ENDELSE
ENDELSE

IF (hour LT 10) THEN BEGIN
    sthour = '0' + STRCOMPRESS(STRING(hour),/REMOVE_ALL)
ENDIF ELSE BEGIN
    sthour = STRCOMPRESS(STRING(hour),/REMOVE_ALL)
ENDELSE

; 00 hour forecast:
IF (FCST EQ 0) THEN BEGIN
    IF (day EQ 1) THEN BEGIN
        monda = monda1
    ENDIF ELSE BEGIN
        monda = monda2
    ENDELSE
ENDIF ELSE BEGIN
    IF (day EQ 1) THEN BEGIN
        monda = monda3
    ENDIF ELSE IF (day EQ 2) THEN BEGIN
        monda = monda4
    ENDIF ELSE BEGIN
        monda = monda5
    ENDELSE
ENDELSE

IF (h LT 2) THEN BEGIN
    FT = '_0' + STRCOMPRESS(STRING(6*h),/REMOVE_ALL)
ENDIF ELSE BEGIN
    FT = '_' + STRCOMPRESS(STRING(6*h),/REMOVE_ALL)
ENDELSE

; To make sure all files are unique, append the forecast hour to the filename
; for both days. For example, FT would = 00, 06, 12, 18, 24, 30, 36

filename = '/workspace/eharris/results/' + Forecast + monda + 'table' + sthour + FT + '.prn'

```

```

table=MAKE_ARRAY(101,101, Type=2, Value=0)
OPENW, 25, filename

;PRINT,'RWM FCST=',FCST,'      Day=',day,'      h=',h,'      Hour=',hour,'      FT=',FT

FOR i=0,60 DO BEGIN
  FOR j=0,60 DO BEGIN
    a=FIX(stotltrim(i,j,h))
    b=FIX(100.*TOTCLD_US(i,j,h))

; account for values of a < 0 and > 100
IF (a GT 100) THEN BEGIN
  a = 100
ENDIF ELSE IF (a LT 0) THEN BEGIN
  a = 0
ENDIF
; account for values of b < 0 and > 100
IF (b GT 100) THEN BEGIN
  b = 100
ENDIF ELSE IF (b LT 0) THEN BEGIN
  b = 0
ENDIF

; Discard the data outside the bounds of 0 to 100
; IF (a LTE 100) or (a GTE 0) THEN
; BEGIN
; table(a,b)=table(a,b)+1
; ENDIF

    table(a,b)=table(a,b)+1

  ENDFOR
ENDFOR
PRINT, 'Table Value = ',max(table)
PRINTF, 25, FORMAT='(101(i4))',table
CLOSE,25

; END the "h check"
ENDIF

ENDFOR
;\----- End building of contingency table -----/
print, '      ... just a few more seconds.'

; I have 8 frames of observed RTNEPH data "converted" (rtotlft, a 61x61x8 array),
; and 8 frames of forecast RWM data (rtotlt, a 61x61x8 array). I'm going to display
; these two images side by side, and then two more under them (each 61x61x8)
; and both being rtotlft(i,j,k) minus rtotlt(i,j,k), with one displaying the

```

```

; pixels with a positive result (underforecast), and the other displaying
; the pixels with a negative result (overforecast). I'll combine all 4 images into one
; array for display, and I will call it icombo.....it has dimension (244,61,7)
; If there is an extra image (i.e., 7 vs 8) the extra image can be a blank image to see clearly the
; beginning of another loop. The eighth image is not necessary but makes the end of the loop
; much more clearer to see.

```

```

icombo=BYTARR(122,122,8)

```

```

;print, 'MAX=',max (rtotlt)
;print, 'MIN=',min (rtotlt)

```

```

RWM=BYTARR(61,61,8)
NEPH=BYTARR(61,61,8)

```

```

RWM=BYTSCL(rtotlt)
NEPH=BYTSCL(rtotltt)

```

```

FOR kk = bgn, fin DO BEGIN
  FOR jj = 0,60,1 DO BEGIN
    FOR ii = 0,60,1 DO BEGIN
      ll=ii+61
      nn=jj+61
    
```

```

; bytscl arranges brightness scale to be from 0 - 255
; 128,128 to 61,61 will have a new array both 61,61
; Transforming from coarser to finer resolution would be incorrect
; and would be degrading the "pixel replication"
; and this would make it "blockier", visually.

```

```

; Upper-left box of icombo with RTNEPH Imagery
  icombo(ii,jj,kk)=NEPH(ii,jj,kk)

```

```

; Upper-right box of icombo with RWM Forecast Imagery
  icombo(ll,jj,kk)=RWM(ii,jj,kk)

```

```

; Calculate difference in bytescale between upper left and upper right
  idiff= FIX(NEPH(ii,jj,kk))-FIX(RWM(ii,jj,kk))

```

```

; If difference is greater than zero, we've underforecasted
  if (idiff ge 0) then begin

```

```

; Put the difference in lower left box and convert to BYTE
    icombo(ii,nn,kk)=BYTE(idiff)

```

```

; Make sure the same pixel location in overforecast box is black
    icombo(ll,nn,kk)=0
  
```

```

; If difference calculated above is less than zero, then it's overforecasted
endif else begin

; make sure pixel location in underforecast box is black
icombo(ii,nn,kk)=0

; and put the difference in that pixel location in overforecast box
icombo(ll,nn,kk)= BYTE(ABS(idiff))
endelse
ENDFOR
ENDFOR
ENDFOR

; Write icombo to file for fast display
get_lun,lun
OPENW,lun,'icombo.dat'
WRITEU,lun,ICOMBO

bigicombo=BYTARR(122*4,122*4,8)
;*****
; Set the environment for postscript then change to encapsulated to input into WORD
set_plot,'ps'

FOR h = 0,6 DO BEGIN
    bigicombo(*,*,h)=congrid(ICOMBO(*,*,h),122*4,122*4)

    IF (h LT 2) THEN BEGIN
        FT = '_0' + STRCOMPRESS(STRING(6*h),/REMOVE_ALL)
    ENDIF ELSE BEGIN
        FT = '_' + STRCOMPRESS(STRING(6*h),/REMOVE_ALL)
    ENDELSE

    DEVICE,filename='/workspace/eharris/results/' + FT + 'table.eps',/encapsulated
    tv, bigicombo(*,*,h)
    DEVICE,/Close_file

ENDFOR

; Set the environment back to X to view the movie
SET_PLOT,'X'
WINDOW, 2, XS=122*4,YS=122*4, Xpos=5, Ypos=750, $
TITLE=' RTNEPH Analysis / RWM Forecast'

; WINDOW, 3, XS=122*4,YS=122*4, Xpos=5, Ypos=470, $
; TITLE=' RWM Under Forecast / RWM Over Forecast'

movie, bigicombo, order=1

```


;/----- Begin Build Persistence contingency table -----\

IF (FCST EQ 0) THEN BEGIN

Forecast = '00_'

ENDIF ELSE BEGIN

Forecast = '12_'

ENDELSE

FOR h=bgn,fin DO BEGIN

IF ((VALIDFCST(h) EQ 0) AND (VALIDOBS(h) EQ 0)) THEN BEGIN

IF (FCST EQ 0) THEN BEGIN

IF (h LE 3) THEN BEGIN

day=1

hour=6*h

ENDIF ELSE BEGIN

day=2

hour=6*(h-4)

ENDELSE

ENDIF ELSE BEGIN

IF (h LE 1) THEN BEGIN

day=1

hour=12+(h*6)

ENDIF ELSE IF (h LE 5) THEN BEGIN

day=2

hour=6*(h-2)

ENDIF ELSE BEGIN

day=3

hour=0

ENDELSE

ENDELSE

;PRINT,"

;PRINT,'RWM FCST=',FCST,' Day=',day,' h=',h,' Hour=',hour

IF (hour LT 10) THEN BEGIN

sthour = '0' + STRCOMPRESS(STRING(hour),/REMOVE_ALL)

ENDIF ELSE BEGIN

sthour = STRCOMPRESS(STRING(hour),/REMOVE_ALL)

ENDELSE

; 00 hour forecast:

IF (FCST EQ 0) THEN BEGIN

IF (day EQ 1) THEN BEGIN

monda = monda1

ENDIF ELSE BEGIN

```

        monda = monda2
    ENDELSE
ENDIF ELSE BEGIN
    IF (day EQ 1) THEN BEGIN
        monda = monda3
    ENDIF ELSE IF (day EQ 2) THEN BEGIN
        monda = monda4
    ENDIF ELSE BEGIN
        monda = monda5
    ENDELSE
ENDELSE

IF (h LT 2) THEN BEGIN
    FT = '_0' + STRCOMPRESS(STRING(6*h),/REMOVE_ALL)
ENDIF ELSE BEGIN
    FT = '_' + STRCOMPRESS(STRING(6*h),/REMOVE_ALL)
ENDELSE

;PRINT,'RWM FCST=',FCST,'      Day=',day,'      h=',h,'      Hour=',hour,'      FT=',FT

filename = '/workspace/eharris/results/' + Forecast + monda + 'perstable' + sthour + FT + '.prn'

perstable=MAKE_ARRAY(101,101, Type=2, Value=0)
OPENW, 24, filename

FOR i=0,60 DO BEGIN
    FOR j=0,60 DO BEGIN
        FT=FIX(stotltrim(i,j,0))
        OBS=FIX(stotltrim(i,j,h))

; account for values of FT < 0 and > 100
        IF (FT GT 100) THEN BEGIN
            FT = 100
        ENDIF ELSE IF (FT LT 0) THEN BEGIN
            FT = 0
        ENDIF
; account for values of OBS < 0 and > 100
        IF (OBS GT 100) THEN BEGIN
            OBS = 100
        ENDIF ELSE IF (OBS LT 0) THEN BEGIN
            OBS = 0
        ENDIF

        perstable(FT,OBS)=perstable(FT,OBS)+1
    ENDFOR
ENDFOR
PRINT, 'Persis_table Value=',max(perstable)
PRINTF, 24, format='(101(i4))',perstable

```

```

CLOSE,24
ENDIF
ENDFOR
; \----- End building of Persistence table array -----/

; /----- Begin persistence movie -----\

; Magnitude: RMSE is a good score but it's limited.
; Qualitatively a forecast may look good and yet have poor RMSE scores.
; A visual check can't be replaced by any score.

; Make a movie with the initial RTNEPH analysis persisted and build table
; like the RWM forecast

persicombo=BYTARR(122,122,8)
persNEPH=BYTARR(61,61,8)
persNEPH=BYTSCL(rtotlft)

FOR kk = bgn, fin DO BEGIN
  FOR jj = 0,60,1 DO BEGIN
    FOR ii = 0,60,1 DO BEGIN
      ll=ii+61
      nn=jj+61

; Upper-left box of icombo with RTNEPH "Analysis" Imagery
      persicombo(ii,jj,kk)=persNEPH(ii,jj,kk)

; Upper-right box of icombo with Persisted RTNEPH "Forecast" Imagery
      persicombo(ll,jj,kk)=NEPH(ii,jj,0)

; Calculate difference in bytescale between upper-left and upper-right box
      persidiff= FIX(persNEPH(ii,jj,kk))-FIX(NEPH(ii,jj,0))

; If difference is greater than zero, we've underforecasted
      IF (persidiff GE 0) THEN BEGIN

; Put the difference in a pixel in lower-left box converted to BYTE
      persicombo(ii,nn,kk)=BYTE(persidiff)

; Make sure the same pixel location is black in overforecast box
      persicombo(ll,nn,kk)=0

; If difference calculated above is less than zero, then it's overforecasted
      ENDIF ELSE BEGIN

; make sure pixel location in underforecast box is black
      persicombo(ii,nn,kk)=0

```

```

; and put the difference in that pixel location in overforecast box
    persicombo(ll,nn,kk)= BYTE(ABS(persidiff))
    ENDELSE

    ENDFOR
    ENDFOR
ENDFOR

get_lun,lun
OPENW,lun,'persicombo.dat'
WRITEU,lun,PERSICOMBO

persbigicombo=BYTARR(122*4,122*4,8)

; Set the environment for poscript then change to encapsulated to input into WORD
set_plot,'ps'

FOR h = 0,7 DO BEGIN
    persbigicombo(*,*,h)=congrid(PERSICOMBO(*,*,h),122*4,122*4)

    IF (h LT 2) THEN BEGIN
        FT = '_0' + STRCOMPRESS(STRING(6*h),/REMOVE_ALL)
    ENDIF ELSE BEGIN
        FT = '_' + STRCOMPRESS(STRING(6*h),/REMOVE_ALL)
    ENDELSE

    DEVICE,filename='/workspace/eharris/results/' + FT + 'persist.eps',/encapsulated
    tv, persbigicombo(*,*,h)
    DEVICE,/Close_file

ENDFOR

; Set the environment back to X to view the movie
SET_PLOT,'X'

WINDOW, 3, XS=122*4,YS=122*4, Xpos=700, Ypos=5, $
TITLE='    RTNEPH Analysis    /    RTNEPH Persisted'

movie, persbigicombo, order=1

END

```

Appendix G: Example of Other Quality Control Data Used.

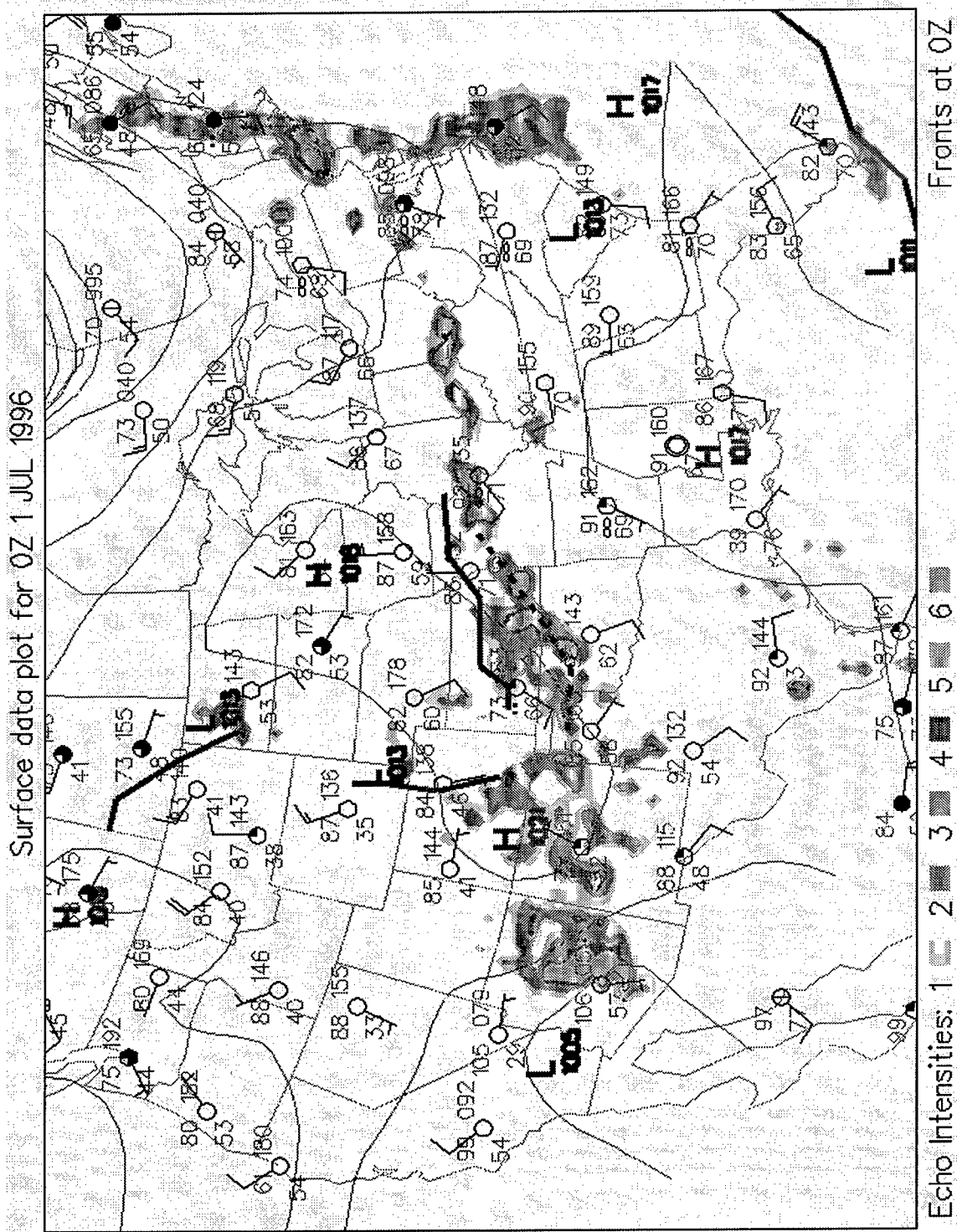


Figure 64: Surface analysis for 1 July 1996 at 00 UTC.

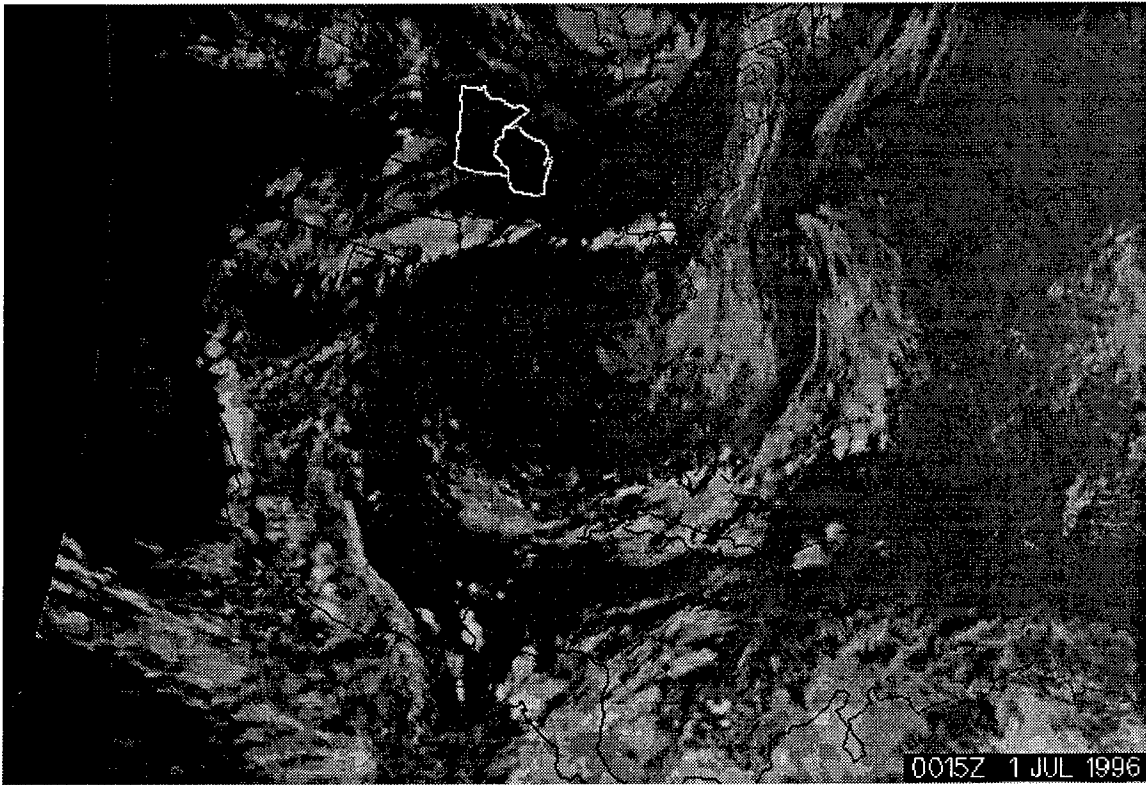


Figure 65: IR satellite picture for 1 July 1996 at 0015 UTC near domain of study (RWM window). A satellite photo is different from a bytescale image. With a satellite photo, a meteorologist can infer low, middle, high and type of cloud. However, a bytescale image only displays the total cloudiness represented by a brightness value. For example, over Northern Minnesota and Wisconsin (highlighted), the satellite photo shows what appears to be overcast low clouds. These low clouds are relatively warm and appear darker than colder, higher clouds. A bytescale representation of the clouds in the same region would display a bytescale of 100 (a brightness of 255 indicating 100% cloud coverage).

Appendix H: Chi-Square Test and Results.

The chi-square (χ^2) test is used in this study as a statistical test, based on frequency of occurrence, applicable to quantitative variables. Among its many uses, the most common are tests of hypothesized probabilities or probability distributions (goodness-of-fit), statistical dependence or independence (association), and common population (homogeneity). When studying only one variable, the interest is how frequently each categorical value of variable occurs among our set of objects. However, in this study, evaluation is in multivariate form, with each object measured on two variables. We want to determine whether the variables are related to one another (dependent) or are independent. During the study, we are only observing a sample from the population of RWM forecasts. The statistical comparison of the observed and expected frequencies of variables is referred to as goodness-of-fit test.

In interpreting the results, one must remember that large samples may produce significant differences that are so small that they have no practical importance. Likewise, if the sample size is very small, a high degree of relationship may exist between the two variables but the χ^2 will not reflect the significance of this relationship. Finally, because χ^2 is computed on interval data, the obtained values of χ^2 can only increase by increments of whole values (Devore, 1995 and Wilks, 1995). The figure on the following page is a scatterplot of the RWM chi-square test through time for all cases and its descriptive statistics.

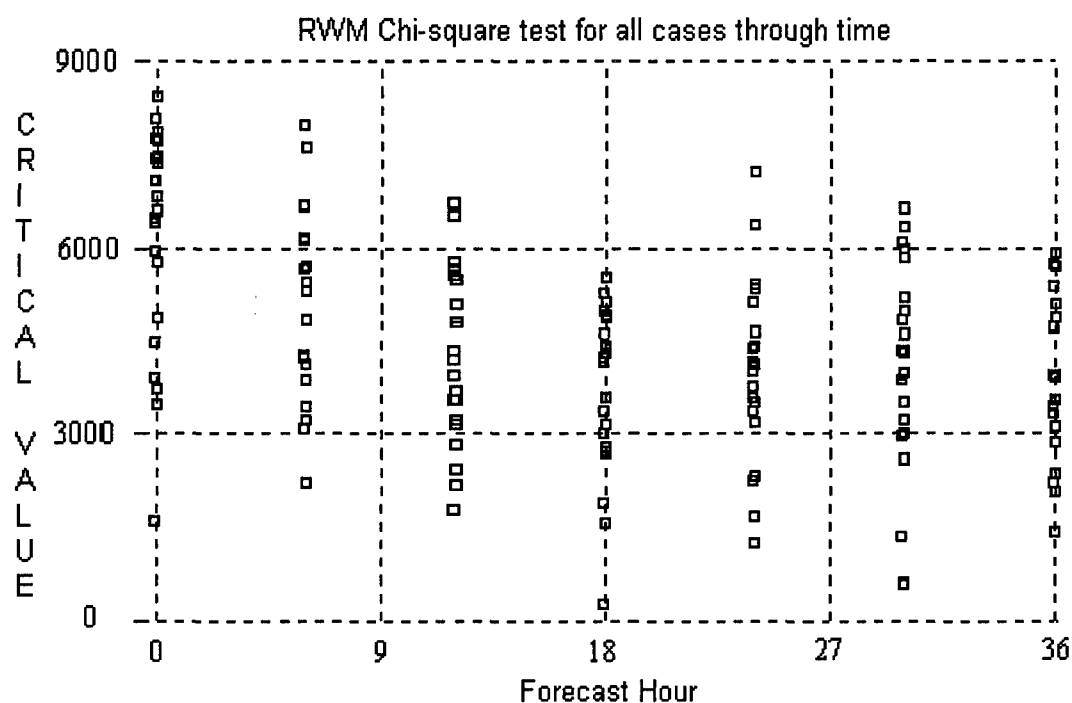


Figure 65: RWM chi-square test of association for all cases through time. Values becoming less positive over time indicates a trend towards dependence of the RWM against the RTNEPH. However, the values all indicate strong independence of the RWM against the RTNEPH. Refer to Table 33 for descriptive statistics.

Table 33: Descriptive statistics for Figure 64.

<u>Chi-Square Test of Association</u>		
	<u>RWM</u>	<u>Persistence</u>
MEAN	4448.8	-12175
SD	1715.3	59671
MINIMUM	-1592.0	-272764
MEDIAN	4328.0	2018.0
MAXIMUM	8465.0	4159.0

Appendix I: Hypothesis Testing.

Hypothesis testing is the process of statistically inferring from sample data whether or not to accept the null hypothesis about the total population from which the data was obtained. The hypothesis to be tested (null hypothesis) is evaluated on the basis of the evidence contained in the sample data. The null hypothesis is then either accepted or rejected by a test applied to the sample data (late spring and early summer data), in this case using the Chi-square test. Rejection carries the meaning that evidence from the sample shows enough doubt about the null hypothesis to say with some identified degree of confidence that the hypothesis is false.

The identified degree of confidence is usually translated into a quantity called the level of significance. This level of significance is defined as the maximum probability of rejecting a true null hypothesis.

The null hypothesis established for this research project is one of independence. The alternate hypothesis, the statement accepted if the null hypothesis is rejected, states the observations under one criteria (RWM forecasts) are dependent on the second criteria (RTHEPH analysis). Dependence is defined as one criteria (variable) being associated with the numerical quantity of the second criteria (variable). Therefore, the analysis has two possible outcomes for any specified level of significance: (1) the null hypothesis is accepted (independence cannot be disproven) or (2) the null hypothesis is rejected (dependence is accepted).

Bibliography

- Campana, K., 1995: Use of cloud analysis to validate and improve model-diagnostic clouds at NMC. Proceedings of a workshop held at ECMWF/GEWEX. *Modeling, validation, and assimilation of clouds*, Reading, U.K., 207-231.
- Cantrell, L., Captain, USAF, Programmer/Analyst, Cloud Models Team, AFGWC, Offutt Air Force Base. Personal Correspondence.
- Conklin, R. J., 1992: *Computer Models used by AFGWC and NMC for Weather Analysis and Forecasting*. AFGWC/TN - 92/001. Air Force Global Weather Central, 69 pp.
- Crum, T. D., 1987: AFGWC cloud forecast models. AFGWC Tech. Note 87/001. Air Force Global Weather Central, 73 pp.
- Devore, J. L., 1995: *Probability and Statistics for Engineering and the Sciences, Fourth Edition*. Duxbury Press, 743 pp.
- Ek, M. and L. Mahrt, 1991: *A formulation for boundary-layer cloud cover*. Annual Geophysicae 9, No. 11, November, 716-724.
- Hamill, T. M., R. P. D'Entremont, and J. T. Bunting, 1992: A description of the Air Force Real-Time Nephanalysis Model. *Wea. Forecasting*, 7, 288-306.
- Hodur, R.M., 1993: Development and testing of the Coupled Ocean/Atmosphere Mesoscale Prediction System (COAMPS). Technical Report NRL/MR/7533-93-7213, Naval Research Laboratory, Monterey, CA 93943-5502, 81 pp.
- Kidder, S. Q. and T. H. VonderHaar, 1995: *Satellite Meteorology, An Introduction*. Academic Press, 466 pp.
- Kiess, R. B., Cox, W. M., 1988: *The AFGWC Automated Real-Time Cloud Analysis Model*. AFGWC/Tech. Note 88/001. Air Force Global Weather Central, 91 pp.
- Lowther, R., M. Surmeier, R. Hartman, C. Coffin, and A. Warren, 1991. *RTNEPH Total Cloud Cover Validation Study*. USAFETAC/PR—91/020. USAF Environmental Technical Applications Center.
- Mathur, M. B., 1983: A Quasi-Lagrangian Regional Model Designed for Operational Weather Prediction. *Monthly Weather Review*, Vol. 111, No. 10, 2087-2099.
- Neel, E., L. Englehart, R. Hughes, and K. Lunn, 1993. *Functional Description AFGWC/SYSM*, The Aerospace Corporation, Orbital Systems Operations, Systems Applications Directorate, 11-72
- Nehrkorn, T., M. Mickelson, M. Zivkovic, and L. W. Knowlton, 1994: *Evaluation of NWP and cloud forecasts from the Phillips Laboratory Global Spectral Model*. PL-TR-94-2296, Phillips Laboratory, Hanscom Air Force Base, 216 pp.
- _____, M. Zivkovic, 1996: A Comparison of Diagnostic Cloud Cover Schemes. *Monthly Weather Review*, Vol. 124, No. 8, 1732-1745.
- Norquist, D., H. Muench, D. Aiken, and D. Hahn, 1994. *Diagnosing Cloudiness from Global Numerical Weather Prediction Model Forecasts*. PL-TR-94-2211, Phillips Laboratory, Hanscom AFB, MA
- Pace, J., M. McAtee, C. Posey, 1989. Planned Use of the AFGWC Relocatable Window Model. *Weather Analysis and Forecasting*, 12, 575-577.
- Slingo, J. M., 1980: A cloud parametrization scheme derived from GATE data for use with a numerical model. *Quart. J. Roy. Meteor. Soc.*, 106, 747-770.

- _____, 1987: The development and verification of a cloud prediction scheme for the ECMWF model. *Quart. J. Roy. Meteor. Soc.*, **113**, 899-927.
- Stobie, J. G., 1986: *AFGWC's Advanced Weather Analysis and Prediction System (AWAPS)*. AWS/TN-86/001, Air Weather Service, Scott AFB, IL, 68 pp.
- Tiedtke, M., 1995: Critical aspects of cloud-parameterization in large-scale models. Proceedings of a workshop held at ECMWF/GEWEX. *Modeling, validation, and assimilation of clouds*, Reading, U.K., 23-42.
- Trapnell, R. N., 1992: Cloud curve algorithm test program, *Report PL-TR-92-2052*, Phillips Laboratory, Hanscom AFB, MA, 170 pp.
- Wilks, D. S., 1995: *Statistical Methods in the Atmospheric Sciences*. Academic Press, 467 pp.
- Wonsick, M., Captain, USAF, Programmer/Analyst, Cloud Models Team, AFGWC, Offutt Air Force Base. Personal Correspondence.
- Zamiska, A., P. Giese, 1995: *RTNEPH, USAFETAC Climatic Database Users Handbook No. 1*. USAFETAC/UH-86/01 (Rev). USAF Environmental Technical Applications Center, 15 pp.

Vita

Edward C. Harris [REDACTED]

[REDACTED] and completed Basic Military Training (BMT) at Lackland AFB, Texas. After BMT, he was assigned to Chanute AFB, Illinois to complete his initial training at the Weather Observing School and concurrently, the Weather Forecasting School (through the fast-track program). After nearly a year of weather training, he was assigned to Columbus AFB, Mississippi. Ed was certified as a weather observer after approximately six months, then certified as a weather forecaster. He had numerous TDY's during his nearly six years at Columbus AFB, including a TDY to Moron AB, Spain during the height of the Persian Gulf War. In 1992, he was selected into the Airman Education and Commissioning Program and chose to attend Florida State University (FSU). Upon graduation from FSU with a Bachelor of Science degree in Meteorology and completing Officer Training School on 11 August 1995, Ed was commissioned a second lieutenant in the U.S. Air Force. He was given the opportunity to enter the inaugural class of the Air Force Institute of Technology meteorology program to earn a Master of Science degree in meteorology. Following AFIT, he was assigned to the 1st Armored Division Headquarters, Bad Kreuznach, Germany, as Cadre Weather Team, Officer in Charge.

Ed is married to the former Tammy Smith of National City, Michigan. They were married on

[REDACTED] and have two children: Matthew, [REDACTED]; and Stephanie, [REDACTED].

[REDACTED]
[REDACTED]
[REDACTED]

REPORT DOCUMENTATION PAGE			Form Approved OMB No. 0704-0188	
<small>Public reporting burden for this collection of information is estimated to average 1 hour per response, including the time for reviewing instructions, searching existing data sources, gathering and maintaining the data needed, and completing and reviewing the collection of information. Send comments regarding this burden estimate or any other aspect of this collection of information, including suggestions for reducing this burden, to Washington Headquarters Services, Directorate for Information Operations and Reports, 1215 Jefferson Davis Highway, Suite 1204, Arlington, VA 22202-4302, and to the Office of Management and Budget, Paperwork Reduction Project (0704-0188), Washington, DC 20503.</small>				
1. AGENCY USE ONLY (Leave blank)		2. REPORT DATE March 1997		3. REPORT TYPE AND DATES COVERED Final
4. TITLE AND SUBTITLE Validation of the Air Force Global Weather Center Relocatable Window Model Total Cloud Forecast			5. FUNDING NUMBERS	
6. AUTHOR(S) Edward C. Harris, 2Lt, USAF				
7. PERFORMING ORGANIZATION NAME(S) AND ADDRESS(ES) AFIT/ENP 2950 P. Street Wright-Patterson AFB, OH 45433 Attn: Lt Col Mike Walters			8. PERFORMING ORGANIZATION REPORT NUMBER AFIT/GM/ENP/97M-07	
9. SPONSORING/MONITORING AGENCY NAME(S) AND ADDRESS(ES) HQ AFGWC/SYSM 106 Peacekeeper Drive Suite 2N3 Offutt AFB, NE 68113-4021 Attn: Capt Lou Cantrell			10. SPONSORING/MONITORING AGENCY REPORT NUMBER	
11. SUPPLEMENTARY NOTES				
12a. DISTRIBUTION AVAILABILITY STATEMENT Distribution Unlimited			12b. DISTRIBUTION CODE	
13. ABSTRACT (Maximum 200 words) <p>Air Force Global Weather Center's (AFGWC) Relocatable Window Model (RWM) total cloud forecasts were validated using data for selected days in May, June, and July, 1996. Forecasts were generated twice daily (00 UTC and 12 UTC) to determine the RWM's ability to accurately forecast total cloud cover during the late spring and early summer. The RWM forecasts were post-processed using the Slingo cloud forecast algorithm and compared against AFGWC's operational real-time nephanalysis (RTNEPH) cloud analysis model. As a minimal-skill baseline comparison to the RWM's total cloud forecast, the RTNEPH initial analysis hour was persisted and evaluated against the same RTNEPH analysis as the RWM forecasts.</p> <p>The results of the study suggest RWM total cloud forecasts did not show improved skill, sharpness, accuracy or bias when compared against RTNEPH persistence through the 36-hour forecast period. The results also suggest the Slingo algorithm, as tested, is not appropriate for use in the RWM as an accurate total cloud forecast method for the late spring and early summer months over the North American Window.</p>				
14. SUBJECT TERMS Air Force Global Weather Center (AFGWC), Relocatable Window Model (RWM), Slingo, Real-Time Nephanalysis (RTNEPH)			15. NUMBER OF PAGES 165	
			16. PRICE CODE	
17. SECURITY CLASSIFICATION OF REPORT Unclassified	18. SECURITY CLASSIFICATION OF THIS PAGE Unclassified	19. SECURITY CLASSIFICATION OF ABSTRACT Unclassified	20. LIMITATION OF ABSTRACT UL	